ADAMA SCIENCE AND TECHNOLOGY UNIVERSITY

SCHOOL OF ENGINEERING AND INFORMATION TECHNOLOGY

Analysis and parametric study of deep excavation

With shoring pile

M.Sc. Thesis by: - Selomie Mequanint

DEPARTMENT OF CIVIL ENGINEERING

Major: - Geotechnical Engineering

Adviser: - Argaw Asha (PhD)

June, 2017

Adama, Ethiopia

ADAMA SCIENCE AND TECHNOLOGY UNIVERSITY

SCHOOL OF GRADUATE STUDIES

ANALYSIS AND PARAMETRIC STUDY OF SHORING PILE WALL AS DEEP EXCAVATION SUPPORT SYSTEM

By: - Selomie Mequanint

June, 2017

Approved by Board of Examiners

Dr. Argaw Asha	____________________	____________________
Advisor	**Signature**	**Date**
Dr.	____________________	____________________
External Examiner	**Signature**	**Date**
Dr.	____________________	____________________
Internal Examiner	**Signature**	**Date**
	____________________	____________________
Chairperson	**Signature**	**Date**

ACKNOWLEDGEMENT

First and foremost, I would like to thank God for the time, strength and wisdom, He gave me to accomplish this thesis.

I would like to express my sincere gratitude to my adviser Dr. Argaw Asha for his supervision, advice, and guidance from the very early stage of this thesis.

A special thanks also goes to GONDWANA ENGNEERING P.L.C for providing me all the necessary data's for the project.

Special thanks are extended to my friend's birhane gebru and hiyaw hatiya for their constant encouragement, and moral support.

Gratitude expressed to my husband, Nigus for his unconditional love and understanding, who has spent countless hours helping me, unwavering support, belief in me and, above all, patience during these most challenging time of my study.

I have no words to express my profound gratitude to my family for their unconditional support, inspiration and love from my child hood. Etye, Gasheye your prayer and blessings have always been the most vital source of inspiration to me.

Furthermore my special Thanks also go to my brothers and sisters for their perseverance unstinted Support and benevolence throughout the study period.

Finally, I would like to thank everybody who was important to the successful realization of this work, as well as expressing my apology that I could not mention personally one by one.

ABSTRACT

The demand for open space in urban areas has increased rapidly in recent years around our country, especially in Addis Ababa. This rapid development has not been matched by the ever decreasing open space commonly associated with urbanization. To fulfill the need for open space in urban centers; a deep excavation into the ground is very crucial. Hence it will provide an open space for different purpose, including parking lots, stores, basement and public utilities, etc. In multi story buildings, Deep excavation should be stable and to limit deformation to acceptable level. Ground deformation around excavation can damage adjacent building streets and public amenities. Thus, it is critically important to accurately predict the damage potential of nearby deep excavations and designing adequate support systems. This thesis will describe the analysis and parametric study of shoring as deep excavation support system. A detailed analysis of deep excavation supporting System using PLAXIS 2D will be performed in this study.

The objectives of this study are to investigate the effect of different parameters on the prediction of ground movement by numerical analysis and to develop a method of estimating these effects quantitatively around deep excavation. Extensive review of relevant literature published in the past four decades was conducted in order to understand the trends and the key developments in this area. It was revealed from the literature review that the concurrent use of the observational method and the finite element method for monitoring and controlling of ground deformations around the excavation has become a norm for deep excavation projects.

This study presents details of different parameters with deep excavation. Parametric study has been conducted to analyze the effects of surcharge and its location, pile diameter and wall embedment depth on horizontal displacement, vertical deformation and bending moment of the support system. Analysis results and discussion from the study are also presented with details of constitutive soil model used during analysis to analyze the suitability of shoring pile wall as deep excavation support system during deep excavation and provide helpful first estimate of probable damages caused on adjacent structures due to excessive excavation. Recommendations for future work are also presented at last.

Key Words: - Deep excavation, support system shoring pile wall, Ground deformation.

Table of Contents

LIST OF ACCRONYMS

C	Cohesion;
C increment	Increment in cohesion;
CS	Clayey soli;
D_{ex}	Excavation Depth;
E	Elastic modulus;
e_0	Void ratio;
EA	Normal stiffness;
EI	Flexural rigidity;
E increment	Increment in Elastic modulus;
EP	Earth Pressure
FE	Finite Element;
FEM	Finite Element Model;
HC	Hard Clay;
He	Final excavation depth;
HS	Hardening soil model;
I	Moment of inertia;
Ka	Active earth pressure ratio;
K	Soil modulus;
K0	initial earth pressure ratio;
Lb	Bond length;
L_s	horizontal anchor spacing;
M	wall bending moment;
MC	Medium Clay;
MCC	Modified Cam Clay;
MCM	Mohr Coulomb Model;
MG	Made Ground;
P	Load intensity;
P_v	Pressure;
Q	Axial load in the wall;
qs	Distributed surface load;

SC	Stiff Clay;
SPT	Standard Penetration Test;
SPW	Sheet pile wall;
SP WALL	shoring pile wall
Sr	relative wall stiffness;
SSM	Soft Soil Model;
t	Thickness;
w	Weight;
X	Distance;
y	Wall horizontal deflection at depth z;
yref	Reference depth;
Z1	Start depth;
Z2	End depth;
ϕ	Angle of internal friction;
ɣ	Unit weight;
δhm	maximum lateral wall deflection;
δvm	maximum ground settlement;
Ψ	Dilatancy angle;
ɣbulk	Bulk unit weight;
ɣr	Partial factor ;
τ	Shear stress;
σ	Compressive stress;
$\Delta\sigma_h$	Increase in lateral earth pressure;
υ	poisons ratio;
ɣ sat	saturated unit weight;

List of Figures

List of Tables

PART I

1. INTRODUCTION

1.1 Background of the study

In many densely populated city areas, there is a big paucity of open land, and most of the buildings are settled close to each other, these conditions increase the tendency to build high rise buildings. Although the application of deep excavation is widely used for the realization of underground space e.g. underground car parks and shopping centers, basement for high rise buildings etc. The integration of underground parking, new building project in urban environments can enhance the aesthetic and economic values of the overall development.

Deep excavations have been used worldwide for underground construction. However, the excavation processes inevitably alter the stress state in the ground and may cause significant wall deformation and ground movements. Especially when the excavation is close to adjacent infrastructure e.g. buildings burred pipe line etc. the excavation induced ground movements must be carefully monitored and controlled within an acceptable amount to avoid any potential damage. “To reduce the excavation-induced deformations, an appropriate retaining wall and support system should be designed, as well as employing adequate construction methods. As the excavation becomes deeper and larger in scale, and may be constructed in problematic soils, challenges arise for the research, design, and construction of deep excavations. Therefore, the performance of deep excavations should be better understood through more sophisticated approaches, e.g. real-time monitoring systems, and advanced numerical predictions” (dong.2014)

Unlike conventional retaining walls, which are often relatively rigid and manly rely on self-weight or soil weight to resist over turning and sliding shoring structure are slender and relatively flexible ,Stiff excavation support systems (such as secant pile walls, diaphragm walls, or tangent pile walls) have been used successfully to limit ground movement-induced damages. Several case histories exist for the use of stiff excavation support systems; example such as the use of anchor shoring for The Shangri-La hotel and luxury condominium tower (Brian Isherwood, Trana Brown Jenny Earle, Paul kreycir, 2013)

The performance of deep excavation should be better understood to limit damage to buildings and nuisance for neighboring residents especially in soft clays and adjacent buildings with shallow foundation. The failure of an excavation may have catastrophic consequence and special care must be taken by Appling numerical analysis which considers both geotechnical and structural aspect to predict the behavior of deep excavation and provide guidelines for construction. Due to the fact that the construction of high rise buildings with deep basement has started recently in Addis Ababa, Ethiopia, much emphasis has not yet given to deep excavation support systems. Therefore in this paper, analysis and parametric study of deep excavation with shoring pile has been studied thoroughly.

1.2 Objectives of the research

In Ethiopia, a number of high rise buildings are being constructed which need deep excavation for parking, etc. It is very important and should be a legal necessity with any construction to provide protection to the adjacent structures when excavating to any appreciable depth. Without adequate lateral support, the new excavation will almost certainly cause loss of bearing capacity, settlements, or lateral movements to existing property and these can damage buildings, streets, and utilities. Therefore, identifying and understanding the factors that affect the performance of deep excavation is an important issue for geotechnical engineers.

Thus, the main objectives of this study was to investigate the effect of different parameters on the performance of deep excavation supported with shoring pile wall and to show a method of estimating these effects quantitatively using analysis and parametric study.

1.3 Significance of the study

The results of this study will have a great importance on the ever growing building infrastructures and high rise buildings in our country, especially for those yet to be constructed in Addis Ababa. In addition the study also provided an estimate of probable damages caused on adjacent structures due to excessive excavation during and after excavation. Hence to come up with such results a careful and detail study in the stress state of soil during excavation was performed.

1.4 Scope of the Investigation

The scope of this study was limited to the analysis and parametric study of shoring pile wall as deep excavation support system in silty soils incase of Akaki Kilinto area in Addis Ababa city using PLAXIS 2D finite element software. The data and parameters which are obtained from the field studies have been used to evaluate in the entire manner, how they affect the ground deformation. Hence by using the field data and the study results the probable and predictable ground deformations had been estimated. In addition possible measures can be taken to reduce the problems arising to the new structures and existing structures during and after construction. The study area Kilinto, Addis Ababa is chosen because it shows rapid development in infrastructure and construction.

1.5 Methodology

To achieve the aforementioned purpose of the study, different soil data's were collected, interpreted and used as an input during the analysis on finite element software and most related researches and journals accomplished on analysis and design of deep excavation support system have been reviewed. Hence Suitable finite element software had been used to determine the effect of those parameters in the design of shoring pile wall and their significance.

1.6 Statement of the problem

Deep excavations have been used worldwide for underground construction, but they also alter the ground conditions and induce ground movements which might cause risks to adjacent infrastructure. For example, O'Rourke(1981) observed that driving and removing foundation piles caused about 30% of the measured ground movement at the Embarcadero 3 project in san Francisco, That's why retaining structure is needed to Prevent and minimize damages to surrounding is of utmost concern to the design engineers and constructor for any excavation work.

Retaining structures should be designed with respect to their lateral displacements, which can be reduced by adopting a stiffer wall, by reinforcing the anchor or strut system, or by pre stressing these components. This general stiffening of the retaining system, however this leads to an increase in lateral soil pressure, bending moments in the retaining wall, and forces in the struts or anchors. Braced excavations with a top-down construction method are usually preferred in practice to reduce wall deformations and ground movements.

Numerical analysis can consider both the geotechnical and structural aspects in the deep excavations such as the soil properties, details of structures, and construction sequences, and provide necessary information on the performance of deep excavations for design purpose. Therefore, accurate predictions of lateral wall deflections and surface settlements are important design criteria in the analysis and design of excavation support systems.

PART II

2. LITERATURE REVIEW

2.1 Introduction

The demand for underground space, for use as transport tunnels, parking garages, storage spaces, etc. in many heavily urbanized areas requires the construction of deep excavation in close proximity to sensitive structures. Advanced excavation techniques, including the use of shoring pile and support construction procedures are effective methods to reduce deformations in the surrounding soil and damage to adjacent structures. Shoring is the process of supporting a building, vessel, structure, or trench with shores (props) when in danger of collapse or during repairs or alterations. Shoring is commonly used when installing the foundation of a building. A shoring system such as piles and lagging or shotcrete will support the surrounding loads until the underground levels of the building are constructed.

However, in deep excavation and walls embedded in deep soil, the soil movements are difficult to control. The prediction of these movements, in such situations, becomes an important part of design of the support structure as well as the construction monitoring stage. Numerical methods are the only methods available to predict deformations caused by complex construction activities. The usefulness of the mechanical behaviour of the soil material and the availability of procedures to model complex construction sequences.

Performance of deep excavation is related to both stability and deformation. Deep excavations are designed to be stable and to limit deformations to acceptable levels. A stable deep excavation is an excavation whose walls do not collapse, and whose base does not heave uncontrollably. Ground deformations around excavations can damage adjacent buildings, streets, and utilities. The severity and extent of damage depends on the magnitude and pattern of ground movements around the excavation. Stability and deformation are related. Thus, prediction of deep excavation performance involves analysis of both stability and deformation. Experience has shown that stability can be evaluated with sufficient accuracy using simple limit equilibrium calculations. Deformations, however, are significantly more difficult to predict, and finite element analyses are often used for this purpose when ground movements are particularly important.

The excavation of soil from a deep excavation has two main effects. The first is that the removal of the weight of the excavated soil results in a decrease in the vertical stress in the soil beneath the excavation. The second is that the removal of the soil in the excavation results in a loss of lateral support for the soil around the excavation.

The purpose of a deep excavation support system is to provide lateral support for the soil around an excavation and to limit movement of the surrounding soil. Support systems for deep excavation consist of two main components. The first is a retaining structure. The second component is the support provided for the retaining structure. Many types of supports have been used in deep excavations. The principal types of supports are shoring piles such as: sheet pile, soldier piles, tangent piles, and contiguous piles. The principal types of supports are struts (braces), rakers, and tieback anchors.

- Approaches to design and analysis of excavation support system

There are a lot of calculation model available for the designing and optimizing retaining structures. But due to the time and financial budget, not all calculation models are adopted in practice. The following procedure is proved to be well balanced among safety, efficiency and accuracy. There are numerous calculation models available for deep excavation retaining structure design. The most essential and popular ones are:

- Analytical model
- Spring model
- Finite element model

2.2 Introduction of analytical model

The analytical model is based on some classical theories that determine the stresses on a retaining structure for the cases of active and passive earth pressure. The most famous and widely used theories among which are Rankine and Coulomb earth pressure theories. By applying these theories, the lateral earth pressure can be calculated, thus the minimum length of the sheet pile wall needed to achieve equilibrium can be determined. The retaining wall will certainly fail when the length of the sheet pile wall length is shorter than the minimum length.

If the length of the wall is longer than minimum required length, the Blum's method can be used to analyses the bending moments and deformation, so that design could be optimized. These theories give a quick first estimation that can be done by hand calculation.

2.3 Introduction of spring model

For a deep excavation process, the soil pressure and deformation change accordingly to the force acting on the retaining structure, the stiffness of retaining wall and so on. The forces are also related to the soil, water condition and excavation plan. It is a coupled process as the excavation induces unbalanced force against retaining structure and causes change in stress state and deformations, and these changes in return affect the unbalanced force. Compared to analytical models, numerical models can simulate and solve more complex conditions, as the computer can easily take over the calculation process. Therefore, the numerical methods can provide more accurate and realistic results. As for geotechnical problems, most commonly used numerical methods are the beam on elastic foundation method (spring method) and finite element method. The finite element model normally requires a lot of computation time and fast computer. Thus the spring method is more favorable for practical design. One of the most widely used geo-technical software for retaining wall design in Netherlands, D-Sheet piling, is based on this beam on elastic foundation theory**.**

2.4 Finite element model

2.4.1 General introduction

The finite element method is the dominant discretization technique that subdivides the mathematical model into non-overlapping disjoint components of simple geometry called elements. The response of each is expressed in terms of a finite number of degrees of freedom at a set of nodal points. It is then approximated by connecting and assembling all elements. Unlike finite difference models, finite elements do not overlap in space.

The common FEM solution procedures are:

1) Divide the system into elements with nodes (discretization/meshing);
2) Assemble all elements at nodes to approximate the whole system (forming element matrices)

3) Solve the system for specific problem by applying governing equations accordingly
4) Calculate desired quantities at selected elements

As stated in the previous sections for the analytical model and spring model, the excavation of soil induces coupled interaction between soil pressure and retaining structure. Theoretically speaking, the finite element method is capable of simulating the change of soil pressure, structure deformation, groundwater pressure and etc. However, finite element method is merely a tool that simulates the problem numerically. It is still down to the proper geotechnical theories applied that solve the problem. Moreover, modern commercial FE software provides rather robust solutions. It requires analysts' knowledge and experience to make sure the model is built up correctly and properly translated when the result presents. Due to the complexity of the FEM and the any small neglect is likely to lead to wrong results; the results of FEM should be checked by other methods.

2.4.2 FEM software for geotechnical problems (PLAXIS)

PLAXIS is special purpose finite element software designed for deformation and stability analysis. It is widely used for analyzing geotechnical problems. Especially the PLAXIS 2D, it gives a more realistic approximation for soil structure interaction compared to analytical model and spring model, without sacrificing too much calculation time.

2.4.3 Advantages and limitations

As mentioned in previous sections, a major advantage of finite element method is that the model has more realistic approximation for the change of deformation of soil and structure, as well as the change of stress state accordingly. For a complete theoretical solution the following four conditions should be satisfied: Equilibrium; Compatibility; Material constitutive behavior; Boundary conditions. The analytical model is not able to fulfill all these conditions at the same time. And it does not provide information on movements or structural forces under working load conditions. Simple numerical methods, such as the beam-spring approach, can provide information on local stability and on wall movements and structural forces under working load conditions. But they do not provide information on overall stability or on movements in the adjacent soil and the effects on adjacent structures or services. Full numerical analysis, for instance the FEM, can provide information on all design requirements.

However, the finite element method especially the three dimensional model requires large amounts of computing resources and an experienced operator. It is becoming widely used for the analysis of geotechnical structures and this trend is likely to increase as the cost of computing continues to decrease. (Potts, D 1999)

2.5 Empirical Method for Prediction of Ground Movement

Many empirical methods have been proposed for prediction of excavation induced ground settlement by researchers such as Peck (1969), Mayne and Kulhawy (1982), Clough and O'Rourke (1990), and Hsieh and Ou (1998). Empirical method is an attempt by the researchers to establish a relationship between the actual ground deformation and construction parameters from many similar projects. Despite its establishment was based on generalized assumption, it is still popular among design engineer for a preliminary study. These methods are based on typical ground deformation profile observed in deep excavation for different stages of excavation and wall installation as shown on the figure below.

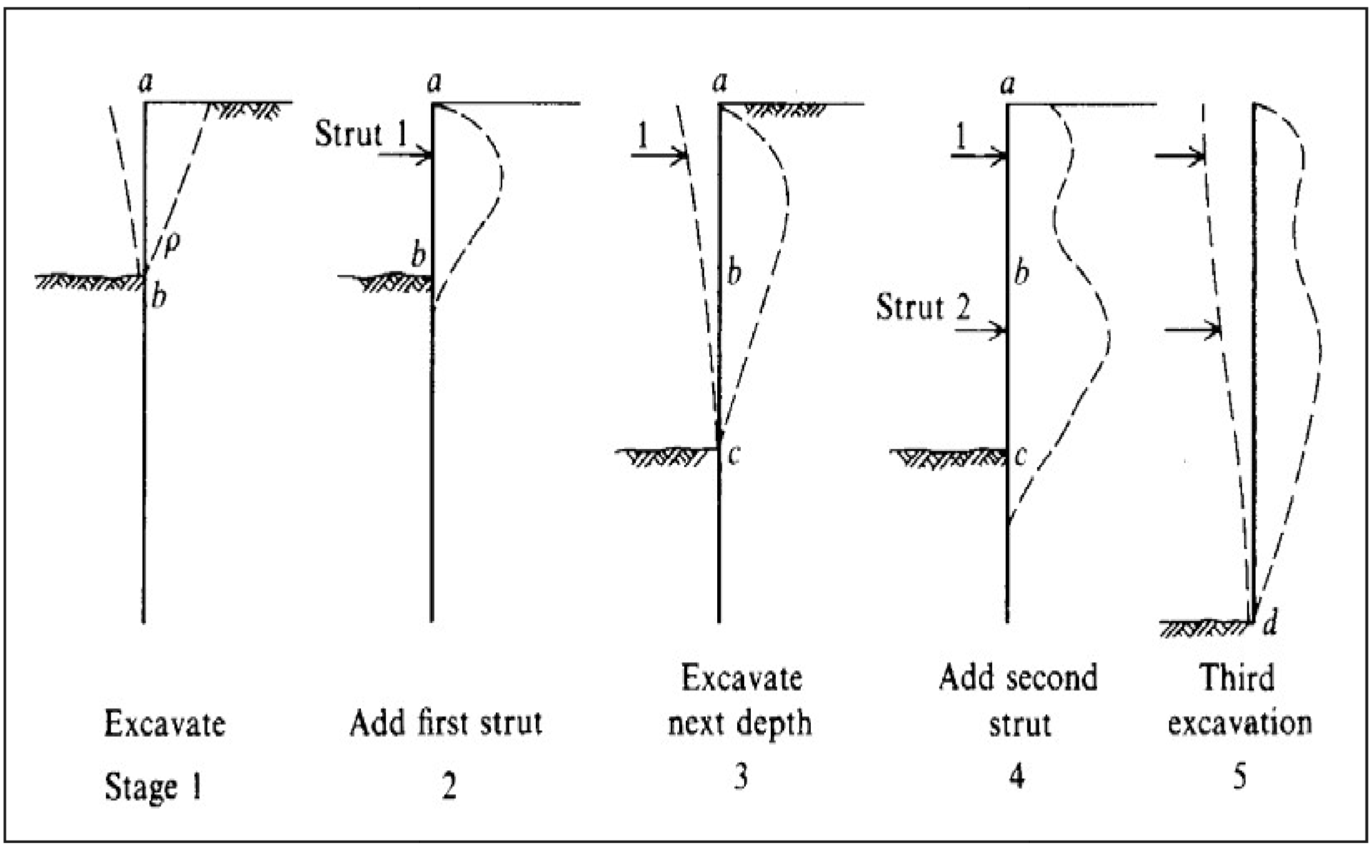

Figure 1: Stage development of earth pressure behind an excavation (Bowles1988)

2.6 Peck's Prediction Method (1969)

Peck (1969) developed the first empirical method to predict the wall movement based on actual ground deformation data collected from temporary braced sheet pile and soldier pile walls with tie back support that normalized by the excavation depth as shown in Figure 2.

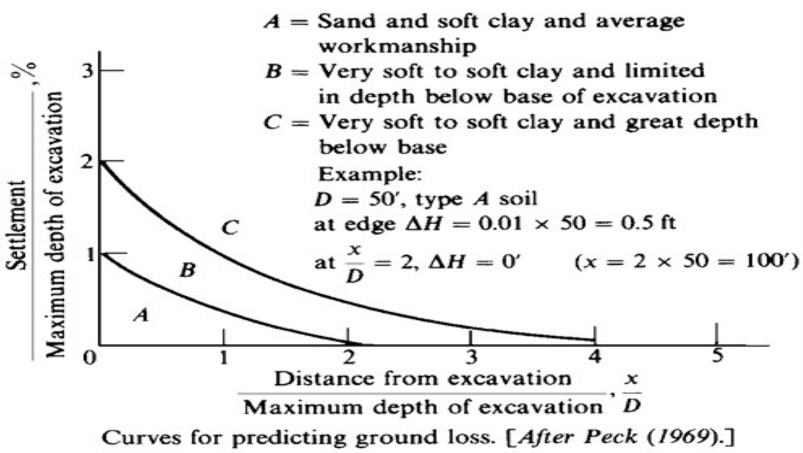

Figure 2: Curve for predicting ground loss (Peck, 1969)

The chart can be used to predict the ground deformation which can extend up to four times the excavated depth from the wall. However, since it is based on data collected from flexible support walls, prediction for much stiffer wall such as diaphragm walls is not reliable.

2.7 Clough and O'Rourke's Prediction Method (1989 &1990)

Clough and O'Rourke (1990) has developed a semi-empirical method for estimating excavation deformation in soft clays where by the maximum lateral deformations induced by excavation are depend on the system stiffness, S, and the factor of safety against basal heave. The overall stiffness is expressed in terms of an effective stiffness of the system as shown in Figure 3.

In this method, the system stiffness is defined as follows: $S = EI\ H\ 4\gamma$

(2.1) where EI is the wall flexural stiffness per horizontal unit of length (E is the modulus of elasticity of the wall element and I is the moment of inertia per length of wall), H is the average vertical spacing between supports, and γ is the total unit weight of the soil behind the wall.

Clough and O'Rourke (1990) concluded from a finite element parametric study on both soft and stiff clay, that the average horizontal and vertical movements of support systems in stiff clays were roughly 0.2 percent and 0.15 percent of the total excavated depth and major portion of movement occurs below excavation bottom in soft clay as a result of basal instability respectively. However, the factor of safety calculated as proposed by Clough et al. (1989) does not consider the increase stability due to wall embedment.

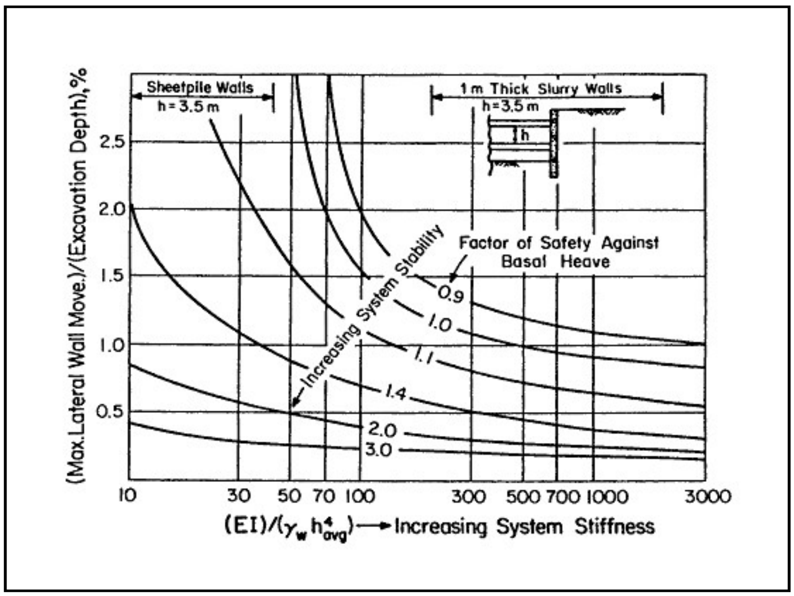

Figure 3: Design Curves for Maximum Lateral Movement in Soft to Medium Clay (Clough et al., 1989)

Clough and O'Rourke (1990) presented a dimensionless settlement profile as shown in Figure 4 for sand, stiff to very hard clays, and soft to medium clays. Based on Figure 6, the settlement influence zone is 3H for excavations in stiff to very hard clays and 2H for excavations in sands and soft to medium clays. Nevertheless, other settlement associated activities, such as dewatering, deep foundation removal or construction, and wall installation as practiced in modern day construction of diaphragm wall are not taken into consideration and it should be used as a conservative settlement prediction method.

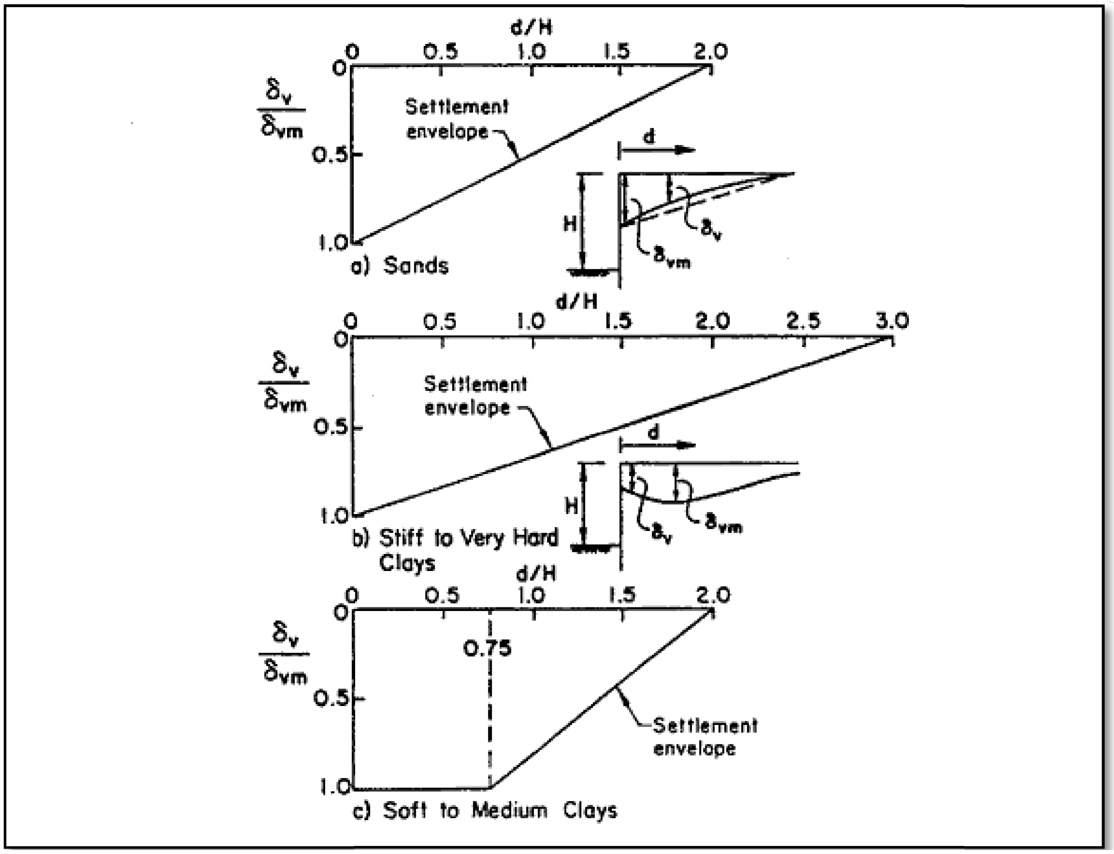

Figure 4: Settlement Profiles Recommended for Estimating settlement distribution adjacent to excavation for different type of soil. (Clough and O'Rourke 1990)

2.8 Hsieh and Ou's Prediction Method (1998)

Hsieh and Ou (1998) observed that there are two types of settlement pattern caused by excavations:

(i) spandrel type, as shown in Figure 5, in which maximum settlement occurs very close to the wall; and

(ii) Concave type, as shown in Figure in which maximum settlement occurs at a distance away from the support wall.

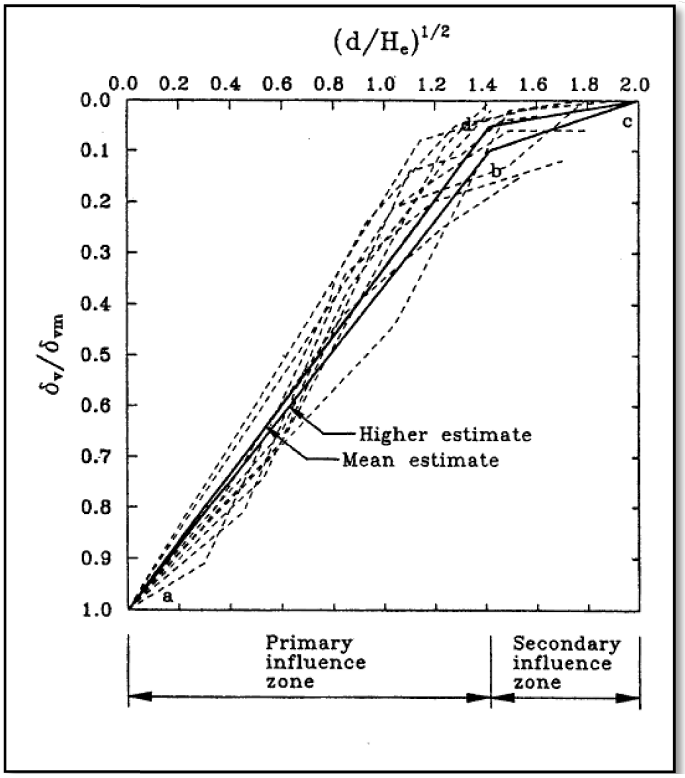

Figure 5: Spandrel type of settlement pattern (Hsieh and Ou 1998)

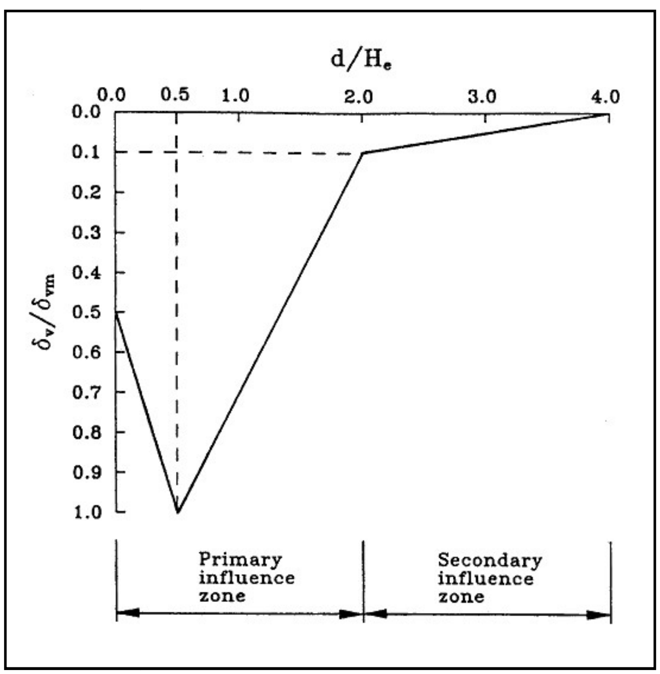

Figure 6: Concave type of settlement pattern (Hsieh and Ou 1998)

The presented normalized data, δ_v/δ_{vm}, where δ_{vm} is the maximum ground surface settlement, versus the square root of the distance-from-the-edge-of-the-excavation divided by the-excavation-depth (d/H_e). Hsieh and Ou (1998) concluded that the distance from the wall to the point where the maximum ground surface settlement occurred was approximately equal to half the excavated depth in concave type of settlement. Hsieh and Ou (1998), based on observations, suggested that δ_{vm} can be estimated using δ_{vm}- δ_{hm} relationship:

$$\delta vm = (0.5 - 1.0)\, \delta hm \text{--} (2.1)$$

Compared to the previous mentioned prediction methods, Hsieh and Ou (1998)'s method appears to be more accurate for predicting maximum surface settlement and the surface settlement profile. However, practical usage of Eq. 2.1 is limited because it yields a wide range of values for δ_{vm}.

2.9 Numerical Prediction Method for Ground Movement

Three main application of the finite element method to deep excavation can be found in the published literature. For design calculation and prediction of ground movement and structural force, it usually forms an important component of observational component. Also back analysis existing case histories using finite element analysis are often accompanied by parametric studies.

Some of the notable uses of finite element method in the analysis and design of deep excavation are given blow:

Palmer and Kenney (1972) used the finite element method to evaluate the relative importance of different parameters on the important of a braced excavation at Oslo subway in Norway. Parametric studies were carried out for a typical excavation with fully penetrating sheet pile walls of the parameters concerning soil condition. The soil deformation modulus was found to have the greatest influence. Other important parameters for deflection of retaining wall were found to be- stiffness of sheet pile and effective stress sheet pile.

Burland and Hancock (1977) described the performance of multi-propped deep excavation in sand and gravel overlaying stiff. Fissured London clay at new palace yard and reported that

Approximately 50% of total ground movement (both horizontal and vertical) occurred due to the construction of diaphragm wall piles.

Tung and Kung (2015) used a simplified soil model, the Modified Pseudo-Plasticity model by conduction a series of small strain triaxial tests on undisturbed Taipei silty clay to analyze the deflection and ground movements caused by braced excavations using Finite element analysis. Two sites having a diaphragm wall 25.6 m deep and 0.9 m thick, 35 m deep, and 0.9m thick were selected to conduct the numerical analyses of excavation. From the results found they concluded that the capability of the soil model adopted in describing the stress-strain-strength of characteristics of soils at a wide range of strain, especially at small strain ranging from 10^{-5} to 10^{2}, plays the crucial role in accurately predicting the excavation-induced ground movements.

Maria et al (2011) studied the performance of the deep excavation support system for 20m diaphragm wall with a single row of prestressed anchors in Berlin using finite element program. Generalized effective stress soil model was employed. The effective stress-strain-strength properties for the three sandy till units were modeled under the assumption that all three units had similar material properties but differed principally in their in situ state (i.e. stress conditions, void ratio, and stress history). Parameters for the soil model were derived from an extensive program of laboratory tests on the local Berlin sands. The study showed that the predictions for excavation performance were strongly affected by the vertical profiles of two key state parameters: the initial earth pressure ratio, K0; and the in situ void ratio, e_0. The results showed good agreement between computed and measured wall deflections and tieback forces.

Popa et al (2007), Presented "Numerical modeling and experimental measurements for a retaining wall of a deep excavation in Bucharest, Romania." They summarized a case history of a diaphragm wall for a deep basement of a new building in the center of Bucharest. The excavation impacted a number of historic structures, leading to the use of "top-down" techniques to support the excavation. The numerical results obtained by plane strain FE simulation were compared with measurements recorded during construction. For the soil, a perfect elasto-plastic constitutive law has been used, with Mohr – Coulomb criteria, using the geotechnical parameters issued from laboratory and in situ tests. From the results obtained they concluded that the computed lateral displacements were 15% and 75% of the observed values, depending on if the comparisons were made in an area with or without a grouted wall – not explicitly modeled in the FE simulations – adjacent to the diaphragm wall. The main factors leading to these differences were the soil parameters.

Schweiger (2005) studied the analysis of a deep excavation project in clayey silt in Salzburg. The excavation was supported by a diaphragm wall, a jet grout panel and three levels of struts. Hardening-Soil model was used as a constitutive model. Because of insufficient information available at the time of design on the material properties of the jet grout panel, the authors varied its stiffness in a parametric study. The effect of taking into account the stiffness of a cracked diaphragm wall on the deformations was also investigated. In some of the 3D calculations a non-perfect contact between diaphragm wall and strut was simulated by means of a non-linear behavior of the strut. The evaluation of the results and comparison with in situ measurements showed that analyses which took into account the reduced stiffness of the diaphragm wall due to cracking achieved the best agreement with the measurements. Furthermore settlements of buildings could be best reproduced by the three-dimensional model.

Manish Kumar (2015): Closely spaced structures in the vicinity of excavation, soft and compressible landfills, presence of underground utilities, and restriction of lateral ground movements have made the supporting systems a formidable task to execute. The support systems commonly adopted include Braced walls, Sheet pile walls, Contiguous or Secant pile walls, Diaphragm walls and RCC retaining walls, unsupported excavations pose several hazards, and the following list gives some of the important ones:

- Very high risk potential of collapse or failure of excavation walls and consequently posing hazard to workers and equipment
- Hazards during excavation due to presence of public utilities, such as electricity, water, gas, or natural gases and oxygen deficient atmosphere
- Dewatering problems
- Ground and/or ground water table changes affecting nearby structures Support provision for excavation depends on the type of soil in the area ,the depth of the excavation, the type of foundation being built, and the space around the excavation.

Erbì and Soccodato (2011) discussed the results of a 3D numerical study of deep excavations in soft clayey soils. The analyses were carried out using non linear, plasticity hardening soil model, an advanced soil model capable to reproduce the significant non-linearity which characterizes soil behavior. The parametric study involved different lengths of excavation sides, considering square and rectangular excavations, and different excavation heights. The attention was focused on horizontal displacements (wall deflections) as well as on vertical displacements (settlement profiles behind wall). Two-dimensional (2D) plane strain numerical analyses were also carried out in order to compare results and to highlight 3D effects on predicted displacement fields. From the results Erbì & Soccodato (2011) confirmed that, especially for excavations characterized by relatively low length to excavation depth or length to width ratios, 3D effects play a significant role in reducing the displacements obtained from 2D plane strain analyses.

Mitew (2005), conducted numerical analysis and parameter study taking into account two calculation methods, based on different constitutive soil models. Numerical back analysis has been divided into two parts. The first part considered the analysis performed using "Geo4-Sheeting analysis" and Rido - software, employing the method of dependent pressures, in which magnitudes of pressures acting upon a structure depend on deformation of the structure. The second part included numerical analysis performed using finite element method software: Geo4-FEM and Plaxis. The results of numerical analysis have been also compared to the results of in-situ measurements. Mitew (2005) concluded that Maximum theoretical displacements of the wall estimated in all FEM analysis were very close to the value of maximum real displacement measured during construction and relatively best results have been obtained when the soil parameters were based on the results of Pressure meter investigations.

Potts and Fourier (1984), studies at the behavior of a propped retaining wall by finite element method, the investigation investigated that for an excavated wall in soil with high initial value of coefficient of earth pressure at rest, props force and wall bending moments greatly exceed those predicted by limit equilibrium calculation. The analysis indicates that the displacement were much smaller in magnitude and that approximately limit equilibrium calculation procedure conservative values of prop force and bending movement.

Wong and broms (1989) proposed a simplified method to estimate the lateral deformation of braced sheet pile walls in clay with average to good workman ship. The study concludes that the settlement, lateral displacement and heave are mainly controlled by the factor of safety with respect to base heave and formed charts to estimate lateral deformation. They suggested that in order to minimize the early deformation of retaining wall, struts should be installed and pre load immediately after the excavation has reached the new strut level and the spacing of the struts be small.

2.10 Field performance studies of deep excavations

Field measurement is an effective method, but it is also expensive and takes a long time to obtain the data, and this process is not repeatable. A number of case histories of deep excavations have been reported worldwide with well-documented field data, e.g. in the UK (Skempton and Ward 1952, Wood and Perrin 1984, Simpson 1992), in Chicago (Wu and Berman 1953, Finno, Atmatzidis et al. 1989, Finno and Nerby 1989), in Shanghai (Liu, Ng et al. 2005, Xu 2007, Wang, Xu et al. 2010, Liu, Jiang et al. 2011, Ng, Hong et al. 2012), in Singapore (Wong, Poh et al. 1996, Lee, Yong et al. 1998), in Hong Kong (Leung and Ng 2007), and in Taiwan (Ou, Hsieh et al).

These case histories vary from one to another in geological conditions, retaining structures, and construction methods, which make the correlation and comparison difficult, but generally they recorded the main excavation behavior, e.g. wall deformations, ground movements, earth and pour water pressures, strut loads and wall bending moments, and deformation of adjacent infrastructure. Therefore, they provide valuable resources for understanding the more comprehensive behavior of deep excavations, and also for calibrating the numerical analyses.

Ahtchi et al (2015): shoring system selection for deep excavation, a study was conducted in the east region of the Middle East to assess the constructability of a shoring system for a 12-meter deep excavation. Several shoring systems were considered in this study including secant concrete piling, contiguous concrete piling, and sheet-piling. The excavation was carried out in very dense sand with the groundwater level located at 3 meters below ground surface. The study included conducting a pilot test for each shoring system listed above. The secant concrete piling included overlapping concrete piles to a depth of 16 meters.

Drilling method with full steel casing was utilized to install the concrete piles. The verticality of the piles was a concern for the overlap. The contiguous concrete piling required the installation of micro-piles to seal the gap between the concrete piles. This method revealed that the gap between the piles was not fully sealed as observed by the ground water penetration to the excavation. The sheet-piling method required pre- drilling due to the high blow count of the penetrated layer of saturated sand. This study concluded that the sheet piling method with pre-drilling was the most cost effective and recommended a method for the shoring system.

Winter et al (1992) described the performance of a 10-m deep excavation supported by a shoring with tiebacks adjacent to the church of the Epiphany in Washington, D.C. Movements measured during wall installation next to the church were 3 mm or less. Very minor displacements were recorded during excavation. Maximum horizontal displacement of wall was 0.15% H.

Ou et al (1993) studied the characteristics of ground surface settlement during excavation by examining data from ten case histories of deep excavations in Taipei. They examined maximum wall deflection and the relationship between wall deflection and ground settlement. Maximum lateral wall deflection often occurs near the bottom of an excavation. Upper limit on maximum ground settlement is the maximum lateral wall deflection; in general ground settlement is about 50% to 70% of the maximum wall deflection. Maximum wall deflections were usually between 0.2% and 0.5% of the excavation depth.

Garvin and Boward (1992) described the cut-and-cover construction of a five level underground parking structure in Pittsburgh. A shoring pile with tiebacks was used to support the 7-m to 8-m excavation. Movements and groundwater levels were monitored during construction. Slurry wall system performed well and permitted dewatering within the excavation within a minimum influence on groundwater levels outside excavation. Maximum lateral movements for the excavation were between 10 and 20 mm. An adjacent 80 year old sandstone structure experienced no distress.

Lings et al (1991) presented and compared the performance of a deep excavation constructed by top-down methods in Gault Clay to design predictions. Earth pressures, heave, and pore pressures were measured. They found diaphragm wall construction caused a significant decrease in lateral stresses and also deflections, prop forces, and bending moments were substantially lower than predicted.

Yu Ou et al (2012) studied the characteristics of ground surface settlement during excavation. Ten excavation cases in Taipei with good-quality construction and field observation data were selected to study the characteristics of excavation behavior. The location of maximum lateral wall deflection, magnitude of maximum lateral wall deflection, relationship of maximum lateral wall deflection and maximum ground surface settlement, location of maximum ground surface settlement, and apparent influence range were thus established based on the actual excavation cases. Finally, an empirical formula was proposed to predict the ground surface settlement profile at the center section of an excavation, where the behavior may be characterized by plane-strain conditions.

Korff and Mair (2013) Studied and discussed ground displacements related to deep excavation in Amsterdam. The settlement measurements for the Amsterdam deep excavations have been compared to several, mostly empirical, relationships to determine the green field surface displacements and displacements at depth. It is concluded that the surface displacement behind the wall was 0.3-1.0% of the excavation depth, if all construction works were included. Surface displacements behind the wall can be much larger than the wall deflections and become negligible at 2-3 times the excavated depth away from the wall. The shape of the displacement fits the profile of Hshieh and Ou (1998) best. In all three of the Amsterdam cases, the largest effect on the ground surface displacement can be attributed to the preliminary activities. The actual excavation stage caused only about 25%-45% of the surface displacements, with 55%-75% attributed to the preliminary activities. At larger excavation depths the influence zone was significantly smaller than 2 times the excavation depth.

The bending moment (M) of the shoring pile can be calculated through the measurements from the reinforcement bar strain gauges, assuming that the variation of stresses over a cross section of the wall is linear and the neutral axis lies along the centre of the wall. Alternatively, the bending moment can be computed from the curvature of the wall deflection curve using the equation $M = EI/r$, where EI is flexural rigidity and r is the radius of curvature. But the bending moments computed from the rebar strain gauges are generally smaller than those from the wall deflection curve, particularly for the location where the maximum lateral wall deflection occurred and its neighboring location. This is because the bending moment from the wall deflection curve is computed without considering cracking concrete so that the moment of inertia (I) is not reduced. As a matter of fact, some cracks actually exist in the concrete because of the deformation of the concrete wall, subsequently thereby reducing the moment of inertia. The reduction factor for the moment of inertia (R) is introduced and then defined as the ratio of the moment obtained from the rebar strain gauge to the moment obtained from the inclinometer measurement. The reduction factor decreases with excavation depth OU, Liao et al (1998).

Gebru (2016) conducted a study on the analysis of Contiguous Pile wall as deep excavation support system in Adam Town. Finite element simulation was used to predict maximum wall movements for deep excavations in cohesive soils. PLAXIS 2D one of the finite element models used in the analyses. In the simulations, soil elements were modeled with 15-node wedge elements that are generated from the projection of two-dimensional 6-node triangular elements between work planes with a width of 105 meters and depth of 30 meters. A surface load of 107.9 kN/m^2, $125kN/m^2$, $150kN/m^2$ and $175kN/m^2$ were used during analysis. Further, medium mesh size were used for modeling of wall and pile, building and the soil. Horizontal displacement was computed at the most vulnerable location. The result showed that The horizontal displacement ratio behind the pile wall increases by 0.00571% but the ratio of settlement to maximum depth of excavation and the maximum bending moment to moment due to active soil mass ratio behind the pile wall decreases by 0.057% and 0.085% respectively as the depth of excavation increases by 2m keeping location of surcharge constant which is 1.5m. Moreover, the horizontal deformation and settlement ratio remains almost constant and the moment ratio increases by 0.0176% as the surcharge to stress at bottom of excavation ratio increases by 1%.

An analysis of secant pile wall as deep excavation support system on silty sand soil in Hawassa town was studied by **Hatiya (2016).** PLAXIS V8.2 2D finite element software was used to analyse the results. A surface load of $100kN/m^2$, $120kN/m^2$ and $140kN/m^2$ were used during analysis. In this study, very fine mesh size were used for modelling of pile and wall, building and the soil. The study found out that as a distance increase from depth of excavation for constant load the ratio of horizontal displacement to maximum depth of excavation decreases .However, for constant distance as the load increases the horizontal displacement ratio behind the pile wall increases.

Finno and Sabatini (2002) presented the damage caused by an adjacent 12.2-m-deep excavation in soft clay in which the excavation support system was a 0.9-m-wide secant pile wall braced by both cross-lot struts and tiebacks on a three-story school supported by shallow foundations. The school was a reinforced concrete frame structure with exterior reinforced concrete foundation walls. The lateral ground movements associated with the excavation were monitored with four inclinometers placed around the school. The building movements were monitored with optical survey points established on interior columns, exterior walls and on the roof, and with tilt meters installed on the exterior foundation walls.

From the study it was found that the damage to the school mainly consisted of 300 to 500-mm-long hairline cracks in non load bearing walls. Only a few cracks had widths greater than 6 mm. The school deformed such that the portion closest to the excavation sagged and the remainder hogged. Damage was first observed in the area of sagging when angular distortions reached 1/940 and the excavation was approximately 5.5m deep. Angular distortions as large as 1/300 was observed at the end of the project, the authors concluded that the angular distortions had to be less than 1/1000 to preclude any damage to the school.

2.11 Constitutive Soil Models

The accuracy of numerical solutions in deep excavation analysis largely depends on the ability of the constitutive model to describe soil behavior in generalized stress conditions. However, considering the complexity of soil behavior, it is not realistic to develop a completely generalized effective stress model for all soils. For a given boundary problem, the complexity of the constitutive model should be closely tied to the major aspects of the problem (e.g., stiffness, strength, deformation, dilation, and anisotropy) to be tackled and/or the accuracy of solution which is required (Whittle 1987). Once the soil model is identified, its application in the finite element analysis requires appropriate procedures to derive the model parameters and calibrate the model through laboratory and/or field tests. A number of advanced soil models have been used in the analysis of deep excavations with certain kinds of success, and their characteristics are discussed briefly in this section.

Yang et al (2008) developed a constitutive model, Plastic Bounding Surface Model for unsaturated cemented and loessic soils under cyclic loading. The developed model was based on the damage theory for structured soils and unsaturated soil mechanics and an elasto plastic model for unsaturated loessic soils under cyclic loading. The description of bond degradation in a damage framework was given, linking the damage of soil's structure to the accumulated strain.

The Barcelona Basic Model (BBM) was considered for the suction effects. The elasto plastic model was then integrated into a bounding surface plasticity framework in order to model strain accumulation along cyclic loading, even under small stress levels. The validation of the proposed model was conducted by comparing its predictions with the experimental results from multi-level cyclic triaxial tests performed on natural loess sampled beside the Northern French railway for high speed train and about 140 km far from Paris. The comparisons showed the capabilities of the model to describe the behavior of unsaturated cemented soils under cyclic loading.

Bolton et al (1994) studied the non linear stress-strain behavior of over consolidated clays at small strains prior to gross plastic yielding and derived a general form of power function for shear modulus and its implementation inside the yield surface of the Modified Cam Clay model within CRISP finite element program. Simulation of triaxial tests, and ground movements due to unneling were compared with appropriate data and contracted with constant stiffness analysis. Results from triaxial tests showed that the shear modulus was under estimated by the MCC model for small strains and over estimated for intermediate large strains. From the observed behavior of ground movements in centrifuge tests on tunnels in clay the author's concluded that the magnitude and shape of surface subsidence above the tunnel could not simultaneously be predicted by the MCC model.

However the SDMCC model fitted observed behavior much better, especially when the critical state ratio (M) was permitted to reflect the local strain path (extension or compression) appropriate to tunnel pressure reduction.

A constitutive model with a single yield surface has been developed for the behavior of frictional materials, such as clay, sand, concrete, and rock by Poul V. L (1990). The model is based on concepts from elasticity and plasticity theories. In addition to Hooke's law for the elastic behavior, the framework for the plastic behavior consists of a failure criterion, a non associated flow rule, a yield criterion that described contours of equal plastic work, and a work-hardening/softening law. The functions that describe these components were all expressed in terms of stress invariants. The model incorporates eleven parameters for normally consolidated clay that can be determined from simple experiments, such as isotropic compression and consolidated-undrained triaxial compression tests.

A study of the three-dimensional behavior of remolded, normally consolidated clay has served as a basis for evaluating the capabilities of the model. In particular, the variations of stress-strain and pore pressure behavior, relation between principal strains, and normalized undrained shear strength with the relative magnitude of the intermediate principal stress were studied. Overall acceptable and accurate predictions were produced for the normally consolidated clay.

Poul et al (2008) developed a Rotational Kinematic Hardening Model for three- dimensional stress reversals in sand. It incorporated rotation and intersection of yield surfaces to achieve a consistent and physically rational fit with experimentally observed soil behavior during large three-dimensional stress reversals. An existing elasto-plastic model with isotropic hardening was used as the basic framework to which the rotational kinematic hardening mechanism has been added. The new combined model preserved the behavior of the isotropic hardening model under monotonic loading conditions, and the extension from isotropic to rotational kinematic hardening under three-dimensional conditions has been accomplished without introducing new material parameters.

Predictions of plastic strain increment vector directions from the proposed Rotational Kinematic Model were made by the authors to compare with experimental results from triaxial compression and extension tests in the triaxial plane. Predictions of stress–strain behavior during large stress reversals were also shown to fit well with experimental data. The model was extended to the principal stress space and theoretical plastic strain increment vector directions were compared with experimental data. Within the scatter of the test results, the model was shown to capture the behavior of soil during large stress reversals with reasonable accuracy.

Cecconi et al.(2002) developed a constitutive model for granular materials within the framework of strain–hardening elasto plasticity, aiming at describing some of the macroscopic effects of the degradation processes associated with grain crushing. The central assumption of the paper was that, upon loading, the frictional properties of the material were modified as a consequence of the changes in grain size distribution.

The effects of these irreversible microscopic processes were described macroscopically as accumulated plastic strain. Plastic strain drives the evolution of internal variables which model phenomenological the changes of mechanical properties induced by grain crushing by controlling the geometry of the yield locus and the direction of plastic flow. The model was applied at Pozzolana Nera to observe the stress–dilatancy relationship to use as guidance for the formulation of hardening laws, and it was concluded that the minimum value of dilatancy always follows the maximum stress ratio experienced by the material.

2.12 Verification Examples from Literature

2.12.1 Modeling of tie back sheet pile wall for deep excavation using plaxis

Dinakar et al (2014) conducted the models of deep excavation and structure at adjacent locations in ground with and without sheet pile wall respectively. For the numerical simulation, two dimensional finite element code PLAXIS version 8.5 was used. Mohr-coulomb model is used to model soil. The linear-elastic-perfectly- plastic Mohr-coulomb model involves five parameters, namely Young’s modulus, Poisson’s ratio, Frictional angle, Cohesion and Dilatancy angle of ground.

The convergence and boundary effects are ensured, the effort to ensure that the convergence criteria are satisfied. For this purpose, modeling of tie back sheet pile, building and the soil is made using very fine mesh size to coarse mesh size. At the most vulnerable location (at 2.5m beside the sheet pile wall) in the ground, horizontal displacement is computed under different mesh sizes. It is observed that idealization with medium mesh size yielded satisfactory results.

The material properties used for the modeling is given in

Table 1: material properties used for the modeling

Soil Properties(Drained)	**Sheet pile**
Modulus Of Elasticity= **20 MPa** Cohesion = **20 kN/m^2** Frictional Angle = **30°** Unit weight = **18 kN/m^3**	Height = **20 m** Pile modulus = **200 Gpa** Thickness = **20mm**
Anchor and Grout body	**Beam elements**
Anchor modulus = **200Gpa** Anchor thickness**= 25mm** Anchor spacing **= 4m** Grout body **M25**	Beam element = **300 mm X 450 mm** Grade of beam **M25**

2.12.2 Construction simulation using Plaxis

The construction in numerical modeling is carried out in stages simulating the exact field procedure to obtain a good correlation. The construction procedure consists of building the structure on the soil and loading it as shown in Figure 7. The displacements with gravity loading are neglected. Later with loading there is a rapid increase in the ground movements which are reduced by constructing the sheet pile wall as shown in Figure 8.

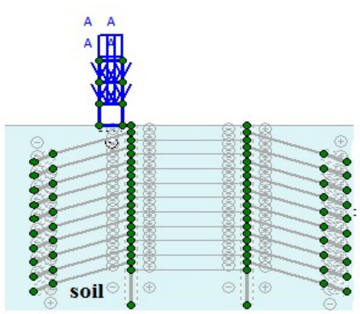

Figure 7: Building construction

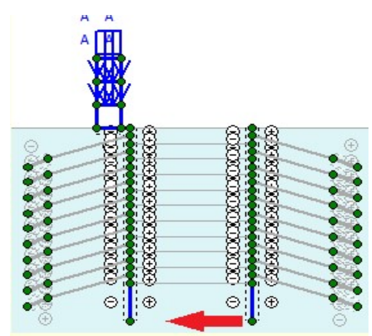

Figure 8: Sheet pile installation and loading

After installation of sheet pile, excavation is carried out in stages. Later the anchors are introduced and pre stressed for wall stability and to bring down the displacements within safe limits.

2.12.3 Results

The objective of the study is to understand the behavior of tie back sheet pile wall system to the ground movements caused by excavation. To focus on the deformation and stress characteristics of adjacent structures due to ground movement, soil structure interaction with and without supporting system is modeled and the parametric study is conducted by varying distance of structure from the face of excavation and ground displacements are measured exactly below the structure. Later the effect of penetration depth, stiffness, pre stressing force is studied to understand the behavior of sheet pile wall. In this paper bending of wall towards backfill is termed as negative bending and bending away from backfill is termed as positive bending.

Effect of Adjacent Structures and Anchorage Point

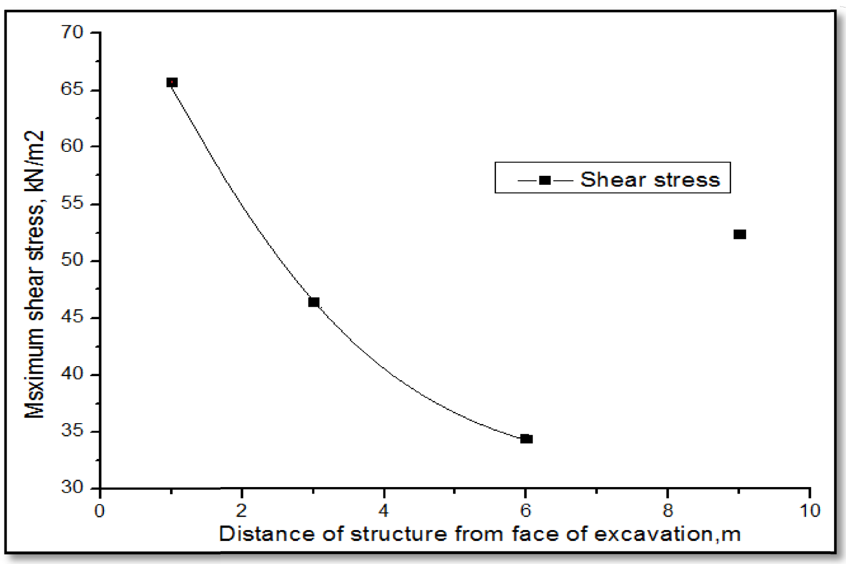

Figure 9: Shear stress variation in ground with increase in distance of Structure from Excavation

Shear stress in soil appears to decrease with increase in the distance from face of excavation. However, near the end of anchor shear stress appears to increase, perhaps due to soil structure interaction. Hence the anchorage should be done far from the adjacent structures. The vertical displacements are unaffected by anchorage point and displacements decreases with increase in distance of structure from excavation

Effect of Prestresing Force

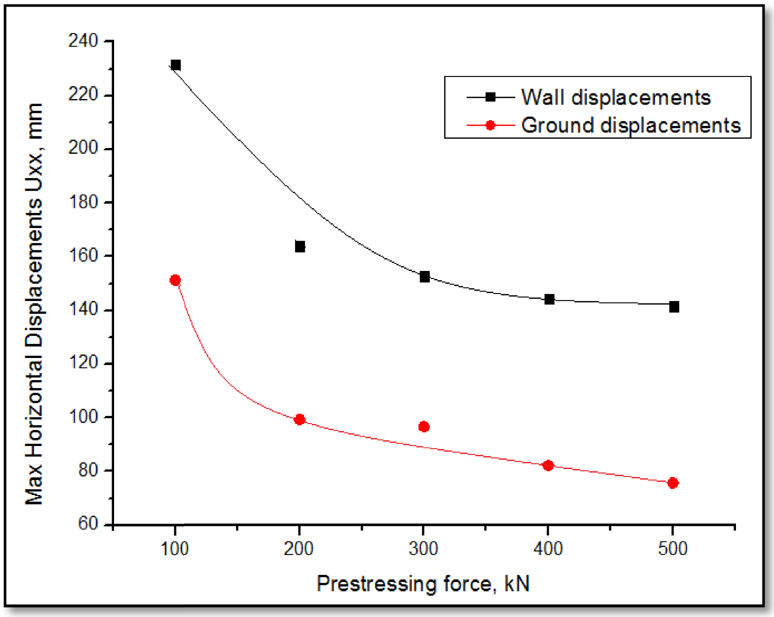

Figure 10: Variation of horizontal displacements with pre stressing force

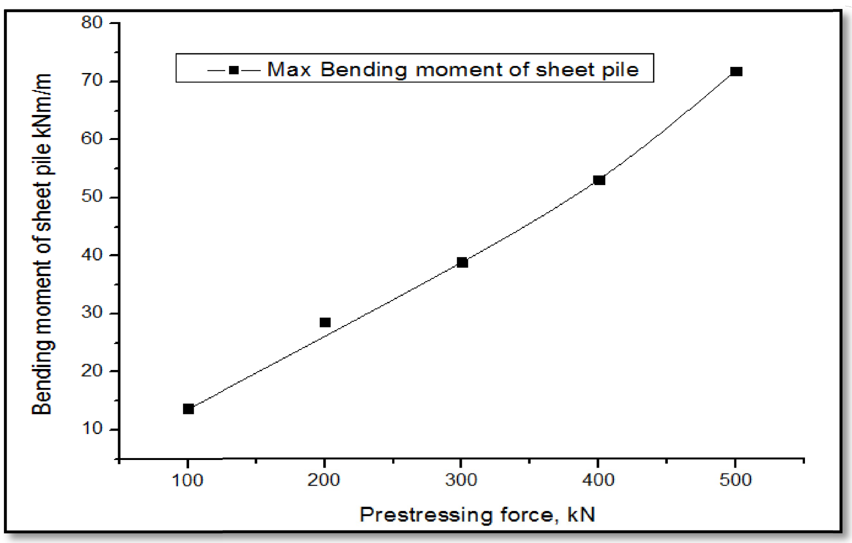

Figure 11: Variation of bending moment of wall with pre stressing force

This parameter helps to identify the force required for the support system to be stable from ground movements. Figure 11 shows the variation of wall, ground displacements of sheet pile wall. Initially displacements are high and are reduced rapidly with increase in force. After reaching optimum force further increase in force may lead to tendon and sheet pile failures. Similar performance is seen with sheet pile bending moment due to the presence of prestressing force the negative bending moment is seen which is shown increasing in Figure 12.

Effect of Stiffness of Sheet Pile

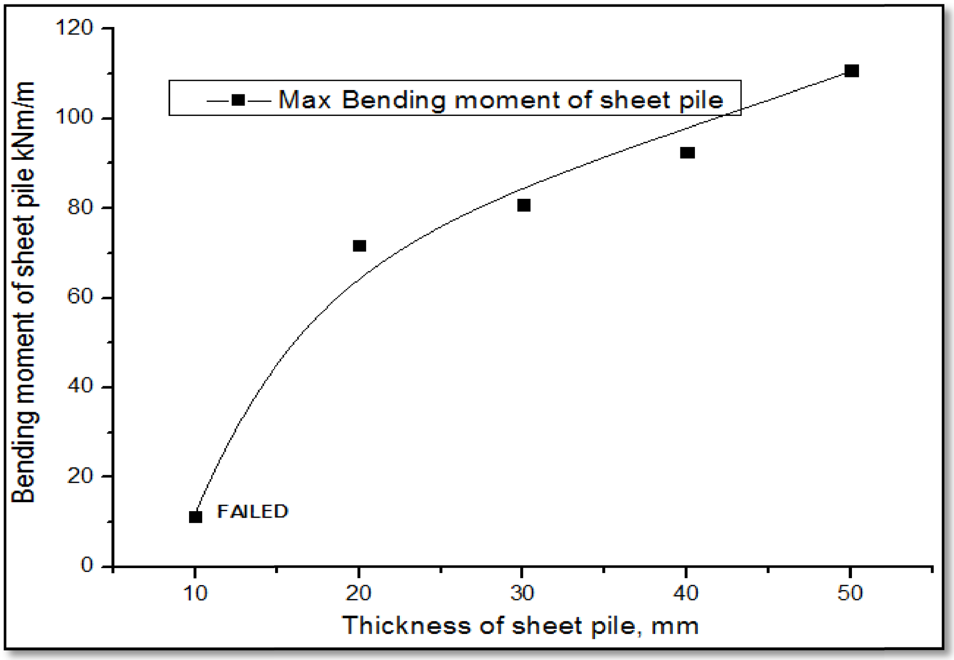

Figure 12: Variation of bending moment with thickness of sheet pile

It can be seen that with 10mm thickness of sheet the displacement value is very high. With the thickness, depth up to 7m was achieved and further excavation was not possible due to failure of pile. On further increase there is a reduction in displacements and bending moments. In present work 30mm is observed as optimum thickness.

Dinakar et al (2014) results provide an understanding of the behavior of tie back sheet pile wall based on the effect of adjacent structures, penetration depth, and pretressing force and stiffness characteristics on the displacements and bending moments of sheet pile. The following are some important inferences from their study.

- Exact field procedure of deep excavation can be simulated in the numerical model using Plaxis and the strength and deformation characteristics of ground and the structure can be computed at any stage.
- Tie back sheet pile wall method acts as a stable supporting system to excavate for greater depths safely without considerable ground deformations.
- Presence of Anchors below the structure increases horizontal displacements in ground hence anchorage should be done far from the structures.

- Increase in penetration depth reduces 10-15% of wall movements only, whereas there is a drastic reduction in maximum bending moments when walls are anchored. Minimum penetration depth of 3-5m shall be preferred.
- Optimum thickness and prestressing force for the system can be predicted from the analysis.

PART III

3. STUDY AREA DESCRIPTION AND BASE MODEL PARAMETRES

3.1 Description of the study area

Kilinto area is located in the south of Addis Ababa city; Kilinto is currently being developed as IPDC's second park in Ethiopia's lively, cosmopolitan capital. With a total size of 337 Ha, Kilinto will be a mixed-use park and the number one destination for manufacturers in agro-processing, pharmaceuticals, electric and electronics products, wood and furniture, both for export and to serve local consumers.

Kilinto will be developed in 2 phases in collaboration with the World Bank Group, with phase 1 on 153 Ha. Serviced land in Kilinto will be available from early 2016, with pre-erected factory sheds available from the 4th quarter of 2016.

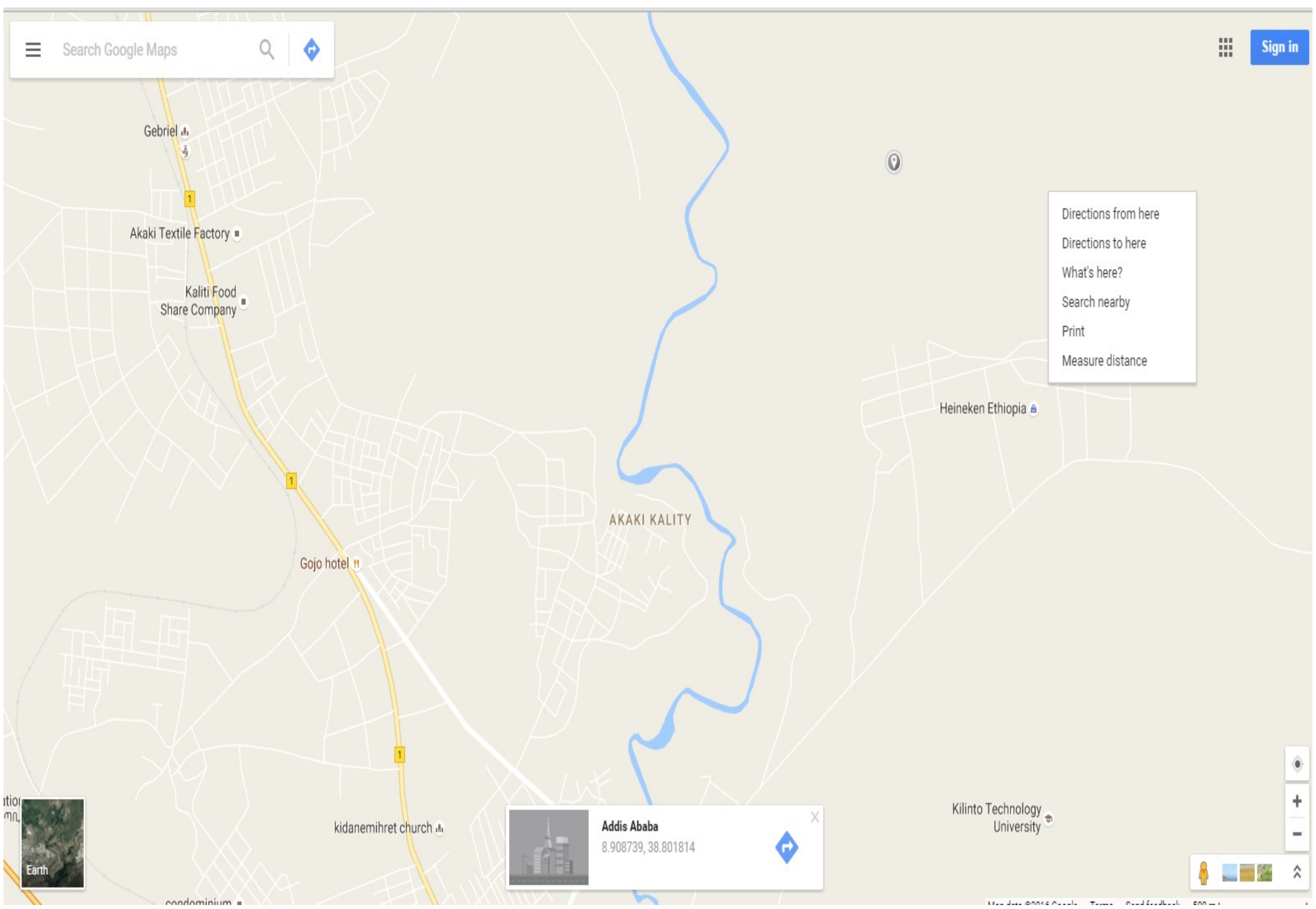

Figure 13: Study area map

3.2 Parameter Identification

During analysis of deep excavation support system, a number of parameters, which has an effect in the performance of shoring pile wall, have to be considered. Therefore based on the Investigations made by GONDWANA ENGNEERING P.L.C. a representative value of SPT test data are chosen and required soil parameter correlations are used and selected based on data quality, soil profile, consistency and availability. Some relevant parameters for the soil are taken from different literatures used to determine the strength parameters of the soil. The soil types considered for this study are silty clay soils from Addis Ababa, Kilinto area. Ground water level is at deep depth from ground surface; hence it has no effect in the analysis, during excavation and construction. The following engineering design parameters are extracted from SPT N values which were conducted by GONDWANA ENGNEERING P.L.C and considered to represent the soil in Addis Ababa, Kilinto area based on availability.

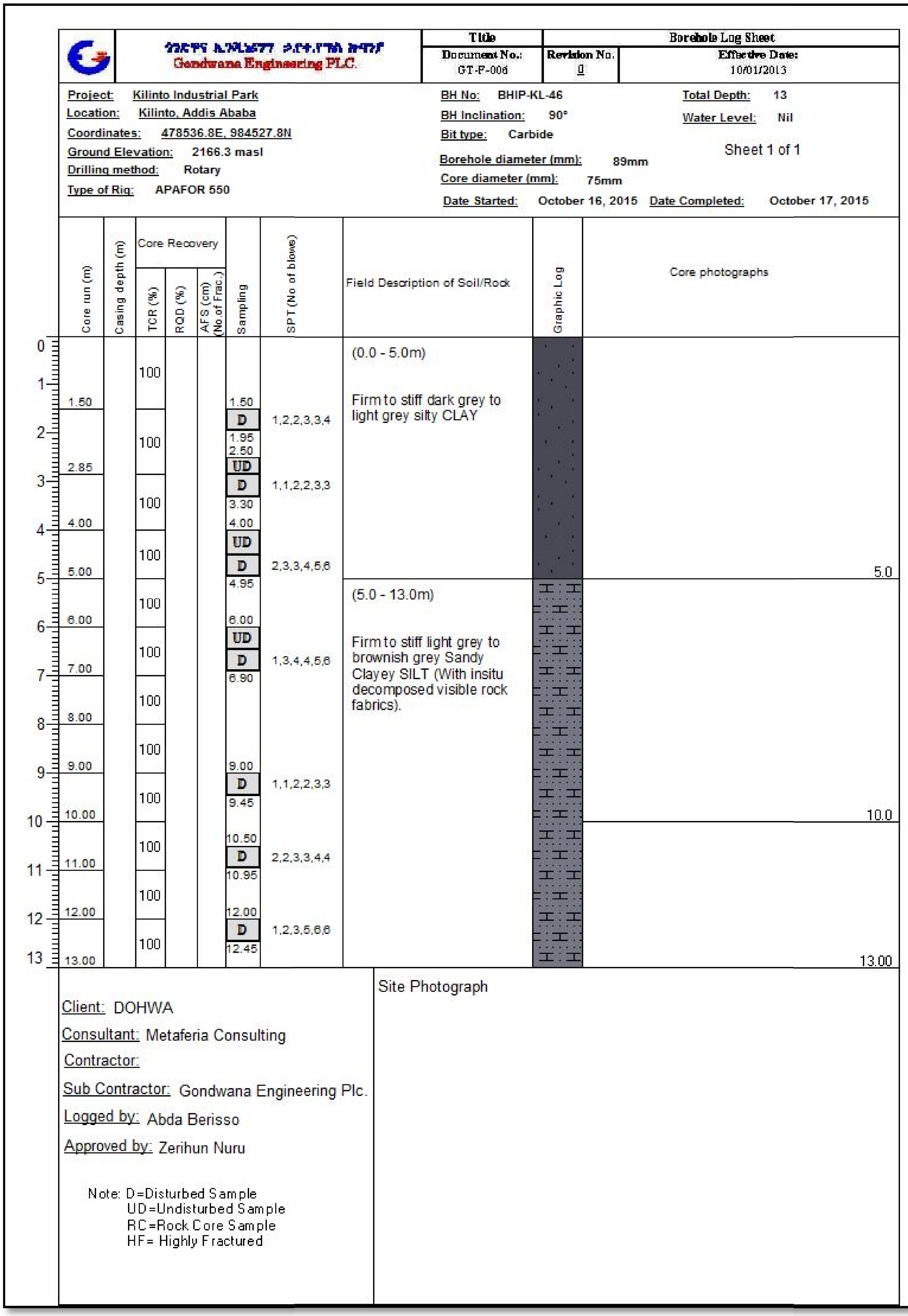

Gondwana Engineering PLC.

Title	Borehole Log Sheet	
Document No.: GT-F-006	Revision No.: 0	Effective Date: 10/01/2013

Project: Kilinto Industrial Park
Location: Kilinto, Addis Ababa
Coordinates: 478536.8E, 984527.8N
Ground Elevation: 2166.3 masl
Drilling method: Rotary
Type of Rig: APAFOR 550

BH No: BHIP-KL-46
BH Inclination: 90°
Bit type: Carbide
Borehole diameter (mm): 89mm
Core diameter (mm): 75mm
Date Started: October 16, 2015 Date Completed: October 17, 2015

Total Depth: 13
Water Level: Nil
Sheet 1 of 1

Core run (m)	Casing depth (m)	Core Recovery: TCR (%)	RQD (%)	AFS (cm) (No.of Frac.)	Sampling	SPT (No of blows)	Field Description of Soil/Rock	Graphic Log	Core photographs
1.50		100			1.50 D 1.95	1,2,2,3,3,4	(0.0 - 5.0m) Firm to stiff dark grey to light grey silty CLAY		
2.85		100			2.50 UD D 3.30	1,1,2,2,3,3			
4.00		100			4.00 UD D 4.95	2,3,3,4,5,6			
5.00		100							5.0
6.00		100			6.00 UD D 6.90	1,3,4,4,5,6	(5.0 - 13.0m) Firm to stiff light grey to brownish grey Sandy Clayey SILT (With insitu decomposed visible rock fabrics).		
7.00		100							
8.00		100							
9.00		100			9.00 D 9.45	1,1,2,2,3,3			
10.00		100							10.0
11.00		100			10.50 D 10.95	2,2,3,3,4,4			
12.00		100			12.00 D 12.45	1,2,3,5,6,6			
13.00		100							13.00

Client: DOHWA
Consultant: Metaferia Consulting
Contractor:
Sub Contractor: Gondwana Engineering Plc.
Logged by: Abda Berisso
Approved by: Zerihun Nuru

Note: D=Disturbed Sample
UD=Undisturbed Sample
RC=Rock Core Sample
HF= Highly Fractured

Site Photograph

Figure 14: Representative borehole log sheet

3.3 Apparent Earth Pressure Diagrams

The earth pressure distribution that develops on an anchored wall depends on the magnitude and distribution of lateral wall deformations. Some relatively flexible non-gravity cantilevered walls (e.g., sheet-pile or soldier beam and lagging walls which are not anchored) can be expected to undergo lateral deformations sufficiently large to induce active earth pressures for the entire wall height. These apparent earth pressure diagrams were developed based upon field measurements rather than theory. Measurements were made of the forces exerted on struts which were supporting a retaining wall as excavation proceeded. The forces in the struts were then divided by the area of wall which they supported to construct the apparent earth pressure diagram. In this study Coulomb's Earth Pressure theory is assumed and wall is assumed as frictional with $\delta=2\phi/3$, where δ is wall friction and ϕ is soil friction angle. Anchor loads are determined by tributary area methods from apparent earth pressure diagrams proposed by Peck (1969).

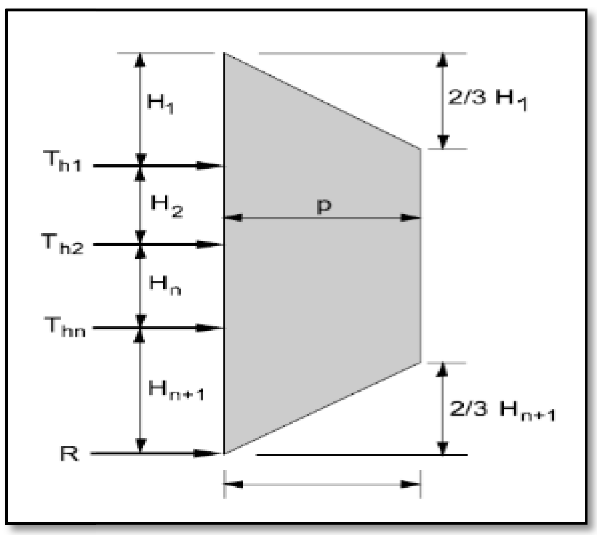

Figure 15: Recommended Earth Pressure Diagram for clay: Walls with multiple levels of

$$Pe = \frac{0.65\tan^2\left(45-\frac{\phi}{2}\right)\gamma H^2}{H-\frac{H1}{3}-\frac{Hn+1}{3}} \text{ --- (3.1)}$$

H_1= Distance from ground surface to upper most ground anchor.

H_{n+1}=Distance from base of excavation to lowermost ground anchor.

T_{hi}=Horizontal load in ground anchor i.

R=Reaction force to be resisted by sub grade (i.e., below base of excavation).

P=Maximum ordinate of diagram.

ɣ= unit weight of soil

H= depth of excavation

H_1= Distance from ground surface to upper most ground anchor.

The trapezoidal diagram is used for anchor load determination for the following reasons:

- ✓ Earth pressures are concentrated at the anchor locations resulting from arching.
- ✓ Earth pressure of zero at the ground surface is appropriate for sands (provided no surcharge loading is present).
- ✓ Earth pressures increase from the ground surface to the upper ground anchor location; and
- ✓ Medium dense to very dense sands, earth pressures reduce below the location of the lowest anchor owing to the passive resistance that is developed below the base of the excavation. (Aiza Malik 2015).

3.4 Lateral Earth Pressure

The lateral earth pressure is linearly proportional to depth and is taken as:

$$a = K\,\gamma_{s.}\,z \text{---} (3.2)$$

Where: σ = lateral earth pressure at a given depth, z.

K = coefficient of lateral earth pressure, to be taken as:

K_a, active, for walls that move or deflect sufficiently to reach the active conditions

K_p, passive, for walls that deflect or move sufficiently to reach a passive Condition, including integral abutments

γ_s = soil unit weight

z = depth

Active and passive earth pressures are the two stages of stress in soils which are of particular interest in the design or analysis of shoring systems. Active pressure is the condition in which the earth exerts a force on a retaining system and the members tend to move toward the excavation. Passive pressure is a condition in which the retaining system exerts a force on the soil. Since soils have a greater passive resistance, the earth pressures are not the same for active and passive conditions.

The resultant lateral earth load due to the weight of the backfill should be assumed to act at a height of H/3 above the base of the wall, where H is the total wall height, measured along a vertical plane extending from the ground surface above the back of the footing down to the bottom of the footing.

3.5 Earth Pressures due to Surface Load

Uniform surcharge loads are vertical loads applied at the ground surface which are assumed to result in uniform increase in lateral stress over the entire height of the wall. The increase in lateral stress for uniform surcharge loading can be written as

$\Delta\sigma_h = Kq_s$--(3.3)

Where:

$\Delta\sigma_h$ =the increase in lateral earth pressure due to the vertical surcharge load (KPa)

q_s =the vertical surcharge stress applied at the ground surface (KPa)

K =an appropriate earth pressure coefficient.

3.6 Calculation of Ground Anchor Loads from Apparent Earth Pressure Diagrams

Ground anchor loads for flexible anchored wall applications can be estimated from apparent earth pressure envelopes. Methods commonly used include the tributary area method and the hinge method. Both methods, when used with appropriate apparent earth pressure diagrams, provide reasonable estimates of ground anchor loads and wall bending moments for anchored systems constructed in competent soils. Tributary area method is used for ground anchor load calculation.

$$\left.\begin{aligned} T1 &= \text{Load over length } H1+ H2/2 \\ T2 &= \text{Load over length } H2/2 + Hn/2 \\ Tn &= \text{Load over length } Hn/2 + Hn+1/2 \\ R &= \text{Load over length } Hn+1/2 \end{aligned}\right\} \text{-------------------------- (3.4)}$$

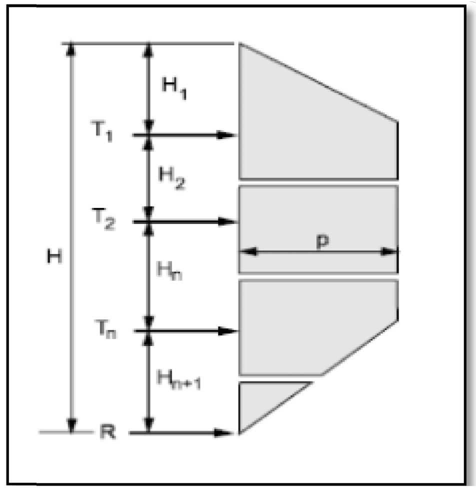

Figure 16: Calculation of Anchor Loads for Multi - Level anchored Wall

3.7 Soil, shoring Pile and Anchor Parameters for base model

Previously reviewed papers show that soil type is a key factor in performance of deep excavations. Soil type is important because the performance of deep excavations is governed by the interaction between the soil and the support system. SPT, N, number gives an idea about the consistency of the soil and the soil may be classified as stiff clay (See the table below).

Table 2: Consistency of clays and approximate correlation to the standard penetration number, N (Das, 1984)

Standard penetration number, N	Consistency	Unconfined compression strength, q_u(kN/m^2)
0-2	Very soft	0-25
2-5	Soft	25-50
5-10	Medium stiff	50-100
10-20	Stiff	100-200
20-30	Very stiff	200-400
>30	Hard	>400

The following soil parameters are used as input for base model generation during analysis of 7, 9, 11 and 13m excavation depth.

Table 3: Soil parameters for base model

depth(m	SPT N30 (uncorrected)	Consistency	Dr	γ bulk (KN/m3)	N30 (coorected)	ϕ(deg)	Cu (Kpa)
1.5							
2.85	12	Stiff	0.38	17.7	19.76107	30.4	152.1942
2.85							
4.5	10	Stiff	0.35	16.4	15.32262	32.6	129.6053
4.5							
6.45	18	Stiff	0.47	17.4	21.18248	31.6	163.0049
6.45							
9	19	Stiff	0.485	17.4	15.56162	31.8	129.6053
9							
10.5	10	Stiff	0.85	17.4	6.181274	30	63.96248
10.5							
12	14	Stiff	0.85	17.4	6.119149	30.8	64.96248
12							
13	20	Stiff	0.55	17.4	6.191635	32	65.96248

Table 4: Pile parameters for base model

		Depth of excavation				
PLATES	Wall parameters	Units	7m	9m	11m	13m
	Wall type		SP	SP	SP	SP
	Material type	Elastic	Elastic	Elastic	Elastic	Elastic
	Adopted pile diameter	m	0.4m	0.4m	0.4m	0.4m
	Equivalent wall thickness, D	m	0.126m	0.126m	0.126m	0.126m
	Normal stiffness, EA,	kN/m	0.653*10^9	0.653*10^9	0.653*10^9	0.653*10^9
	Flexural Rigidity, EI,	kNm	27.5*10^6	27.5*10^6	27.5*10^6	27.5*10^6
	Weight, w	KN/m	6.27	6.27	6.27	6.27
	Poisson's ratio		0.32	0.32	0.32	0.32
	Pile spacing		100mm	100mm	100mm	100mm

Notes: SP – shoring pile

EA and EI are per unit length of the pile

EA = Et, t = equivalent thickness of the pile

$EI = Et^3/12$

Anchor load calculation (sample calculation for H=7m)

The tributary area method is used to calculate the horizontal anchor loads, T1, T2, T3and the reaction force to be resisted by the sub grade, Rc.

The horizontal anchor loads were calculated using the tributary area method, as follows

$T_1=\left(\frac{2H1}{3}+\frac{H2}{2}\right)Pe+\left(H1+\frac{H}{2}\right)Ps$ = 167.09kN/m------------------------------ (3.5)

$T_2=\left(\frac{H2}{2}+\frac{H3}{2}\right)Pe+\left(\frac{H2}{2}+\frac{H3}{2}\right)Ps$ = 131.68kN/m------------------------------- (3.6)

$T_3=\left(\frac{H3}{2}+\frac{23H4}{48}\right)Pe+\left(\frac{H3}{2}+\frac{H4}{2}\right)Ps$ = 78.46kN/m------------------------------ (3.7)

$Rc=\left(\frac{3H4}{16}\right)Pe+\left(\frac{H4}{2}\right)Ps$ = 18.24kN/m--- (3.8)

Anchor design load

The inclination of all anchors is assumed to be 15º and center-to-center spacing is taken as 3 m.

1. Upper anchor: The anchor design load (DL) was calculated as follows:

$DL_1=T1*\frac{Lc}{cos\Theta}$ = 345.95 kN-- (3.9)

2. middle anchor: The anchor design load (DL) was calculated as follows

$DL_2=T2*\frac{Lc}{cos\Theta}$ = 340.78 kN--- (3.10)

2. Lower anchor: The anchor design load (DL) was calculated as follows

$DL_3=T3*\frac{Lc}{cos\Theta}$ = 203.07 kN--- (3.11)

The maximum calculated anchor design load is 345.95 kN.

Tendon selection

A 64-mm diameter, Grade 150 prestressing bar may be selected, based on an allowable tensile capacity of 60 percent of the specified minimum tensile strength (SMTS) with allowable tensile capacity that exceeds the calculated maximum design load. (From Properties of prestressing steel bars, ASTM A722.).

Table 5: Anchor parameters for the base model

Anchor parameters	Depth of excavation	7m	9m	11m	13m
	Type	Elastic	Elastic	Elastic	Elastic
	EA, kN/m	1*10^5	1*10^5	1*10^5	1*10^5
	Prestressed load Kn	150	150	150	150
	No of Anchors	3	3	4	5
	Anchor spacing	Anchor1=3m Anchor2=2m Anchor3=1m	Anchor1=3m Anchor2=3m Anchor3=1m	Anchor1=3m Anchor2=3m Anchor3=2m Anchor4=1	Anchor 1=3m Anchor 2= 3m Anchor3=2m Anchor4=3m Anchor 5=1m

Table 6: Excavation and embedment depth parameters for the base model

Parameters	Unit	D_{ex1}	D_{ex2}	D_{ex3}	D_{ex}
Depth of excavation	M	7	9	11	13
Depth of embedment	M	5m	7m	9m	11m

PART IV

4. ANALYSIS AND PARAMETRIC STUDY

4.1 Introduction

The purpose of parametric study is to investigate which parameters that affect the design of a shoring pile wall used for staged excavation. There are a number of parameters to be considered if one is interested in conducting a comprehensive parametric study, some of the variables have little or no effect in the performance of deep excavation supported by shoring wall. In this paper, variables that have practical importance and reported to have significant influence in the performance of deep excavations were considered. To do this, a generalized mohr- coulomb model is used for simulation in PLAXIS 2D, the soil/structure model.

The problem is modeled with a geometry model of 100 m width and 13 m depth. Parametric study is conducted for excavation depth of 7,9,11 and 13m. In this study the ground anchor is modeled by a combination of a node-to-node anchor and a geotextile. The geotextile simulates the grout body whereas the node-to-node anchor simulates the anchor rod. In reality, there is a complex three-dimensional state of stress around the grout body. Although the precise stress state and interaction with the soil cannot be modeled with this 2D model, it is possible in this way to estimate the stress distribution, the deformations and the stability of the structure on a global level, assuming that the grout body does not slip relative to the soil. With this model it is certainly not possible to evaluate the pull-out force of the ground anchor. The pile wall is modeled as a beam. The interfaces around the beam are used to model soil-structure interaction effects. Interfaces should not be used around the geotextile that represent the grout body. The excavation is constructed in several excavation stages. The separation between the stages is modeled by geometry lines.

Based on scientific verifications and investigations Mohr coulomb model gives precise prediction of ground deformation for the selected deep excavation support system in the chosen area (For details, see Appendix 1). Since the performance of deep excavation support system and lateral wall, movements are influenced by several factors including wall installation, soil conditions, support system stiffness, and methods of support system installation and interaction between the soil and the support, parameters has to be identified accordingly. Finite element software PLAXIS V8.1 2D is used for analysis. Since the support system contains wall and pile, analysis is done for the less thick wall, which governs the design, and the analysis results are presented.

4.2 Base Model generation

In the Model mode, the geometry is built. Soil layer boundaries and material properties are set. Construction element, such as walls and beams are placed in the model and interface properties are defined. In the simulations, soil elements were modeled with 15-node wedge elements that are generated from the projection of two-dimensional 6-node triangular elements between work planes with a width of 100 meters and depth of 30 meters. A surface load of 95 kN/m^2, 120kN/m^2 and 150kN/m^2 are used during analysis. For this purpose, modeling of wall and pile, building and the soil is made using medium mesh size. Horizontal displacement is computed at the most vulnerable location. Excavations in silty clay soils with depth of 7m, 9m, 11m and 13m were considered in this study. Typical base model geometry and general dimensions for the study is shown in Figure 17.

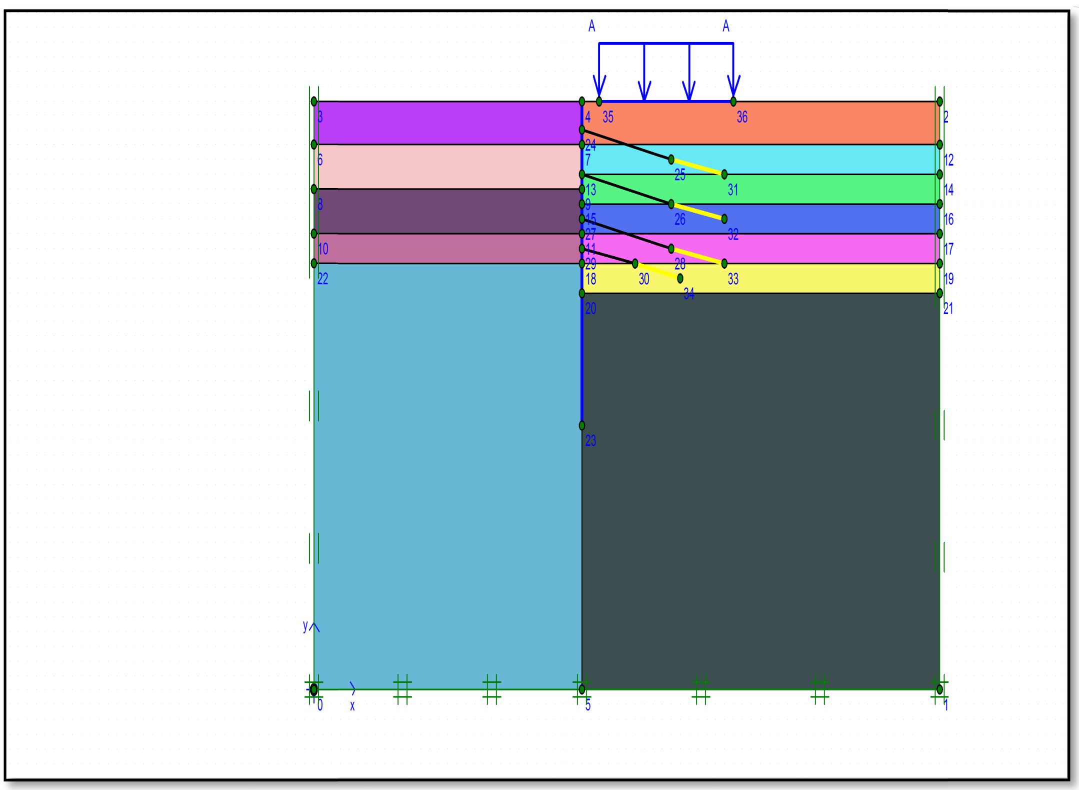

Figure 17: Finite element model used in plaxis for deep excavation

Finally, the mesh is generated and refined to a proper level. The choice of soil model is very important, and Note that the mesh is very fine in and around the excavation and along the shoring pile wall. This is because this is the area where most displacements are expected. It is important to know that a very fine mesh will give more deformations. This is why it is important to have a very fine mesh in the excavation, where the deflection of the shoring pile wall has its Maximum.

4.3 Parametric study and discussion

In this section, the details of the effects of surcharge location, increase in surcharge, change in pile diameter and change in embedment depth in horizontal displacement of the pile $\delta hmax_p$, ground settlement behind the pile $\delta vmax_p$ and bending moment of pile $Mmax_p$ are presented and discussed for excavation depth of 7m, 9m, 11m and 13m including their construction stages.

The typical phases in staged construction which are assumed to be carried out by intervals of shown below

Typical phases in staged construction for 7m excavation

Initial Phase

Phase 1: Installation of pile wall

Phase 2: Excavation to first level RL-3.00m

Phase 3: Installation of anchor at RL-1.00m

Phase 4: Excavation to second level RL-6.00m

Phase 5: Installation of anchor at RL-4.00m

Phase 6: Excavation to final level RL-7.00m

Phase 7: Installation of anchor at RL-6.00m

4.3.1 Effect of Change in magnitude of surcharge

In this part of the analysis, the study concentrates on how change in magnitude of surcharge affects the performance of deep excavations supported by shoring pile wall for each of 7m, 9m, 11m and 13m depth of excavation. The output of this analysis is presented for each soil for varying surcharge load increased from 95kN/m^2 to 150kN/m^2, 300kN/m^2 and 400kN/m^2 placed on at a distance of 1.5m from edge of excavation and the horizontal displacement ratio, settlement ratio and bending moment ratio results behind the pile wall are presented and discussed. For analysis, the soil, pile and anchor parameters listed from table to table are used.

4.3.1.1 Vertical Displacement

The vertical displacement ratio occurred in the pile for excavation depth of 7m, 9m, 11m and 13m are presented in the figure below.

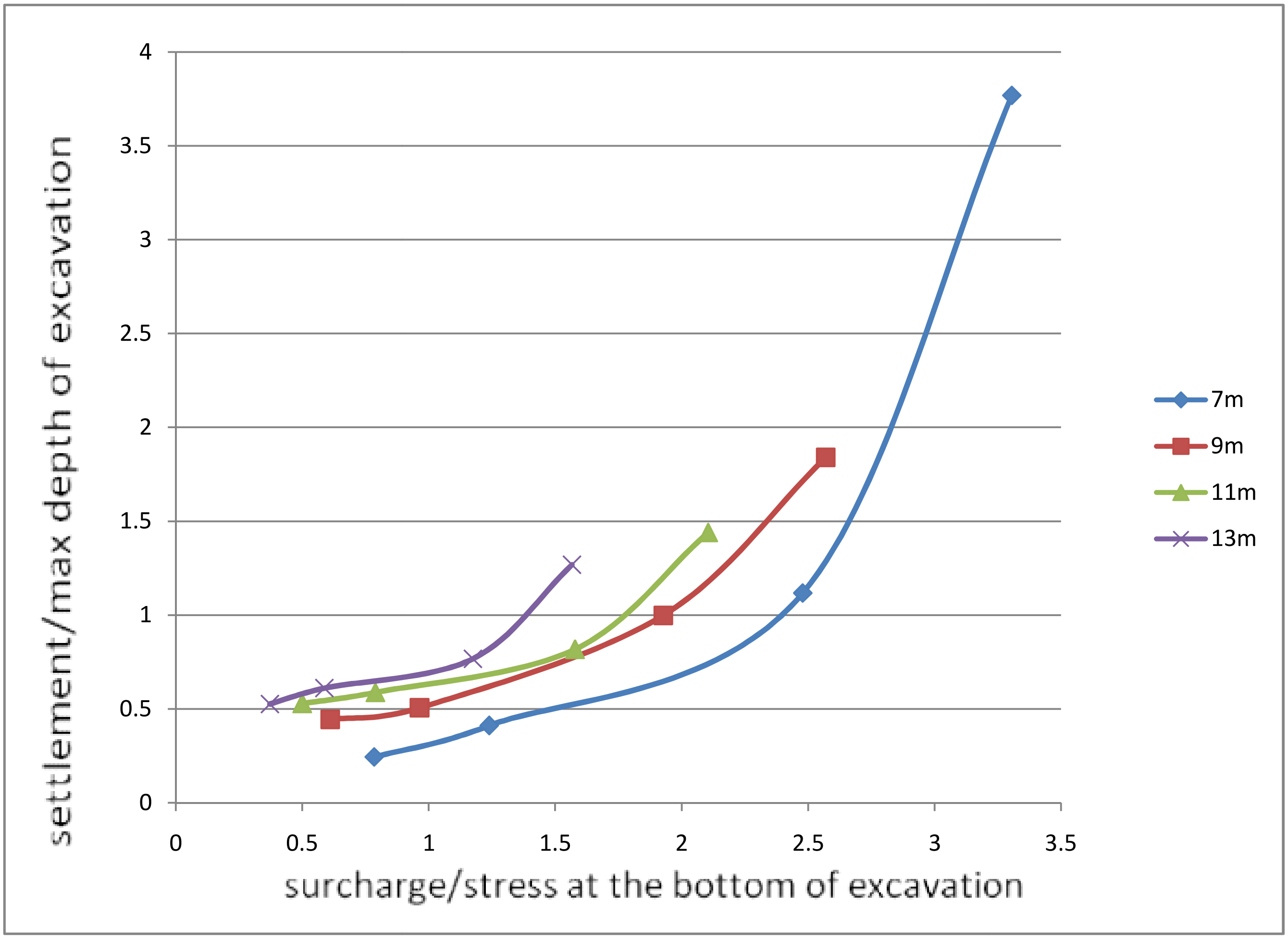

Figure 18: Vertical displacement ratio behind shoring pile wall

The above figure shows the ratio of surcharge to stress at the bottom of excavation increases rapidly as the ratio of settlement to maximum depth of excavation increase. The settlement ratio for excavation depth of 7m is greater than all because it has more effect than the other depth of excavation.

4.3.1.2 Horizontal Displacement

The horizontal displacement ratio occurred in the pile for excavation depth of 7m, 9m, 11m and 13m are presented in the figure below.

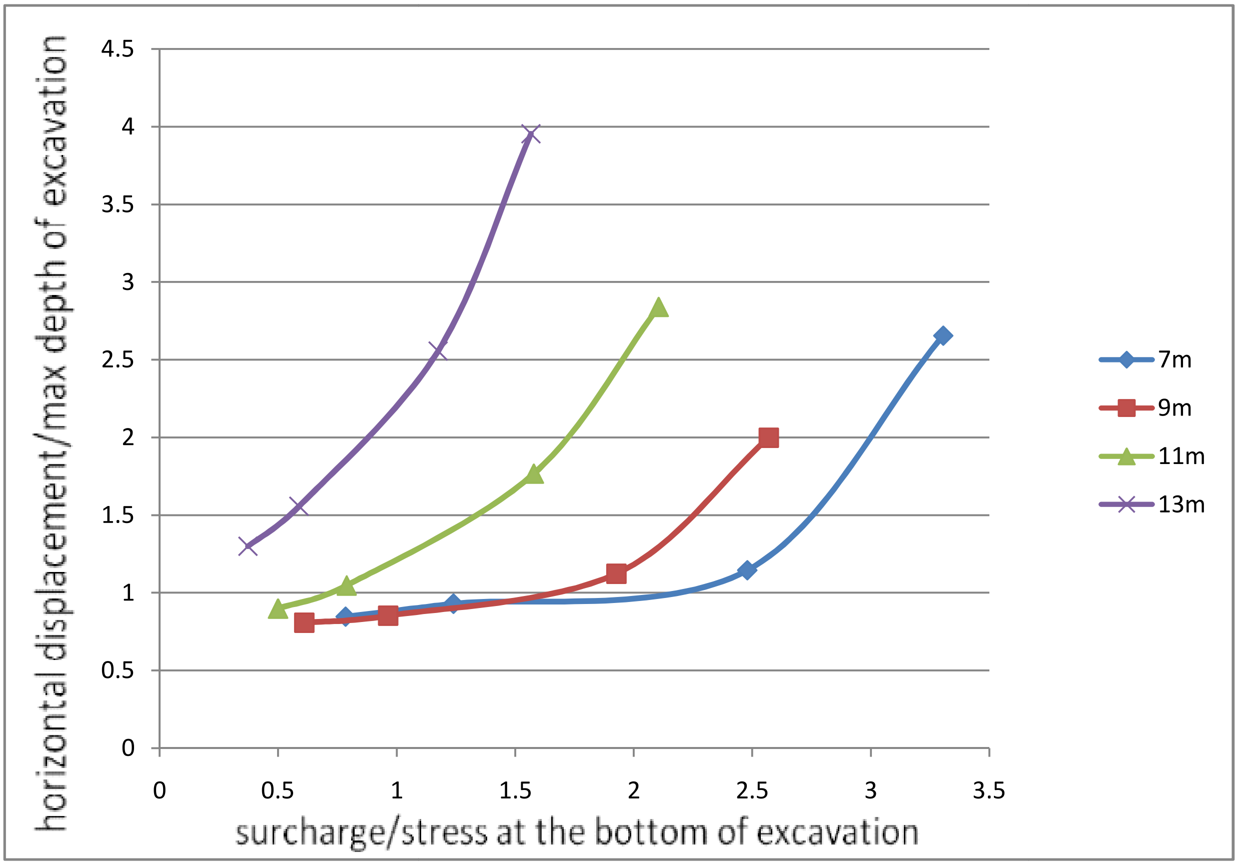

Figure 19: Horizontal displacement ratio behind shoring wall

From the figure above as the ratio of surcharge to stress at the bottom of excavation increases, the ratio of horizontal displacement depth of excavation increase.

4.3.1.3 Bending moment

This section deals with the bending moments occurred in the pile for excavation depth of 7m, 9m, 11m and 13m

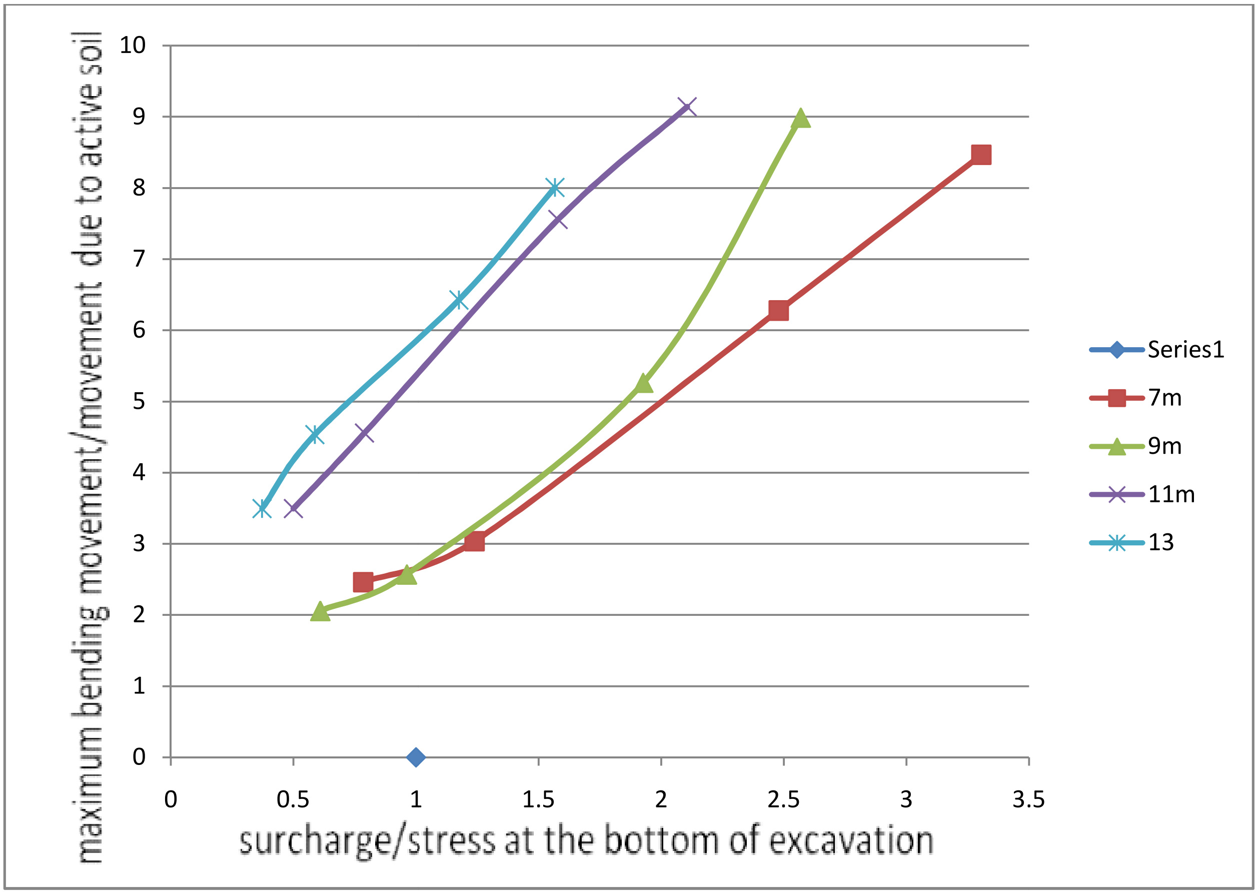

Figure 20: Bending movement behind shoring wall

The figure above demonstrated that an increased in the ratio of surcharge to stress at the bottom of excavation resulted in an increased bending moment due to active soil mass ratio behind the pile wall.

From the above findings, it can be inferred that the change in magnitude of surcharge from 95kN/m^2 to 150kN/m^2, 300kN/m^2 and 400kN/m^2 resulted in an increased in vertical settlement, horizontal settlement and bending movement. Similar results reported in Hatiya (2016) study on the analysis of secant pile wall as deep excavation support system on silty sand soil. However, this finding was not reported on Gebru (2016) study. Gebru (2016) performed a study on the analysis of Contiguous Pile wall as deep excavation support system in Adam Town. The study found out that the ratio of settlement to maximum depth of excavation remains the same despite an increase in the ratio of surcharge to stress due to soil increases. Although the three studies focused on excavation support system, Gebru's study produced different results. This could be due to the fact that a maximum of 150kN/m^2 surcharge used in Gebru's study. On the current study a maximum of 400kN/m^2 surcharge used. In addition, as it was demonstrated on the graph vertical settlement, horizontal settlement and bending movement significantly increased when the amount of surcharge were 150kN/m^2 and above.

4.3.2 Effect of Change in location of surcharge

Change in location of surcharge is one of a key factor influencing performance of deep excavation, this section will concentrate on a surcharge of 300kN/m^2 is placed at a distance of 1.5m, 10m , 15m and 20m the horizontal displacement ratio, settlement ratio and bending moment ratio results behind the pile wall are presented and discussed. For analysis the soil, pile and anchor parameters listed from table to table are used.

4.3.2.1 Vertical Displacement

The vertical displacement ratio occurred in the pile for excavation depth of 7m, 9m, 11m and 13m are presented in the figure below.

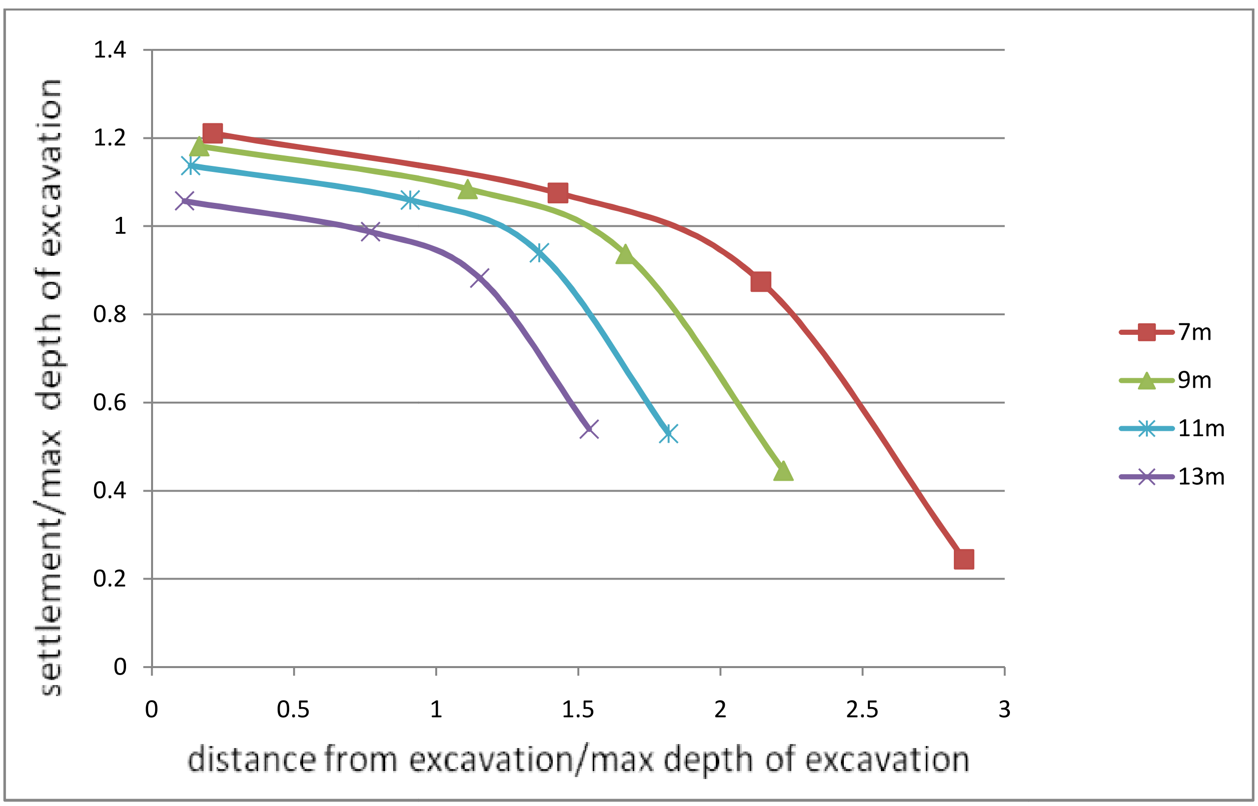

Figure 21: Vertical displacement ratio behind shoring wall

The ratio of settlement to maximum depth of excavation decreases as the ratio of distance from excavation to maximum depth of excavation increases for all excavation depths. The settlement ratio for excavation depth of 7m is greater than all.

4.3.2.2 Horizontal Displacement

The horizontal displacement ratio occurred in the pile for excavation depth of 7m, 9m, 11m and 13m are presented in the figure below.

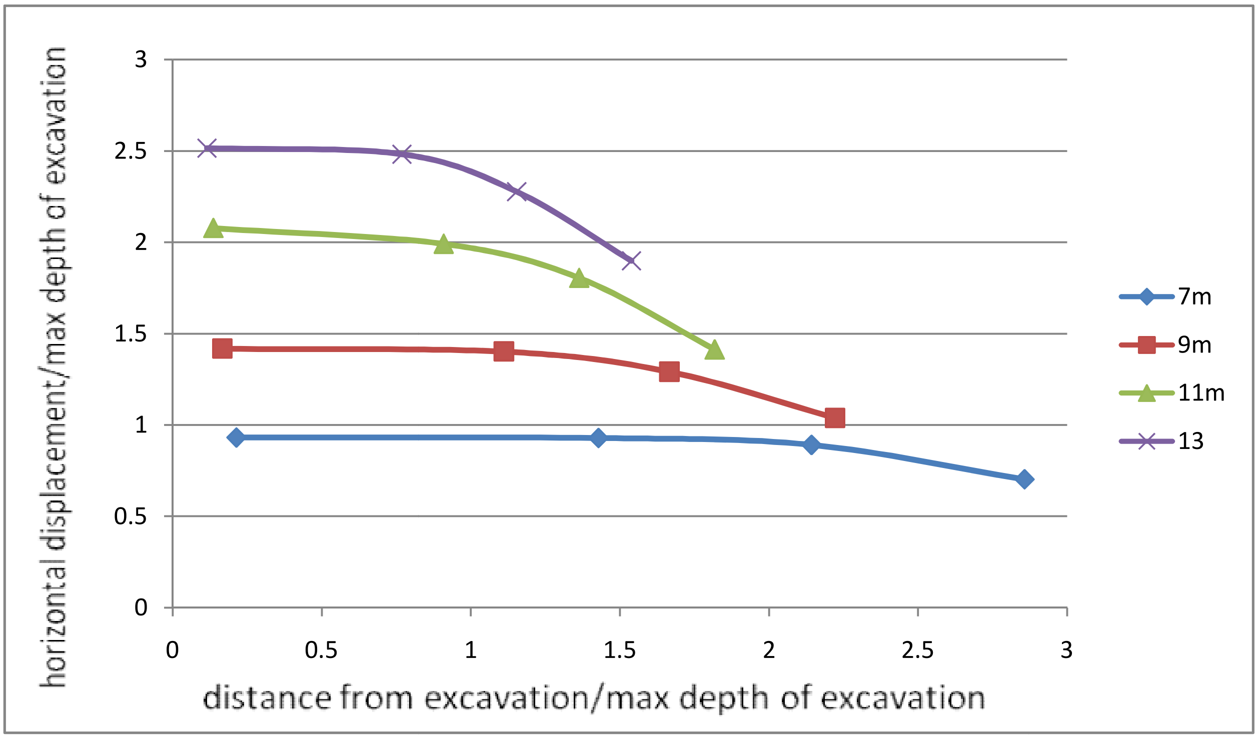

Figure 22: Horizontal displacements behind shoring wall

The ratio of horizontal displacement to maximum depth of excavation decrease as the depth of excavation increases. But the ratio of distance from excavation to maximum depth of excavation increase.

4.3.2.3 Bending moment

This section deals with the bending moments occurred in the pile for excavation depth of 7m, 9m, 11m and 13m.

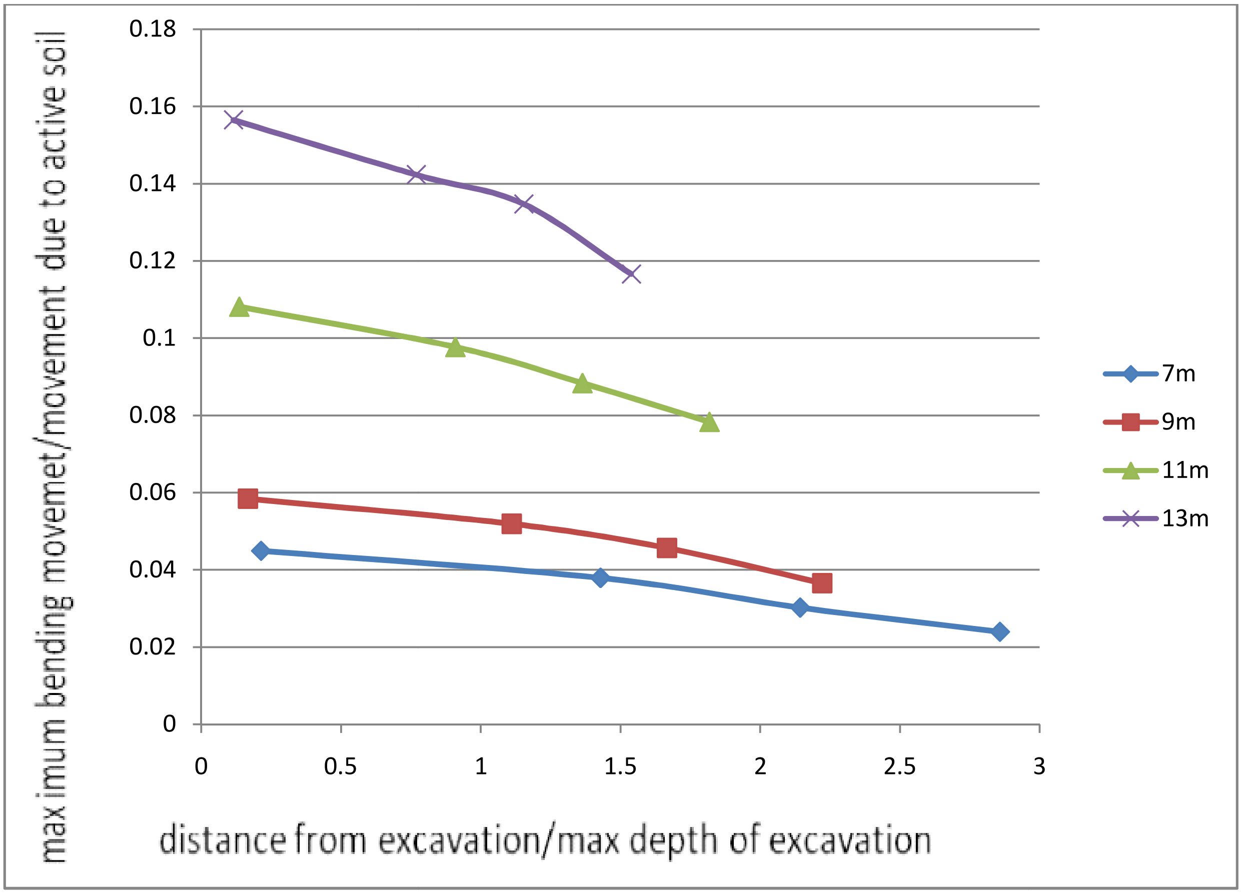

Figure 23: Bending movement behind shoring wall

The above figure shows that the maximum bending moment to active soil moment ratio has decreasing pattern as the ratio of distance from excavation to maximum depth of excavation has increasing pattern.

From the above findings it can be inferred that the change in location of surcharge from the face of excavation placed at 1.5m, 10m , 15m and 20m distance resulted in a decreased in vertical settlement , horizontal settlement and bending movement. The vertical displacement, horizontal displacement and bending movement decreased by 29,49% ,41.16% and 2.82% constrictively when location of surcharge was placed at 1.5m to 20m away from the face of excavation. Similar results reported in Hatiya (2016) study on the analysis of secant pile wall as deep excavation support system on silty sand soil.

4.3.3 Effect of Change in pile diameter

In this section, the pile diameter is increased from 40cm to 60cm and 80cm and its effect on the horizontal displacement ratio; settlement ratio and bending moment ratio results behind the pile wall are presented and discussed. For analysis surcharge is kept constant and placed 1.5m away from edge of excavation. The soil and anchor parameters listed from table to table are used.

4.3.3.1 Vertical Displacement

The settlement ratio occurred in the pile for excavation depth of 7m, 9m, 11m and 13m when the pile diameter ratio changes are presented in the figure below.

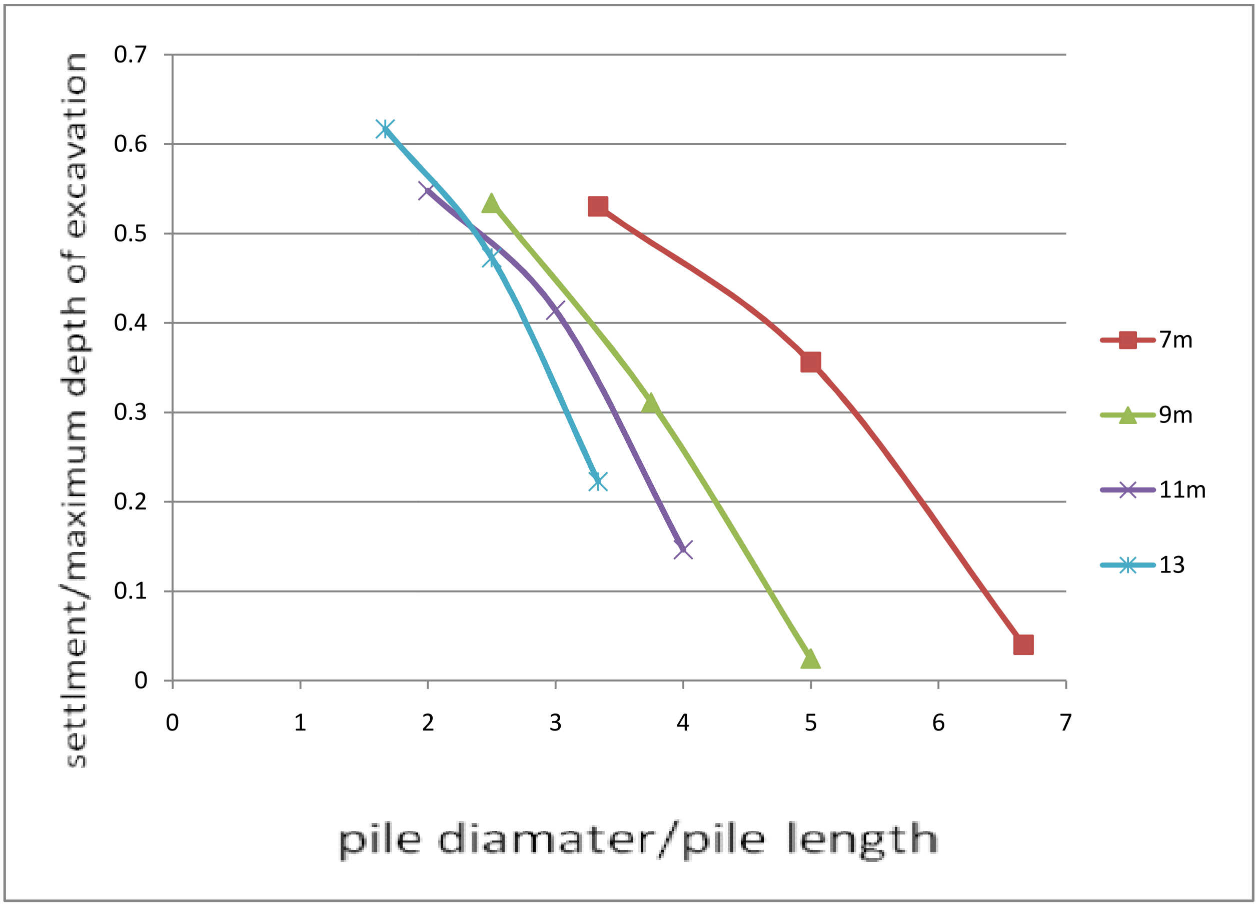

Figure 24: Vertical displacement behind shoring wall

The above figure demonstrated that as pile diameter to pile length increases the settlement to maximum depth of excavation ratio has a decreasing pattern.

4.3.3.2 Horizontal Displacement

The horizontal displacement ratio occurred in the pile for excavation depth of 7m, 9m, 11m and 13m when the pile diameter ratio changes are presented in the figure below.

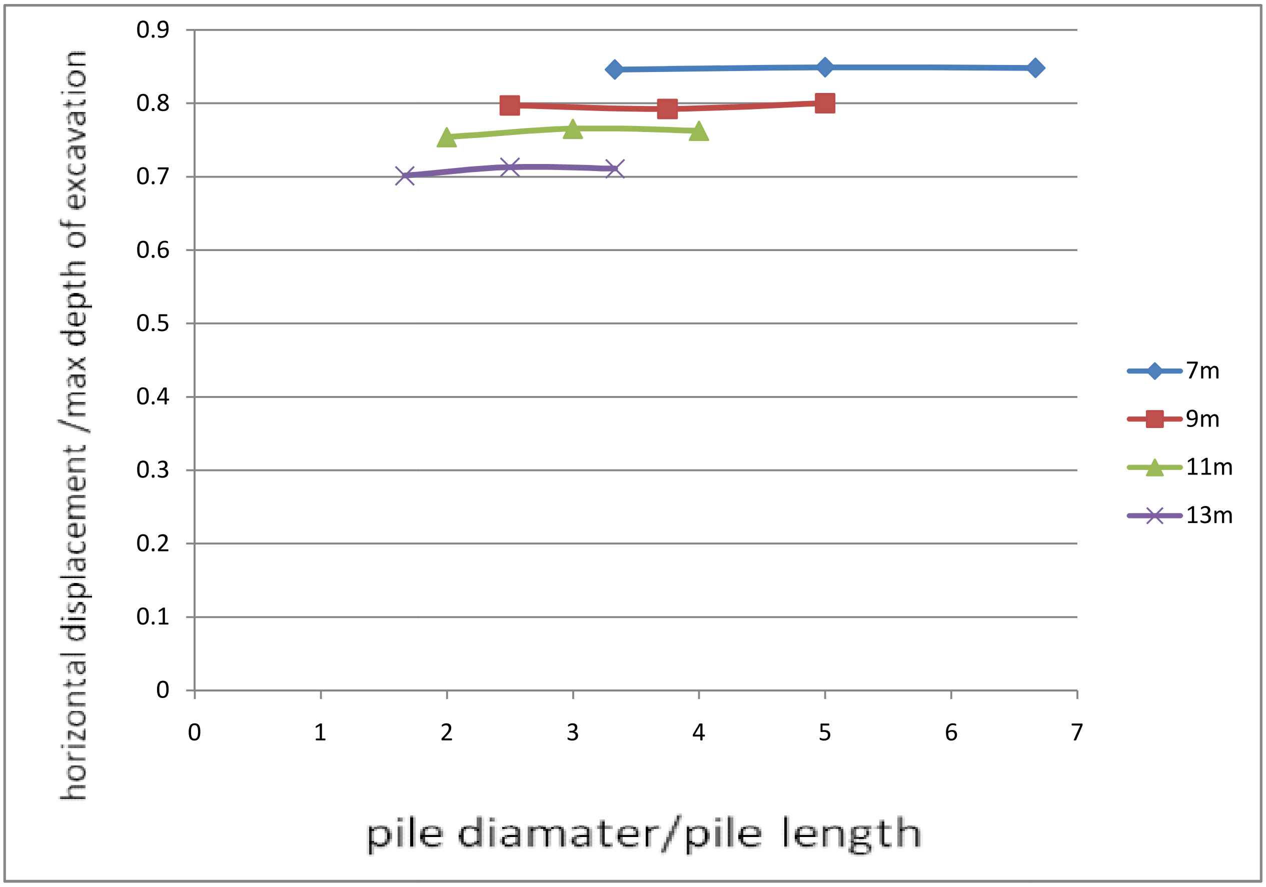

Figure 25: Horizontal displacement behind shoring wall

The above figure highlighted that the ratio of horizontal displacement to maximum depth of excavation has an increasing pattern when the ratio of pile diameter to pile length increases.

4.3.3.3 Bending moment

This section deals with the bending moments occurred in the pile for excavation depth of 7m, 9m, 11m and 13m and the results are presented in the figure below. The ratio of maximum bending moment to moment due to active soil mass has an increasing pattern while the ratio of pile diameter to pile length increases.

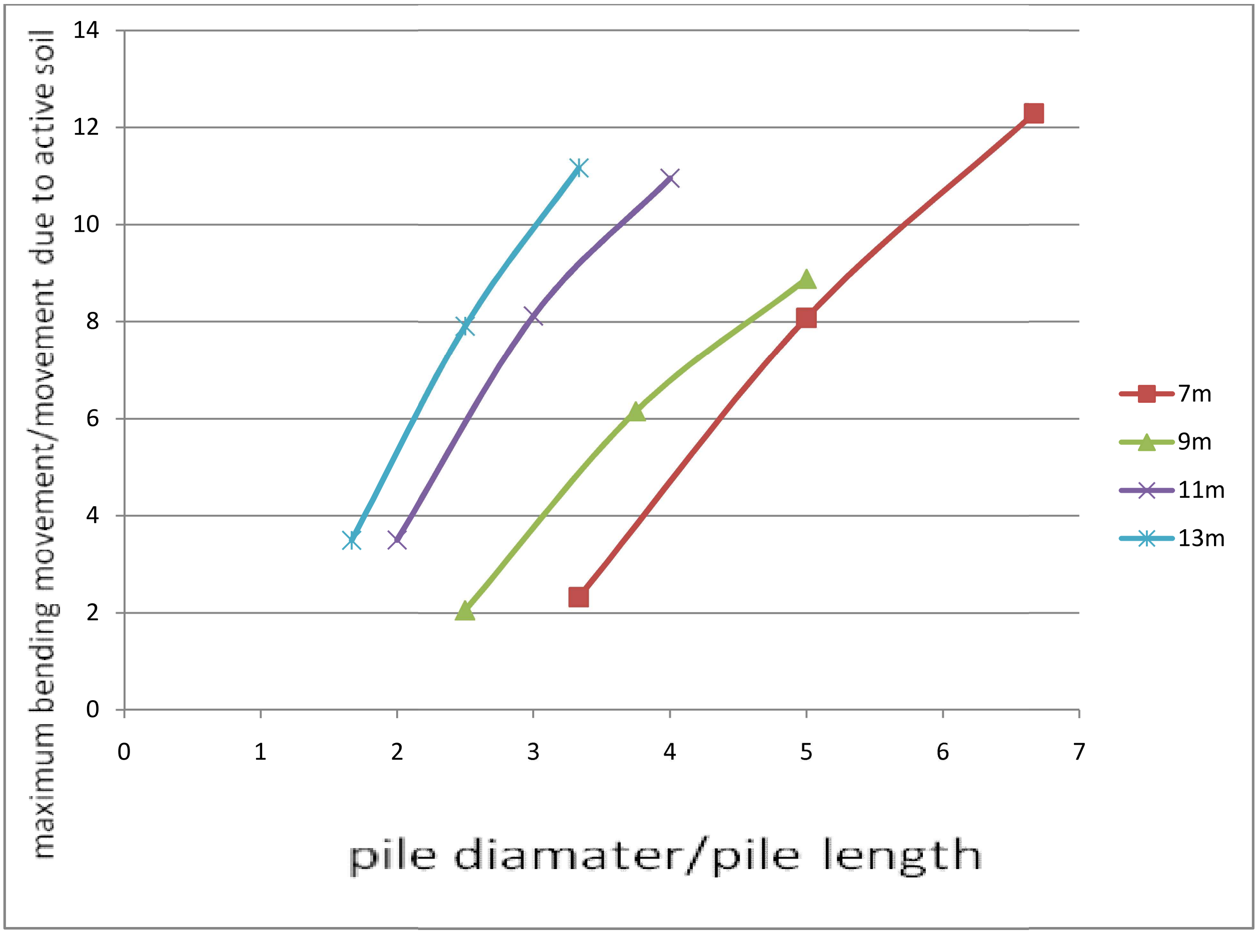

Figure 26: Bending movement behind shoring wall

According to the above findings it can be inferred that the change in pile diameter from 40cm to 60cm and 80cm resulted in a decreased in vertical settlement by 11.92% however horizontal settlement and bending movement has an increasing pattern. Horizontal displacement and bending movement have increased by 2.58% and 16.80% consecutively. Similarly, Gebru's (2016) study on the analysis of Contiguous Pile wall as deep excavation support system in Adam Town reported that the change in pile diameter from 45cm to 60 and 75 cm resulted in a decreased in vertical settlement by 4.47% but horizontal displacement and bending movement have increased by 1.38% and 3.04%. Although both studies demonstrated somehow similar pattern, the percentage of the displacement on the current study seems larger than Gebru's study. This could be due to several reasons such as wall type, different pill diameters and parameters being used.

4.3.4 Effect of Change in Wall Embedment Depth

In this section, the effect of change in wall embedment depth on the performance of deep excavation supported by shoring pile wall will be studied into two cases. One is wall embedment is increased by 30% and 40%, for 7m,9m,11m and 13m depth of deep excavation. The output from this analysis is given below.

4.3.4.1 Vertical Displacement

The settlement ratio occurred in the pile for excavation depth of 7m, 9m, 11m and 13m when the pile diameter ratio changes are presented in the figure below.

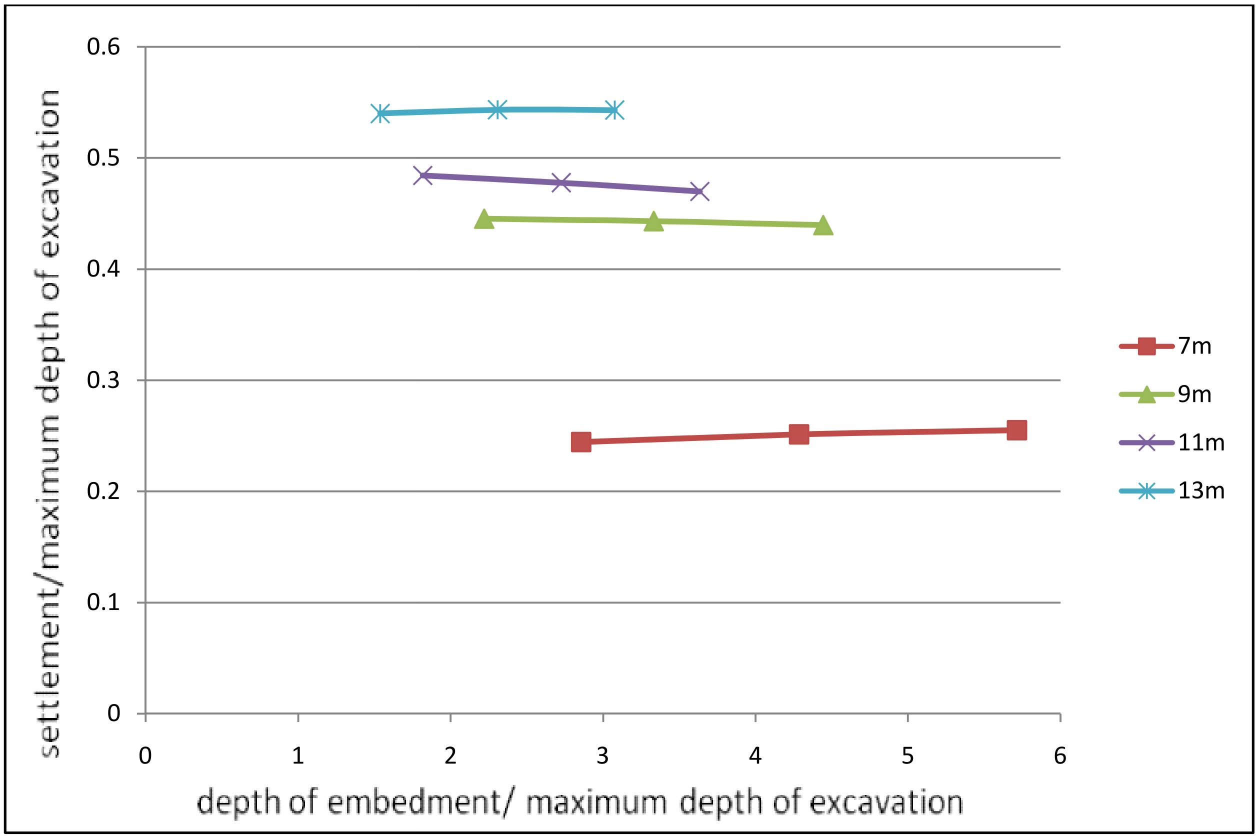

Figure 27: Vertical displacement behind shoring wall

It's observed that, the ratio of settlement to maximum depth of excavation slightly decrease as the ratio of depth of embedment to maximum depth of excavation increases.

4.3.4.2 Horizontal Displacement

The horizontal displacement ratio occurred in the pile for excavation depth of 7m, 9m, 11m and 13m, when the pile diameter ratio changes are presented in the figure below. The horizontal displacement to maximum depth of excavation ratio has slightly decreasing pattern when the depth of embedment to maximum depth of excavation increased.

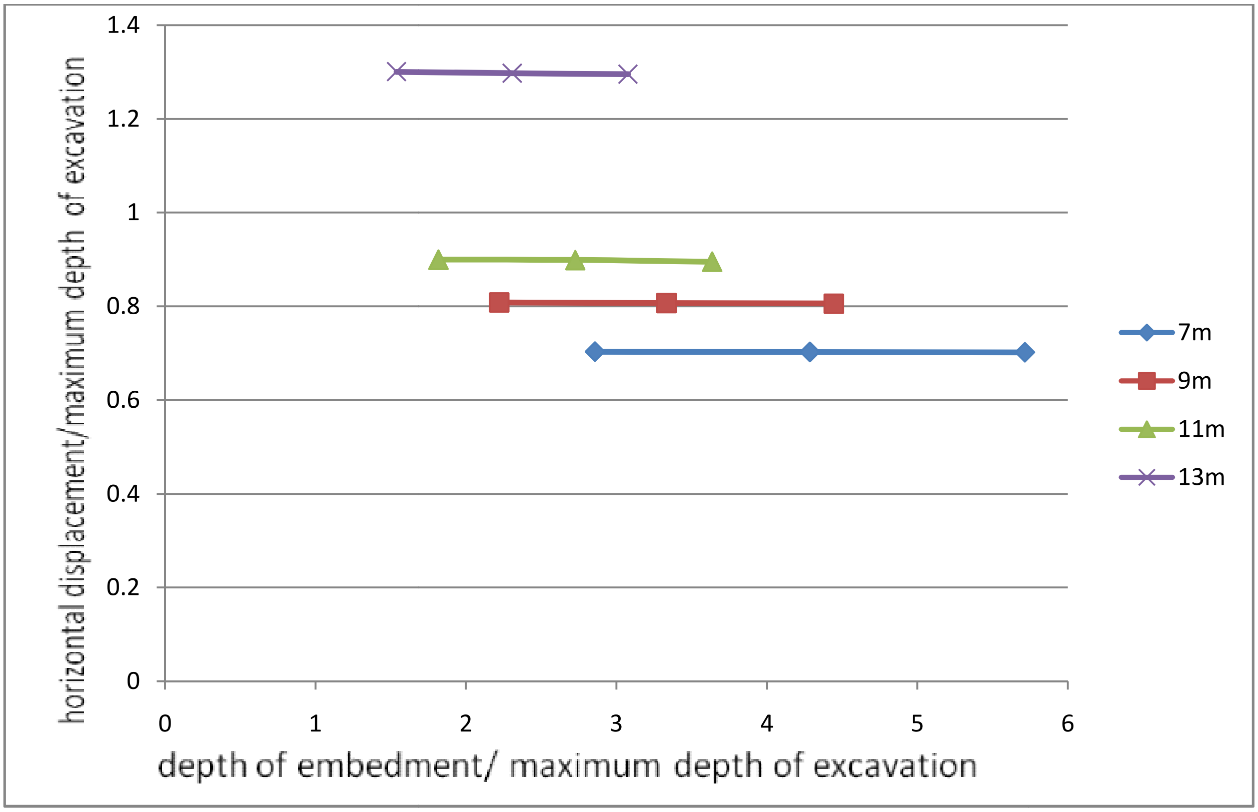

Figure 28: Horizontal displacement behind shoring wall

4.3.4.3 Bending moment

This section deals with the bending moments occurred in the pile for excavation depth of 7m, 9m, 11m and 13m and the results are presented in the figure below.

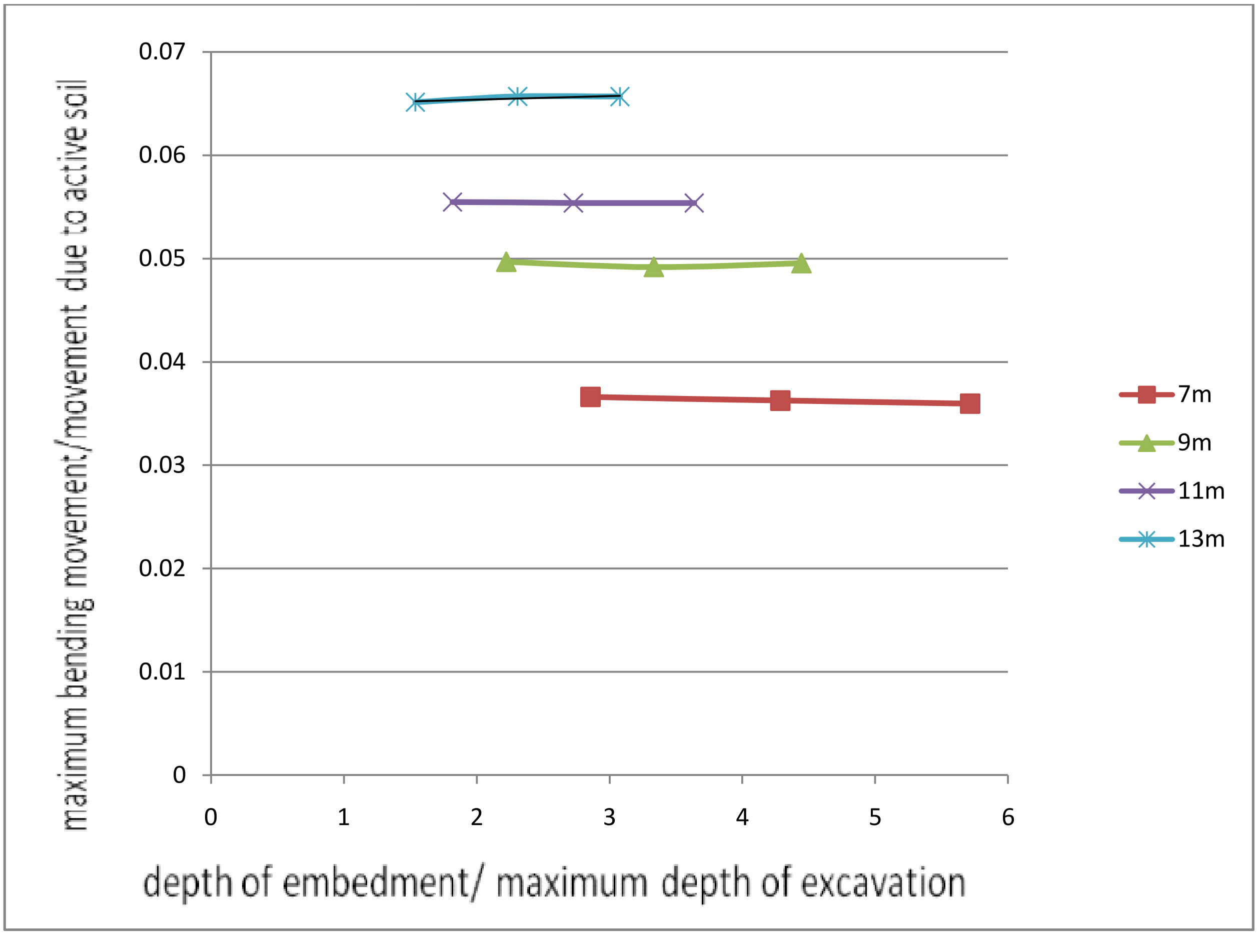

Figure 29: Bending movement behind shoring wall

It's observed that while the ratio of depth of embedment to maximum depth of excavation has increasing pattern, the ratio of maximum bending movement to movement due to active soil slightly decreased.

According to the above findings it can be inferred that the change in embedment depth from 20% to 30% and 40% resulted in a decreased in vertical settlement, horizontal settlement and bending movement. Vertical settlement, horizontal displacement and bending movement have been decreased by 5.93%, 1.08% and 0.58% consecutively.

PART V

5. CONCLUSION AND RECOMMENDATIONS

5.1 Conclusion

The previous chapters have investigated that which parameters affect deep excavations and the influence of various key aspects through parametric studies on a simplified excavation and analysis. In this section conclusions and recommendations drawn from this study are given below.

The ground deformations around a deep excavation are significantly influenced by soil parameters. Therefore obtaining accurate estimation of soil parameters is important in order to get accurate estimation of ground deformation. The performance of shoring pile walls is affected by the magnitude and location of surcharge, change in pile diameter and change in embedment depth.

- Change in magnitude of surcharge as depth of excavation increased
  - vertical deformations increased by 84.67 %
  - Horizontal deformations increased by 50.49%.
  - Maximum bending moment increased by 22.47%.
- Change in location of surcharge as depth of excavation increased
  - vertical deformations increased by 29.49 %
  - Horizontal deformations increased by 41.16%.
  - Maximum bending moment increased by 2.82%.
- Change in pile diameter as depth of excavation increased
  - vertical deformations increased by 11.92%
  - Horizontal deformations increased by 2.58%.
  - Maximum bending moment increased by 16.8%.
- Change in wall embedment depth as depth of excavation increased
  - vertical deformations increased by 5.93%
  - Horizontal deformations increased by 1.08%.
  - Maximum bending moment increased by 0.58%.

- Applying anchor significantly reduces ground deformation around deep excavation, however decreasing strut spacing beyond some limit do not reduce ground deformation appreciably.

5.2 Recommendations for future work

Deep excavation analysis requires a number of parameters and different parameters have been addressed in this study, based on that various conclusions are drawn and listed above. Nevertheless there are still some unsolved problems worth further investigations on this matter; hence some of the matters on this issue are identified and listed below for students and professionals in the field to carry on the study, by doing so the study will be a first hand document for decision makers including engineers, consultants and contractors to solve the

- Due to the short coming of the PLAIXS 2D, on handling the corner effects of the excavation on deformation and bending moment, It is advisable to use PLAXIS 3D for further analysis.
- In addition, results from plaxis with Mohr coulomb model could be compared with different constitutive model results, like hardening soil model or softening model. By doing so, it is quite possible to get a better image of the analysis result for the problem.

Appendixes

Appendix A. Constitutive Soil Model

A.1 Mohr-Coulomb Model

The Mohr-Coulomb model coded in Plaxis version 8.1 is based on ideal elasto-plastic constitutive law with a fixed yield surface that does not affected by plastic straining and stress state represented by point fall on the yield surface are perfectly elastic. There is no hardening or softening law required for the Mohr-Coulomb model as it is assumed to be perfectly plastic.

Mohr-Coulomb model is a simple and applicable to three-dimensional stress space model (Refer Fig A.1.1) with only two strength parameters to describe the plastic behavior. Regarding its strength behavior, this model performs better. This model is applicable to analyze the stability of dams, slopes, embankments and shallow foundations. Although failure behavior is generally well captured in drained conditions, the effective stress path that is followed in undrained materials may deviate significantly from observations. It is preferable to use undrained shear parameters in an undrained analysis, with friction angle set equal to zero. The stiffness (hence also deformation) behavior before reaching the local shear is poorly modeled. For perfect plasticity, model does not include strain hardening or softening effect of the soil.

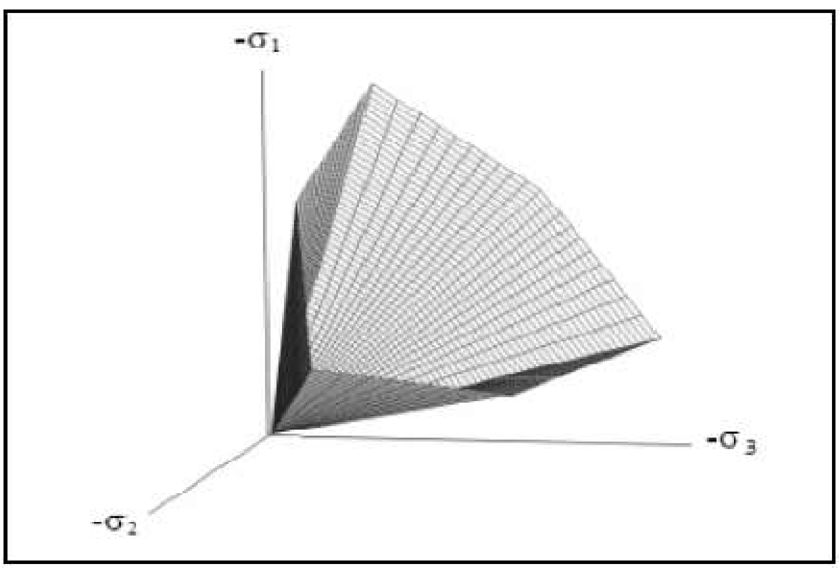

Figure 30: The Mohr-Coulomb yield surface in principal stress space (c = 0)

The Mohr-Coulomb model requires five parameters. Parameters related to elastic behavior are E and ν, whereas parameters related to plastic behavior are c and ϕ, and ψ, angle of dilatancy. These parameters with their standard units are listed below.

Parameter		Unit
E	Young's Modulus	KN/m2
υ	Poisson's ratio	-
Φ	Friction angle	Degree
C	Cohesion	KN/m2
Φ	Dilatancy angle	Degree

Table A.1.1 Mohr Coulomb parameters

PLAXIS uses the Young's modulus as the basic stiffness modulus in the Mohr Coulomb model. E_{ur} which tend to increase with the confining pressure is needed for unloading modeling such as in the case of excavations. This behavior in turn results in the deep soil layers tend to have greater stiffness than shallow layers. Hence, when using a constant stiffness modulus to represent soil behavior, a value that is consistent with the stress level and the stress path development should be chosen.

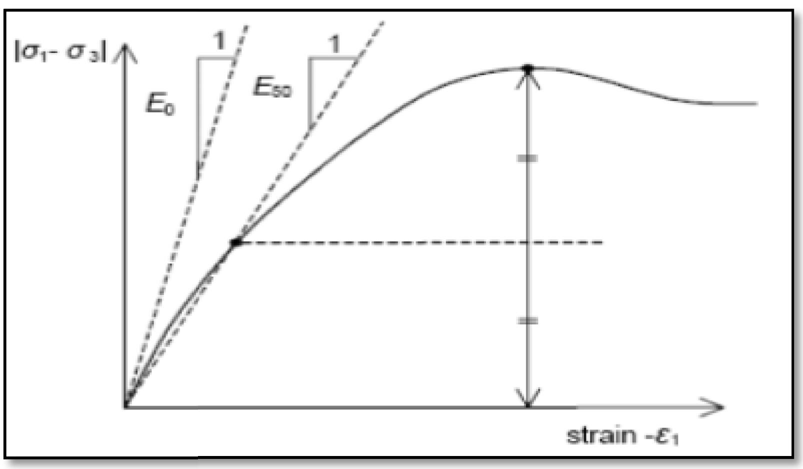

Figure 31: Definition of E0 and E50 for standard drained triaxial test results

Since standard drained triaxial tests yields a significant rate of volume decrease at the very beginning of axial loading, a low initial value of Poisson's ratio is used. However, when using the Mohr Coulomb model the use of a higher value is recommended. PLAXIS recommends the value of Poisson's ratio between 0.3-0.4 for loading conditions and 0.15-0.25 for unloading condition.

Plaxis can handle Cohesionless soil (c=0), but some options will not perform well. To avoid complications its advised to use a small value of c (c > 0.2 kPa). The friction angle ϕ is entered in degrees. High friction angles, as sometimes obtained for dense sands, will substantially increase plastic computational effort. The dilatancy angle, Ψ ,is specified in degrees. Apart from heavily over consolidated layers, clay soils tend to show little dilatancy (Ψ=0).

Appendix B. Results from plaxis

B.1 Effect of Change in magnitude of surcharge on pile

B.1.1 For depth of excavation of 7m

	95Kpa			150kPa			300kPa			400kPa		
Y	Ux	Uy	M	Ux	Uy	M	Ux	Uy	M	Ux	Uy	M
[m]	[m]	[m]	[kNm/m]	[m]	[m]	[kNm/m]	[m]	[m]	[kNm/m]	[m]	[m]	[kNm/m]
40.00	0.09	0.02	0.00	0.12	-0.02	0.00	0.14	-0.12	0.00	-0.19	-0.06	0.00
39.75	0.08	0.02	3.67	0.11	-0.02	3.58	0.13	-0.12	3.72	-0.18	-0.06	12.41
39.50	0.08	0.02	11.14	0.11	-0.02	10.79	0.12	-0.12	11.11	-0.17	-0.06	33.55
39.25	0.08	0.02	22.02	0.10	-0.02	21.23	0.12	-0.12	21.63	-0.17	-0.06	60.85
39.00	0.07	0.02	35.97	0.10	-0.02	34.53	0.11	-0.12	34.84	-0.16	-0.06	92.26
39.00	0.07	0.02	35.97	0.10	-0.02	34.53	0.11	-0.12	34.84	-0.16	-0.06	92.26
38.50	0.06	0.02	6.63	0.09	-0.02	2.49	0.09	-0.12	-5.43	-0.15	-0.06	65.03
38.00	0.06	0.02	-13.02	0.07	-0.02	-20.86	0.08	-0.12	-39.28	-0.15	-0.06	46.41
37.50	0.05	0.02	-23.64	0.06	-0.02	-36.31	0.06	-0.12	-68.55	-0.14	-0.06	31.87
37.00	0.04	0.02	-25.46	0.05	-0.02	-44.17	0.05	-0.12	-93.83	-0.13	-0.06	17.15
37.00	0.04	0.02	-25.46	0.05	-0.02	-44.17	0.05	-0.12	-93.83	-0.13	-0.06	17.15
36.75	0.04	0.02	-22.58	0.05	-0.02	-44.42	0.04	-0.12	-102.88	-0.12	-0.06	12.81
36.50	0.03	0.02	-16.88	0.04	-0.02	-41.58	0.04	-0.12	-108.48	-0.12	-0.06	14.92
36.25	0.03	0.02	-7.95	0.04	-0.02	-35.12	0.03	-0.12	-109.51	-0.12	-0.06	24.15
36.00	0.02	0.02	4.58	0.03	-0.02	-24.52	0.02	-0.12	-104.76	-0.11	-0.06	40.99
36.00	0.02	0.02	4.58	0.03	-0.02	-24.52	0.02	-0.12	-104.76	-0.11	-0.06	40.99
35.75	0.02	0.02	-8.17	0.03	-0.02	-39.00	0.02	-0.12	-125.53	-0.11	-0.06	27.48
35.50	0.02	0.02	-16.95	0.02	-0.02	-48.66	0.01	-0.12	-139.02	-0.10	-0.06	20.76
35.25	0.01	0.02	-21.64	0.02	-0.02	-53.45	0.01	-0.12	-145.00	-0.10	-0.06	20.32
35.00	0.01	0.02	-22.18	0.01	-0.02	-53.31	0.00	-0.12	-143.30	-0.10	-0.06	25.64
35.00	0.01	0.02	-22.18	0.01	-0.02	-53.31	0.00	-0.12	-143.30	-0.10	-0.06	25.64
34.75	0.00	0.02	-17.81	0.01	-0.02	-46.99	0.00	-0.12	-135.03	-0.09	-0.06	31.41
34.50	0.00	0.02	-9.33	0.01	-0.02	-35.68	-0.01	-0.12	-118.20	-0.09	-0.06	40.52
34.25	0.00	0.02	3.28	0.00	-0.02	-19.36	-0.01	-0.12	-92.62	-0.09	-0.06	56.07
34.00	-0.01	0.02	20.02	0.00	-0.02	1.96	-0.01	-0.12	-58.13	-0.08	-0.06	80.87
34.00	-0.01	0.02	20.02	0.00	-0.02	1.96	-0.01	-0.12	-58.13	-0.08	-0.06	80.87
33.75	-0.01	0.02	4.52	-0.01	-0.02	-8.09	-0.02	-0.12	-50.84	-0.08	-0.06	79.83
33.50	-0.01	0.02	-7.03	-0.01	-0.02	-13.36	-0.02	-0.12	-34.33	-0.08	-0.06	90.10
33.25	-0.02	0.02	-14.74	-0.01	-0.02	-13.94	-0.03	-0.12	-8.10	-0.07	-0.06	112.47
33.00	-0.02	0.02	-18.75	-0.02	-0.02	-9.89	-0.03	-0.12	28.51	-0.07	-0.06	147.76
33.00	-0.02	0.02	-18.75	-0.02	-0.02	-9.89	-0.03	-0.12	28.51	-0.07	-0.06	147.76
32.96	-0.02	0.02	-19.51	-0.02	-0.02	-9.61	-0.03	-0.12	34.04	-0.07	-0.06	153.53
32.93	-0.02	0.02	-20.64	-0.02	-0.02	-9.93	-0.03	-0.12	38.93	-0.07	-0.06	159.06
32.89	-0.02	0.02	-22.05	-0.02	-0.02	-10.74	-0.03	-0.12	43.14	-0.07	-0.06	164.25
32.86	-0.02	0.02	-23.62	-0.02	-0.02	-11.89	-0.03	-0.12	46.64	-0.07	-0.06	168.95
32.86	-0.02	0.02	-23.62	-0.02	-0.02	-11.89	-0.03	-0.12	46.64	-0.07	-0.06	168.95

32.75	-0.02	0.02	-29.27	-0.02	-0.02	-17.11	-0.03	-0.12	53.73	-0.07	-0.06	181.10
32.64	-0.03	0.02	-35.42	-0.02	-0.02	-23.75	-0.03	-0.12	55.61	-0.07	-0.06	189.27
32.52	-0.03	0.02	-41.77	-0.03	-0.02	-31.25	-0.04	-0.12	53.14	-0.07	-0.06	193.89
32.41	-0.03	0.02	-48.09	-0.03	-0.02	-39.18	-0.04	-0.12	47.21	-0.07	-0.06	195.54
32.41	-0.03	0.02	-48.09	-0.03	-0.02	-39.18	-0.04	-0.12	47.21	-0.07	-0.06	195.54
32.06	-0.03	0.02	-66.94	-0.03	-0.02	-65.20	-0.04	-0.12	13.19	-0.06	-0.06	185.03
31.71	-0.04	0.02	-83.46	-0.04	-0.02	-90.95	-0.05	-0.12	-35.17	-0.06	-0.06	155.80
31.35	-0.04	0.02	-96.33	-0.04	-0.02	-113.48	-0.05	-0.12	-85.65	-0.06	-0.06	116.64
31.00	-0.05	0.02	-103.80	-0.05	-0.02	-129.11	-0.06	-0.12	-124.16	-0.06	-0.06	78.07
31.00	-0.05	0.02	-103.80	-0.05	-0.02	-129.11	-0.06	-0.12	-124.16	-0.06	-0.06	78.07
30.50	-0.05	0.02	-94.58	-0.05	-0.02	-121.27	-0.07	-0.12	-119.27	-0.06	-0.06	55.81
30.00	-0.05	0.02	-85.65	-0.06	-0.01	-113.15	-0.07	-0.12	-118.28	-0.07	-0.06	34.03
29.50	-0.06	0.02	-77.07	-0.06	-0.01	-104.57	-0.07	-0.12	-119.74	-0.07	-0.06	11.52
29.00	-0.06	0.02	-66.69	-0.06	-0.01	-92.05	-0.08	-0.11	-117.70	-0.07	-0.06	-13.37
29.00	-0.06	0.02	-66.69	-0.06	-0.01	-92.05	-0.08	-0.11	-117.70	-0.07	-0.06	-13.37
28.50	-0.06	0.02	-48.32	-0.06	-0.01	-66.11	-0.08	-0.11	-92.16	-0.07	-0.06	-33.82
28.00	-0.06	0.02	-32.61	-0.06	-0.01	-43.41	-0.08	-0.11	-65.25	-0.07	-0.06	-42.68
27.50	-0.06	0.02	-19.52	-0.06	-0.01	-24.16	-0.08	-0.11	-38.60	-0.07	-0.06	-42.18
27.00	-0.06	0.02	-8.70	-0.06	-0.01	-8.13	-0.08	-0.11	-13.35	-0.07	-0.06	-34.09
27.00	-0.06	0.02	-8.70	-0.06	-0.01	-8.13	-0.08	-0.11	-13.35	-0.07	-0.06	-34.09
26.58	-0.06	0.02	-4.04	-0.06	-0.01	-1.27	-0.08	-0.11	-3.81	-0.08	-0.06	-30.48
26.17	-0.06	0.02	-1.59	-0.06	-0.01	2.30	-0.08	-0.11	-0.20	-0.08	-0.06	-30.96
25.75	-0.06	0.02	-0.52	-0.06	-0.01	3.81	-0.08	-0.11	-0.52	-0.08	-0.06	-33.86
25.33	-0.06	0.02	-0.09	-0.06	-0.01	4.32	-0.08	-0.11	-2.87	-0.08	-0.06	-36.96
25.33	-0.06	0.02	-0.09	-0.06	-0.01	4.32	-0.08	-0.11	-2.87	-0.08	-0.06	-36.96
24.92	-0.06	0.02	0.00	-0.06	-0.01	4.27	-0.08	-0.11	-6.99	-0.07	-0.06	-42.38
24.50	-0.06	0.02	0.04	-0.06	-0.01	4.02	-0.08	-0.11	-11.34	-0.07	-0.06	-47.69
24.08	-0.06	0.02	0.15	-0.06	-0.01	3.68	-0.08	-0.11	-14.99	-0.07	-0.06	-51.98
23.67	-0.06	0.02	0.38	-0.06	-0.01	3.29	-0.08	-0.11	-16.87	-0.07	-0.06	-53.94
23.67	-0.06	0.02	0.38	-0.06	-0.01	3.29	-0.08	-0.11	-16.87	-0.07	-0.06	-53.94
23.25	-0.06	0.02	0.73	-0.06	-0.01	2.84	-0.08	-0.11	-16.73	-0.07	-0.06	-50.33
22.83	-0.06	0.02	0.93	-0.06	-0.01	1.62	-0.08	-0.11	-15.19	-0.07	-0.06	-40.91
22.42	-0.06	0.02	0.74	-0.06	-0.01	0.27	-0.08	-0.11	-10.49	-0.07	-0.06	-24.65
22.00	-0.06	0.02	0.00	-0.07	-0.01	0.00	-0.08	-0.11	0.00	-0.06	-0.06	0.00

B.1.2 For depth of excavation of 9m

	95kPa			150kPa			300kPa			400kPa		
Y	Ux	Uy	M	Ux	Uy	M	Ux	Uy	M	Ux	Uy	M
[m]	[m]	[m]	[kNm/m]	[m]	[m]	[kNm/m]	[m]	[m]	[kNm/m]	[m]	[m]	[kNm/m]
40.00	0.06	0.04	0.00	0.07	0.00	0.00	0.03	-0.09	0.00	-0.04	-0.17	0.00
39.50	0.05	0.04	5.62	0.06	0.00	6.00	0.01	-0.09	2.38	-0.05	-0.17	7.27
39.00	0.05	0.04	17.74	0.05	0.00	18.86	0.00	-0.09	6.13	-0.07	-0.17	22.16
38.50	0.04	0.04	36.63	0.04	0.00	38.58	-0.01	-0.09	10.49	-0.08	-0.17	41.75
38.00	0.03	0.04	62.85	0.04	0.00	65.43	-0.02	-0.09	15.08	-0.10	-0.17	63.40
32.00	-0.05	0.04	-51.02	-0.06	0.01	-60.78	-0.10	-0.09	-95.08	-0.16	-0.16	-202.28
31.75	-0.05	0.04	-64.44	-0.06	0.01	-76.24	-0.10	-0.09	-93.45	-0.16	-0.16	-178.50
31.50	-0.06	0.04	-69.37	-0.06	0.01	-81.87	-0.10	-0.08	-81.09	-0.15	-0.16	-143.59
31.25	-0.06	0.04	-64.28	-0.06	0.01	-75.43	-0.10	-0.08	-50.30	-0.14	-0.16	-87.76
31.00	-0.06	0.04	-47.31	-0.06	0.01	-54.03	-0.09	-0.08	8.76	-0.14	-0.16	-0.29
38.00	0.03	0.04	62.85	0.04	0.00	65.43	-0.02	-0.09	15.08	-0.10	-0.17	63.40
37.75	0.03	0.04	43.58	0.03	0.00	44.80	-0.03	-0.09	-2.96	-0.10	-0.17	14.81
37.50	0.02	0.04	26.49	0.03	0.00	26.03	-0.03	-0.09	-21.62	-0.11	-0.17	-33.95
37.25	0.02	0.04	11.64	0.02	0.00	9.19	-0.04	-0.09	-40.84	-0.12	-0.17	-81.72
37.00	0.02	0.04	-0.91	0.02	0.00	-5.60	-0.04	-0.09	-60.40	-0.13	-0.17	-127.11
37.00	0.02	0.04	-0.91	0.02	0.00	-5.60	-0.04	-0.09	-60.40	-0.13	-0.17	-127.11
36.50	0.01	0.04	-18.61	0.01	0.00	-28.24	-0.06	-0.09	-97.46	-0.14	-0.17	-194.04
36.00	0.00	0.04	-25.64	0.00	0.01	-39.35	-0.07	-0.09	-122.51	-0.15	-0.17	-229.39
35.50	-0.01	0.04	-21.14	-0.01	0.01	-37.37	-0.08	-0.09	-129.12	-0.16	-0.16	-231.84
35.00	-0.02	0.04	-4.15	-0.02	0.01	-20.60	-0.08	-0.09	-111.69	-0.17	-0.16	-199.77
23.50	-0.07	0.05	-7.02	-0.08	0.01	-4.90	-0.09	-0.07	-7.45	-0.09	-0.15	-36.04
23.06	-0.07	0.05	-6.75	-0.08	0.01	-4.91	-0.09	-0.07	-11.14	-0.10	-0.15	-44.64
22.63	-0.07	0.05	-6.28	-0.08	0.01	-4.72	-0.09	-0.07	-16.27	-0.10	-0.14	-51.54
22.19	-0.07	0.05	-5.60	-0.08	0.01	-4.40	-0.09	-0.07	-22.50	-0.10	-0.14	-55.49
21.75	-0.07	0.05	-4.68	-0.08	0.01	-4.00	-0.09	-0.07	-28.98	-0.10	-0.14	-54.88
25.25	-0.07	0.05	-6.96	-0.08	0.01	-2.75	-0.09	-0.08	6.13	-0.09	-0.15	23.85
24.81	-0.07	0.05	-7.01	-0.08	0.01	-3.50	-0.09	-0.07	2.32	-0.09	-0.15	5.06
24.38	-0.07	0.05	-7.09	-0.08	0.01	-4.16	-0.09	-0.07	-1.02	-0.09	-0.15	-11.36
23.94	-0.07	0.05	-7.12	-0.08	0.01	-4.65	-0.09	-0.07	-4.17	-0.09	-0.15	-25.16
23.50	-0.07	0.05	-7.02	-0.08	0.01	-4.90	-0.09	-0.07	-7.45	-0.09	-0.15	-36.04
27.00	-0.07	0.04	-13.85	-0.08	0.01	-8.51	-0.09	-0.08	18.85	-0.09	-0.15	103.45
26.56	-0.07	0.04	-9.86	-0.08	0.01	-3.97	-0.09	-0.08	18.24	-0.09	-0.15	88.34
26.13	-0.07	0.04	-7.93	-0.08	0.01	-2.32	-0.09	-0.08	14.77	-0.09	-0.15	67.08
25.69	-0.07	0.04	-7.20	-0.08	0.01	-2.27	-0.09	-0.08	10.26	-0.09	-0.15	44.35
25.25	-0.07	0.05	-6.96	-0.08	0.01	-2.75	-0.09	-0.08	6.13	-0.09	-0.15	23.85
29.00	-0.07	0.04	-51.49	-0.07	0.01	-58.78	-0.09	-0.08	25.10	-0.10	-0.15	189.11
28.50	-0.07	0.04	-41.38	-0.07	0.01	-44.87	-0.09	-0.08	14.07	-0.10	-0.15	156.71
28.00	-0.07	0.04	-31.67	-0.08	0.01	-31.86	-0.09	-0.08	9.83	-0.09	-0.15	131.66
27.50	-0.07	0.04	-22.47	-0.08	0.01	-19.77	-0.09	-0.08	11.74	-0.09	-0.15	113.95

27.00	-0.07	0.04	-13.85	-0.08	0.01	-8.51	-0.09	-0.08	18.85	-0.09	-0.15	103.45
33.00	-0.04	0.04	-83.60	-0.05	0.01	-84.41	-0.10	-0.09	-188.74	-0.18	-0.16	-348.34
32.75	-0.05	0.04	-81.63	-0.05	0.01	-83.40	-0.10	-0.09	-167.15	-0.17	-0.16	-322.40
32.50	-0.05	0.04	-76.46	-0.05	0.01	-80.58	-0.10	-0.09	-146.93	-0.17	-0.16	-289.91
32.25	-0.05	0.04	-66.75	-0.05	0.01	-73.77	-0.10	-0.09	-124.45	-0.17	-0.16	-250.07
32.00	-0.05	0.04	-51.02	-0.06	0.01	-60.78	-0.10	-0.09	-95.08	-0.16	-0.16	-202.28
35.00	-0.02	0.04	-4.15	-0.02	0.01	-20.60	-0.08	-0.09	-111.69	-0.17	-0.16	-199.77
34.75	-0.02	0.04	-25.32	-0.02	0.01	-42.06	-0.09	-0.09	-146.73	-0.17	-0.16	-247.01
34.50	-0.02	0.04	-43.22	-0.03	0.01	-59.44	-0.09	-0.09	-174.97	-0.18	-0.16	-288.14
34.25	-0.03	0.04	-57.84	-0.03	0.01	-72.87	-0.09	-0.09	-196.17	-0.18	-0.16	-322.00
34.00	-0.03	0.04	-69.18	-0.03	0.01	-82.48	-0.10	-0.09	-210.09	-0.18	-0.16	-347.40
31.00	-0.06	0.04	-47.31	-0.06	0.01	-54.03	-0.09	-0.08	8.76	-0.14	-0.16	-0.29
30.50	-0.06	0.04	-36.37	-0.07	0.01	-36.55	-0.09	-0.08	94.24	-0.13	-0.16	152.98
30.00	-0.06	0.04	-39.69	-0.07	0.01	-40.31	-0.09	-0.08	100.36	-0.12	-0.16	216.41
29.50	-0.07	0.04	-47.63	-0.07	0.01	-51.84	-0.09	-0.08	64.69	-0.11	-0.15	219.46
29.00	-0.07	0.04	-51.49	-0.07	0.01	-58.78	-0.09	-0.08	25.10	-0.10	-0.15	189.11
34.00	-0.03	0.04	-69.18	-0.03	0.01	-82.48	-0.10	-0.09	-210.09	-0.18	-0.16	-347.40
33.75	-0.03	0.04	-77.45	-0.04	0.01	-88.35	-0.10	-0.09	-216.33	-0.18	-0.16	-363.28
33.50	-0.04	0.04	-82.54	-0.04	0.01	-90.64	-0.10	-0.09	-215.20	-0.18	-0.16	-369.44
33.25	-0.04	0.04	-84.57	-0.04	0.01	-89.34	-0.10	-0.09	-206.22	-0.18	-0.16	-364.89
33.00	-0.04	0.04	-83.60	-0.05	0.01	-84.41	-0.10	-0.09	-188.74	-0.18	-0.16	-348.34
21.75	-0.07	0.05	-4.68	-0.08	0.01	-4.00	-0.09	-0.07	-28.98	-0.10	-0.14	-54.88
21.31	-0.07	0.05	-3.55	-0.08	0.01	-3.21	-0.09	-0.07	-32.99	-0.09	-0.14	-52.49
20.88	-0.07	0.05	-2.28	-0.08	0.01	-3.67	-0.09	-0.07	-31.13	-0.09	-0.14	-43.80
20.44	-0.07	0.05	-1.04	-0.08	0.01	-3.66	-0.09	-0.07	-20.91	-0.09	-0.14	-27.13
20.00	-0.07	0.05	0.00	-0.08	0.01	0.00	-0.09	-0.07	0.00	-0.09	-0.14	0.00

B.1.3 For depth of excavation of 11m

	95kPa			150kPa			300kPa			400kPa		
Y	Ux	Uy	M	Ux	Uy	M	Ux	Uy	M	Ux	Uy	M
[m]	[m]	[m]	[kNm/m]	[m]	[m]	[kNm/m]	[m]	[m]	[kNm/m]	[m]	[m]	[kNm/m]
40.00	0.03	0.06	0.00	0.03	0.02	0.00	0.00	-0.08	0.00	-0.12	-0.16	0.00
39.50	0.03	0.06	6.90	0.02	0.02	7.56	-0.02	-0.08	8.86	-0.14	-0.16	8.78
39.00	0.02	0.06	21.50	0.01	0.02	23.54	-0.03	-0.08	27.44	-0.15	-0.16	26.44
38.50	0.01	0.06	43.72	0.00	0.02	47.57	-0.04	-0.08	54.39	-0.17	-0.16	50.30
38.00	0.00	0.06	73.82	0.00	0.02	79.62	-0.06	-0.08	88.72	-0.19	-0.16	78.09
38.00	0.00	0.06	73.82	0.00	0.02	79.62	-0.06	-0.08	88.72	-0.19	-0.16	78.09
37.75	0.00	0.06	54.62	-0.01	0.02	59.25	-0.07	-0.08	60.31	-0.20	-0.16	29.12
37.50	-0.01	0.06	37.68	-0.01	0.02	40.92	-0.07	-0.08	33.25	-0.21	-0.16	-18.97
37.25	-0.01	0.06	23.00	-0.02	0.02	24.65	-0.08	-0.08	7.45	-0.22	-0.16	-65.26
37.00	-0.02	0.06	10.63	-0.02	0.02	10.48	-0.09	-0.08	-17.08	-0.23	-0.16	-108.70
37.00	-0.02	0.06	10.63	-0.02	0.02	10.48	-0.09	-0.08	-17.08	-0.23	-0.16	-108.70
36.50	-0.02	0.06	-6.92	-0.03	0.02	-11.05	-0.11	-0.08	-61.12	-0.24	-0.16	-170.87
36.00	-0.03	0.06	-14.22	-0.05	0.02	-21.31	-0.12	-0.08	-91.73	-0.26	-0.16	-200.27
35.50	-0.04	0.06	-10.73	-0.05	0.02	-19.35	-0.14	-0.08	-104.37	-0.27	-0.16	-197.10
35.00	-0.05	0.06	4.13	-0.06	0.02	-4.17	-0.15	-0.08	-95.24	-0.29	-0.16	-161.45
35.00	-0.05	0.06	4.13	-0.06	0.02	-4.17	-0.15	-0.08	-95.24	-0.29	-0.16	-161.45
34.75	-0.06	0.06	-21.50	-0.07	0.02	-31.26	-0.16	-0.08	-142.10	-0.29	-0.16	-220.63
34.50	-0.06	0.06	-44.22	-0.07	0.02	-54.72	-0.16	-0.08	-182.51	-0.30	-0.16	-274.71
34.25	-0.06	0.06	-64.00	-0.08	0.02	-74.68	-0.17	-0.08	-216.50	-0.30	-0.16	-322.53
34.00	-0.07	0.06	-80.84	-0.08	0.02	-91.27	-0.18	-0.08	-244.09	-0.31	-0.16	-362.89
34.00	-0.07	0.06	-80.84	-0.08	0.02	-91.27	-0.18	-0.08	-244.09	-0.31	-0.16	-362.89
33.75	-0.07	0.06	-95.02	-0.09	0.02	-104.64	-0.18	-0.08	-265.03	-0.31	-0.16	-394.93
33.50	-0.08	0.06	-106.45	-0.09	0.02	-115.06	-0.18	-0.08	-279.46	-0.31	-0.16	-418.44
33.25	-0.08	0.06	-115.25	-0.10	0.02	-122.49	-0.19	-0.08	-287.16	-0.31	-0.16	-432.52
33.00	-0.08	0.06	-121.53	-0.10	0.02	-126.89	-0.19	-0.08	-287.86	-0.31	-0.16	-435.94
33.00	-0.08	0.06	-121.53	-0.10	0.02	-126.89	-0.19	-0.08	-287.86	-0.31	-0.16	-435.94
32.75	-0.09	0.06	-127.66	-0.10	0.02	-136.55	-0.19	-0.08	-287.03	-0.31	-0.15	-433.47
32.50	-0.09	0.06	-131.72	-0.11	0.02	-146.12	-0.19	-0.07	-291.25	-0.31	-0.15	-428.17
32.25	-0.09	0.06	-132.49	-0.11	0.02	-153.58	-0.19	-0.07	-296.91	-0.31	-0.15	-419.76
32.00	-0.09	0.06	-128.79	-0.11	0.02	-156.89	-0.19	-0.07	-299.82	-0.30	-0.15	-408.47
32.00	-0.09	0.06	-128.79	-0.11	0.02	-156.89	-0.19	-0.07	-299.82	-0.30	-0.15	-408.47
31.75	-0.10	0.06	-159.73	-0.11	0.02	-197.85	-0.19	-0.07	-353.84	-0.30	-0.15	-458.53
31.50	-0.10	0.06	-183.97	-0.11	0.02	-231.69	-0.19	-0.07	-401.31	-0.29	-0.15	-503.20
31.25	-0.10	0.06	-199.49	-0.11	0.03	-255.49	-0.19	-0.07	-434.00	-0.29	-0.15	-532.22
31.00	-0.10	0.06	-204.20	-0.12	0.03	-266.13	-0.19	-0.07	-441.23	-0.28	-0.15	-533.69
31.00	-0.10	0.06	-204.20	-0.12	0.03	-266.13	-0.19	-0.07	-441.23	-0.28	-0.15	-533.69
30.75	-0.10	0.06	-191.13	-0.11	0.03	-252.97	-0.18	-0.07	-407.99	-0.27	-0.15	-490.94
30.50	-0.10	0.06	-167.60	-0.11	0.03	-226.81	-0.18	-0.07	-357.33	-0.26	-0.15	-428.13

30.25	-0.10	0.06	-133.86	-0.11	0.03	-188.06	-0.17	-0.07	-290.70	-0.25	-0.15	-346.22
30.00	-0.10	0.06	-90.32	-0.11	0.03	-137.43	-0.17	-0.07	-210.10	-0.23	-0.15	-246.71
30.00	-0.10	0.06	-90.32	-0.11	0.03	-137.43	-0.17	-0.07	-210.10	-0.23	-0.15	-246.71
29.75	-0.10	0.06	-72.76	-0.11	0.03	-110.21	-0.16	-0.07	-150.69	-0.22	-0.15	-165.89
29.50	-0.09	0.06	-44.56	-0.11	0.03	-69.91	-0.15	-0.07	-75.88	-0.21	-0.15	-67.64
29.25	-0.09	0.06	-4.56	-0.10	0.03	-14.84	-0.14	-0.07	17.64	-0.19	-0.15	49.27
29.00	-0.09	0.06	48.24	-0.10	0.03	56.45	-0.13	-0.07	132.90	-0.18	-0.15	185.96
29.00	-0.09	0.06	48.24	-0.10	0.03	56.45	-0.13	-0.07	132.90	-0.18	-0.15	185.96
28.50	-0.09	0.06	88.98	-0.10	0.03	125.97	-0.12	-0.07	274.92	-0.15	-0.14	370.11
28.00	-0.09	0.06	87.95	-0.09	0.03	133.66	-0.11	-0.07	321.94	-0.13	-0.14	456.46
27.50	-0.09	0.06	69.12	-0.09	0.03	112.69	-0.10	-0.06	309.43	-0.11	-0.14	471.74
27.00	-0.09	0.06	52.27	-0.09	0.03	90.45	-0.09	-0.06	271.18	-0.10	-0.14	443.27
27.00	-0.09	0.06	52.27	-0.09	0.03	90.45	-0.09	-0.06	271.18	-0.10	-0.14	443.27
26.55	-0.09	0.06	35.25	-0.09	0.03	66.33	-0.09	-0.06	219.09	-0.09	-0.14	393.38
26.10	-0.09	0.06	20.36	-0.09	0.03	44.35	-0.09	-0.06	163.83	-0.09	-0.14	329.20
25.65	-0.09	0.06	8.27	-0.09	0.03	25.88	-0.09	-0.06	112.32	-0.08	-0.14	261.11
25.20	-0.09	0.06	-0.62	-0.09	0.03	11.84	-0.09	-0.06	70.26	-0.08	-0.14	198.14
25.20	-0.09	0.06	-0.62	-0.09	0.03	11.84	-0.09	-0.06	70.26	-0.08	-0.14	198.14
24.75	-0.09	0.06	-6.88	-0.09	0.03	1.56	-0.09	-0.06	38.00	-0.08	-0.14	142.05
24.30	-0.09	0.06	-10.97	-0.09	0.03	-5.51	-0.09	-0.06	14.95	-0.09	-0.14	94.65
23.85	-0.09	0.06	-13.40	-0.09	0.03	-10.02	-0.09	-0.06	-0.52	-0.09	-0.13	55.91
23.40	-0.09	0.06	-14.63	-0.09	0.03	-12.63	-0.09	-0.06	-10.07	-0.09	-0.13	25.28
23.40	-0.09	0.06	-14.63	-0.09	0.03	-12.63	-0.09	-0.06	-10.07	-0.09	-0.13	25.28
22.95	-0.09	0.06	-15.01	-0.09	0.03	-13.82	-0.10	-0.06	-15.17	-0.09	-0.13	1.71
22.50	-0.09	0.06	-14.85	-0.09	0.03	-14.03	-0.10	-0.06	-17.22	-0.10	-0.13	-15.96
22.05	-0.09	0.06	-14.30	-0.09	0.03	-13.54	-0.10	-0.06	-17.15	-0.10	-0.13	-28.31
21.60	-0.09	0.06	-13.52	-0.09	0.03	-12.57	-0.10	-0.06	-15.78	-0.10	-0.13	-35.98
21.60	-0.09	0.06	-13.52	-0.09	0.03	-12.57	-0.10	-0.06	-15.78	-0.10	-0.13	-35.98
21.15	-0.09	0.06	-12.55	-0.09	0.03	-11.22	-0.10	-0.06	-13.63	-0.10	-0.13	-40.42
20.70	-0.09	0.06	-11.41	-0.09	0.03	-9.60	-0.10	-0.06	-11.29	-0.10	-0.13	-42.56
20.25	-0.09	0.06	-10.07	-0.09	0.03	-7.74	-0.10	-0.06	-9.13	-0.11	-0.13	-42.59
19.80	-0.09	0.06	-8.49	-0.09	0.03	-5.68	-0.10	-0.05	-7.47	-0.11	-0.13	-40.39
19.80	-0.09	0.06	-8.49	-0.09	0.03	-5.68	-0.10	-0.05	-7.47	-0.11	-0.13	-40.39
19.35	-0.09	0.06	-6.66	-0.09	0.03	-3.51	-0.10	-0.05	-7.40	-0.11	-0.13	-34.58
18.90	-0.09	0.06	-4.44	-0.09	0.03	-1.52	-0.10	-0.05	-7.40	-0.11	-0.13	-27.30
18.45	-0.09	0.06	-2.10	-0.09	0.03	-0.19	-0.10	-0.05	-5.34	-0.11	-0.13	-16.80
18.00	-0.09	0.06	0.00	-0.09	0.03	0.00	-0.10	-0.05	0.00	-0.11	-0.13	0.00

B.1.4 For depth of excavation of 13m

	95kPa			150kPa			300kPa			400kPa		
Y	Ux	Uy	M	Ux	Uy	M	Ux	Uy	M	Ux	Uy	M
[m]	[m]	[m]	[kNm/m]	[m]	[m]	[kNm/m]	[m]	[m]	[kNm/m]	[m]	[m]	[kNm/m]
40.00	0.01	0.07	0.00	0.01	0.03	0.00	-0.07	-0.07	0.00	-0.23	-0.21	0.00
39.75	0.00	0.07	4.65	0.00	0.03	4.78	-0.08	-0.07	5.45	-0.24	-0.21	5.43
39.50	0.00	0.07	13.97	-0.01	0.03	14.35	-0.09	-0.07	16.47	-0.26	-0.21	16.56
39.25	-0.01	0.07	27.34	-0.01	0.03	28.07	-0.10	-0.07	32.31	-0.27	-0.21	32.45
39.00	-0.01	0.07	44.19	-0.02	0.03	45.37	-0.11	-0.07	52.27	-0.28	-0.21	52.22
39.00	-0.01	0.07	44.19	-0.02	0.03	45.37	-0.11	-0.07	52.27	-0.28	-0.21	52.22
38.50	-0.02	0.07	17.77	-0.03	0.03	17.71	-0.13	-0.07	21.14	-0.31	-0.21	0.95
38.00	-0.03	0.07	1.95	-0.05	0.03	0.62	-0.14	-0.07	-0.34	-0.33	-0.21	-44.31
37.50	-0.04	0.07	-4.43	-0.06	0.03	-7.37	-0.16	-0.07	-15.10	-0.35	-0.21	-84.34
37.00	-0.06	0.07	-2.22	-0.07	0.03	-7.43	-0.18	-0.07	-25.18	-0.38	-0.21	-118.07
37.00	-0.06	0.07	-2.22	-0.07	0.03	-7.43	-0.18	-0.07	-25.18	-0.38	-0.21	-118.07
36.75	-0.06	0.07	2.23	-0.08	0.03	-4.18	-0.19	-0.07	-27.27	-0.39	-0.21	-125.35
36.50	-0.07	0.07	9.14	-0.08	0.03	1.61	-0.20	-0.07	-27.05	-0.40	-0.21	-124.00
36.25	-0.07	0.07	18.83	-0.09	0.03	10.40	-0.21	-0.07	-23.52	-0.41	-0.21	-113.24
36.00	-0.08	0.07	31.66	-0.10	0.03	22.66	-0.22	-0.07	-15.57	-0.42	-0.21	-92.54
36.00	-0.08	0.07	31.66	-0.10	0.03	22.66	-0.22	-0.07	-15.57	-0.42	-0.21	-92.54
35.75	-0.08	0.07	9.38	-0.10	0.03	-2.58	-0.23	-0.07	-60.31	-0.43	-0.21	-149.32
35.50	-0.09	0.07	-9.61	-0.11	0.03	-23.93	-0.24	-0.07	-99.50	-0.44	-0.21	-197.26
35.25	-0.09	0.07	-25.49	-0.12	0.03	-41.67	-0.25	-0.07	-133.00	-0.45	-0.21	-236.82
35.00	-0.10	0.07	-38.45	-0.12	0.03	-56.06	-0.26	-0.07	-160.78	-0.46	-0.21	-268.10
35.00	-0.10	0.07	-38.45	-0.12	0.03	-56.06	-0.26	-0.07	-160.78	-0.46	-0.21	-268.10
34.75	-0.10	0.07	-48.20	-0.13	0.03	-66.36	-0.27	-0.07	-184.82	-0.47	-0.21	-295.09
34.50	-0.11	0.07	-55.20	-0.14	0.03	-73.27	-0.27	-0.07	-202.75	-0.48	-0.21	-316.31
34.25	-0.11	0.07	-59.35	-0.14	0.03	-76.70	-0.28	-0.07	-214.32	-0.48	-0.21	-330.84
34.00	-0.12	0.07	-60.60	-0.15	0.03	-76.59	-0.29	-0.07	-219.30	-0.49	-0.21	-337.69
34.00	-0.12	0.07	-60.60	-0.15	0.03	-76.59	-0.29	-0.07	-219.30	-0.49	-0.21	-337.69
33.75	-0.12	0.07	-59.02	-0.15	0.03	-72.83	-0.30	-0.07	-217.22	-0.50	-0.21	-335.28
33.50	-0.13	0.07	-54.35	-0.16	0.03	-65.44	-0.30	-0.07	-208.12	-0.50	-0.21	-324.13
33.25	-0.13	0.07	-46.55	-0.16	0.03	-54.30	-0.31	-0.07	-191.62	-0.50	-0.21	-303.24
33.00	-0.14	0.07	-35.60	-0.17	0.03	-39.28	-0.31	-0.07	-167.21	-0.51	-0.21	-271.37
33.00	-0.14	0.07	-35.60	-0.17	0.03	-39.28	-0.31	-0.07	-167.21	-0.51	-0.21	-271.37
32.50	-0.15	0.07	-106.66	-0.18	0.03	-123.31	-0.32	-0.07	-260.05	-0.51	-0.21	-383.93
32.00	-0.16	0.07	-167.13	-0.19	0.03	-204.40	-0.33	-0.07	-365.32	-0.51	-0.20	-496.92
31.50	-0.16	0.07	-210.38	-0.20	0.04	-269.84	-0.33	-0.07	-458.28	-0.51	-0.20	-600.86
31.00	-0.17	0.07	-228.60	-0.20	0.04	-307.38	-0.33	-0.07	-512.09	-0.50	-0.20	-681.10
31.00	-0.17	0.07	-228.60	-0.20	0.04	-307.38	-0.33	-0.07	-512.09	-0.50	-0.20	-681.10
30.50	-0.17	0.07	-293.53	-0.20	0.04	-384.67	-0.33	-0.06	-578.12	-0.49	-0.20	-729.91
30.00	-0.17	0.07	-323.85	-0.20	0.04	-420.03	-0.32	-0.06	-595.54	-0.47	-0.20	-725.41
29.50	-0.17	0.07	-317.97	-0.20	0.04	-411.69	-0.30	-0.06	-564.19	-0.44	-0.20	-671.57

29.00	-0.16	0.07	-272.24	-0.19	0.04	-354.72	-0.28	-0.06	-478.14	-0.41	-0.20	-569.15
29.00	-0.16	0.07	-272.24	-0.19	0.04	-354.72	-0.28	-0.06	-478.14	-0.41	-0.20	-569.15
28.75	-0.16	0.07	-226.52	-0.18	0.04	-296.16	-0.27	-0.06	-401.96	-0.39	-0.20	-496.90
28.50	-0.15	0.07	-170.90	-0.17	0.04	-225.89	-0.25	-0.06	-309.99	-0.37	-0.20	-410.30
28.25	-0.15	0.07	-105.63	-0.17	0.04	-144.37	-0.24	-0.06	-202.59	-0.35	-0.19	-309.18
28.00	-0.14	0.07	-30.97	-0.16	0.04	-52.10	-0.23	-0.06	-79.87	-0.33	-0.19	-192.83
28.00	-0.14	0.07	-30.97	-0.16	0.04	-52.10	-0.23	-0.06	-79.87	-0.33	-0.19	-192.83
27.75	-0.14	0.07	16.84	-0.15	0.04	14.12	-0.21	-0.06	21.01	-0.30	-0.19	-62.78
27.50	-0.13	0.08	74.03	-0.14	0.04	90.86	-0.20	-0.06	136.47	-0.28	-0.19	82.20
27.25	-0.12	0.08	140.61	-0.14	0.04	177.97	-0.18	-0.06	265.72	-0.26	-0.19	241.52
27.00	-0.12	0.08	216.52	-0.13	0.04	275.17	-0.17	-0.06	408.07	-0.24	-0.19	415.21
27.00	-0.12	0.08	216.52	-0.13	0.04	275.17	-0.17	-0.06	408.07	-0.24	-0.19	415.21
26.54	-0.11	0.08	258.23	-0.12	0.04	344.45	-0.15	-0.06	546.24	-0.20	-0.19	636.34
26.08	-0.11	0.08	236.90	-0.11	0.04	331.69	-0.13	-0.05	575.90	-0.17	-0.19	737.12
25.63	-0.10	0.08	187.04	-0.11	0.04	275.19	-0.12	-0.05	532.43	-0.14	-0.19	742.17
25.17	-0.10	0.08	137.63	-0.10	0.04	209.69	-0.11	-0.05	452.74	-0.12	-0.19	686.50
25.17	-0.10	0.08	137.63	-0.10	0.04	209.69	-0.11	-0.05	452.74	-0.12	-0.19	686.50
24.71	-0.10	0.08	92.68	-0.10	0.04	147.25	-0.10	-0.05	362.45	-0.11	-0.18	600.52
24.25	-0.10	0.08	56.83	-0.10	0.04	96.09	-0.10	-0.05	273.39	-0.10	-0.18	509.77
23.79	-0.10	0.08	29.61	-0.10	0.04	56.30	-0.10	-0.05	191.11	-0.09	-0.18	417.01
23.33	-0.10	0.08	10.30	-0.10	0.04	27.49	-0.10	-0.05	121.05	-0.09	-0.18	326.17
23.33	-0.10	0.08	10.30	-0.10	0.04	27.49	-0.10	-0.05	121.05	-0.09	-0.18	326.17
22.88	-0.10	0.08	-2.77	-0.10	0.04	7.48	-0.10	-0.05	66.27	-0.08	-0.18	243.92
22.42	-0.10	0.08	-11.11	-0.10	0.04	-5.70	-0.10	-0.05	26.83	-0.08	-0.18	171.54
21.96	-0.10	0.08	-15.95	-0.10	0.04	-13.72	-0.10	-0.05	0.28	-0.09	-0.18	108.63
21.50	-0.10	0.08	-18.43	-0.10	0.05	-18.15	-0.10	-0.05	-16.11	-0.09	-0.18	54.98
21.50	-0.10	0.08	-18.43	-0.10	0.05	-18.15	-0.10	-0.05	-16.11	-0.09	-0.18	54.98
21.04	-0.10	0.08	-19.30	-0.10	0.05	-20.05	-0.11	-0.05	-24.93	-0.09	-0.18	9.68
20.58	-0.10	0.08	-19.21	-0.10	0.05	-20.35	-0.11	-0.04	-28.73	-0.09	-0.18	-27.86
20.13	-0.10	0.08	-18.51	-0.10	0.05	-19.58	-0.11	-0.04	-29.18	-0.10	-0.18	-58.85
19.67	-0.10	0.08	-17.49	-0.10	0.05	-18.20	-0.11	-0.04	-27.79	-0.10	-0.17	-84.03
19.67	-0.10	0.08	-17.49	-0.10	0.05	-18.20	-0.11	-0.04	-27.79	-0.10	-0.17	-84.03
19.21	-0.10	0.08	-16.26	-0.10	0.05	-16.39	-0.11	-0.04	-25.44	-0.10	-0.17	-102.94
18.75	-0.10	0.08	-14.86	-0.10	0.05	-14.33	-0.11	-0.04	-23.07	-0.10	-0.17	-116.03
18.29	-0.10	0.08	-13.26	-0.10	0.05	-12.03	-0.11	-0.04	-21.10	-0.10	-0.17	-122.45
17.83	-0.10	0.08	-11.40	-0.10	0.05	-9.51	-0.11	-0.04	-19.78	-0.10	-0.17	-120.75
17.83	-0.10	0.08	-11.40	-0.10	0.05	-9.51	-0.11	-0.04	-19.78	-0.10	-0.17	-120.75
17.38	-0.10	0.08	-9.23	-0.10	0.05	-6.83	-0.11	-0.04	-20.55	-0.10	-0.17	-108.74
16.92	-0.10	0.08	-6.38	-0.10	0.05	-4.20	-0.11	-0.04	-21.42	-0.10	-0.17	-87.26
16.46	-0.10	0.08	-3.15	-0.10	0.05	-1.85	-0.11	-0.04	-16.35	-0.09	-0.17	-52.87
16.00	-0.10	0.08	0.00	-0.10	0.05	0.00	-0.11	-0.04	0.00	-0.09	-0.17	0.00

B.2 Effect of Change in location of surcharge on pile

B.2.1 For depth of excavation of 7m

	1.5m			10m			15m			20m		
Y	Ux	Uy	M	Ux	Uy	M	Ux	Uy	M	Ux	Uy	M
[m]	[m]	[m]	[kNm/m]	[m]	[m]	[kNm/m]	[m]	[m]	[kNm/m]	[m]	[m]	[kNm/m]
40.00	0.09	0.02	0.00	0.07	0.06	0.00	0.04	0.08	0.00	0.02	0.09	0.00
39.75	0.08	0.02	3.67	0.06	0.06	-0.02	0.04	0.08	-0.02	0.01	0.09	0.10
39.50	0.08	0.02	11.14	0.06	0.06	-0.07	0.03	0.08	-0.07	0.01	0.09	0.27
39.25	0.08	0.02	22.02	0.05	0.06	-0.15	0.03	0.08	-0.15	0.01	0.09	0.48
39.00	0.07	0.02	35.97	0.05	0.06	-0.25	0.03	0.08	-0.26	0.00	0.09	0.69
39.00	0.07	0.02	35.97	0.05	0.06	-0.25	0.03	0.08	-0.26	0.00	0.09	0.69
38.50	0.06	0.02	6.63	0.04	0.06	-6.19	0.02	0.08	-4.94	0.00	0.09	-4.40
38.00	0.06	0.02	-13.02	0.03	0.06	-12.13	0.01	0.08	-9.68	-0.01	0.09	-9.46
37.50	0.05	0.02	-23.64	0.02	0.06	-17.99	0.00	0.08	-14.44	-0.02	0.09	-14.47
37.00	0.04	0.02	-25.46	0.01	0.06	-23.66	0.00	0.08	-19.17	-0.02	0.09	-19.41
37.00	0.04	0.02	-25.46	0.01	0.06	-23.66	0.00	0.08	-19.17	-0.02	0.09	-19.41
36.75	0.04	0.02	-22.58	0.01	0.06	-26.46	-0.01	0.08	-21.54	-0.02	0.09	-`21.85
36.50	0.03	0.02	-16.88	0.00	0.06	-29.21	-0.01	0.08	-23.90	-0.03	0.09	-24.27
36.25	0.03	0.02	-7.95	0.00	0.06	-31.89	-0.02	0.08	-26.25	-0.03	0.09	-26.64
36.00	0.02	0.02	4.58	-0.01	0.06	-34.50	-0.02	0.08	-28.58	-0.03	0.09	-28.96
36.00	0.02	0.02	4.58	-0.01	0.06	-34.50	-0.02	0.08	-28.58	-0.03	0.09	-28.96
35.75	0.02	0.02	-8.17	-0.01	0.06	-39.41	-0.02	0.08	-33.26	-0.04	0.09	-33.62
35.50	0.02	0.02	-16.95	-0.01	0.06	-44.26	-0.03	0.08	-37.92	-0.04	0.09	-38.25
35.25	0.01	0.02	-21.64	-0.02	0.06	-49.07	-0.03	0.08	-42.57	-0.04	0.09	-42.81
35.00	0.01	0.02	-22.18	-0.02	0.06	-53.86	-0.03	0.08	-47.21	-0.04	0.09	-47.28
35.00	0.01	0.02	-22.18	-0.02	0.06	-53.86	-0.03	0.08	-47.21	-0.04	0.09	-47.28
34.75	0.00	0.02	-17.81	-0.03	0.06	-58.49	-0.04	0.08	-51.63	-0.05	0.09	-51.21
34.50	0.00	0.02	-9.33	-0.03	0.06	-62.68	-0.04	0.08	-55.46	-0.05	0.09	-53.98
34.25	0.00	0.02	3.28	-0.03	0.06	-65.92	-0.04	0.08	-58.29	-0.05	0.09	-55.36
34.00	-0.01	0.02	20.02	-0.04	0.06	-67.70	-0.05	0.08	-59.78	-0.05	0.09	-55.08
34.00	-0.01	0.02	20.02	-0.04	0.06	-67.70	-0.05	0.08	-59.78	-0.05	0.09	-55.08
33.75	-0.01	0.02	4.52	-0.04	0.06	-67.69	-0.05	0.08	-59.58	-0.06	0.09	-52.86
33.50	-0.01	0.02	-7.03	-0.04	0.06	-65.58	-0.05	0.08	-57.36	-0.06	0.09	-48.41
33.25	-0.02	0.02	-14.74	-0.05	0.06	-61.16	-0.05	0.08	-52.79	-0.06	0.09	-41.40
33.00	-0.02	0.02	-18.75	-0.05	0.06	-54.21	-0.06	0.08	-45.55	-0.06	0.09	-31.51
33.00	-0.02	0.02	-18.75	-0.05	0.06	-54.21	-0.06	0.08	-45.55	-0.06	0.09	-31.51
32.96	-0.02	0.02	-19.51	-0.05	0.06	-53.51	-0.06	0.08	-44.76	-0.06	0.09	-30.33
32.93	-0.02	0.02	-20.64	-0.05	0.06	-53.15	-0.06	0.08	-44.31	-0.06	0.09	-29.51
32.89	-0.02	0.02	-22.05	-0.05	0.06	-53.04	-0.06	0.08	-44.09	-0.06	0.09	-28.97
32.86	-0.02	0.02	-23.62	-0.05	0.06	-53.10	-0.06	0.08	-44.03	-0.06	0.09	-28.61
32.86	-0.02	0.02	-23.62	-0.05	0.06	-53.10	-0.06	0.08	-44.03	-0.06	0.09	-28.61
32.75	-0.02	0.02	-29.27	-0.05	0.06	-54.09	-0.06	0.08	-44.61	-0.06	0.09	-28.38

32.64	-0.03	0.02	-35.42	-0.05	0.06	-55.82	-0.06	0.08	-45.88	-0.06	0.09	-28.96
32.52	-0.03	0.02	-41.77	-0.05	0.06	-58.03	-0.06	0.08	-47.59	-0.06	0.09	-30.09
32.41	-0.03	0.02	-48.09	-0.06	0.06	-60.49	-0.06	0.08	-49.51	-0.06	0.09	-31.52
32.41	-0.03	0.02	-48.09	-0.06	0.06	-60.49	-0.06	0.08	-49.51	-0.06	0.09	-31.52
32.06	-0.03	0.02	-66.94	-0.06	0.06	-69.05	-0.06	0.08	-56.24	-0.07	0.09	-37.02
31.71	-0.04	0.02	-83.46	-0.06	0.06	-77.58	-0.07	0.08	-62.69	-0.07	0.09	-42.52
31.35	-0.04	0.02	-96.33	-0.06	0.06	-84.39	-0.07	0.08	-67.67	-0.07	0.09	-46.96
31.00	-0.05	0.02	-103.80	-0.07	0.06	-87.62	-0.07	0.08	-69.85	-0.07	0.09	-49.31
31.00	-0.05	0.02	-103.80	-0.07	0.06	-87.62	-0.07	0.08	-69.85	-0.07	0.09	-49.31
30.50	-0.05	0.02	-94.58	-0.07	0.06	-79.81	-0.07	0.08	-64.73	-0.07	0.09	-47.36
30.00	-0.05	0.02	-85.65	-0.07	0.06	-72.67	-0.07	0.08	-59.68	-0.07	0.09	-44.88
29.50	-0.06	0.02	-77.07	-0.07	0.06	-65.48	-0.07	0.08	-54.12	-0.07	0.09	-41.45
29.00	-0.06	0.02	-66.69	-0.07	0.06	-55.86	-0.08	0.08	-46.22	-0.08	0.09	-35.84
29.00	-0.06	0.02	-66.69	-0.07	0.06	-55.86	-0.08	0.08	-46.22	-0.08	0.09	-35.84
28.50	-0.06	0.02	-48.32	-0.07	0.06	-39.51	-0.08	0.08	-33.20	-0.08	0.09	-26.46
28.00	-0.06	0.02	-32.61	-0.07	0.06	-25.78	-0.07	0.08	-22.29	-0.08	0.09	-18.57
27.50	-0.06	0.02	-19.52	-0.07	0.06	-14.58	-0.07	0.08	-13.42	-0.07	0.09	-12.11
27.00	-0.06	0.02	-8.70	-0.07	0.06	-5.61	-0.07	0.08	-6.31	-0.07	0.09	-6.85
27.00	-0.06	0.02	-8.70	-0.07	0.06	-5.61	-0.07	0.08	-6.31	-0.07	0.09	-6.85
26.58	-0.06	0.02	-4.04	-0.07	0.06	-2.04	-0.07	0.08	-3.46	-0.07	0.09	-4.68
26.17	-0.06	0.02	-1.59	-0.07	0.06	-0.54	-0.07	0.08	-2.33	-0.07	0.09	-3.87
25.75	-0.06	0.02	-0.52	-0.07	0.06	-0.32	-0.07	0.08	-2.28	-0.07	0.09	-3.93
25.33	-0.06	0.02	-0.09	-0.07	0.06	-0.72	-0.07	0.08	-2.76	-0.07	0.09	-4.41
25.33	-0.06	0.02	-0.09	-0.07	0.06	-0.72	-0.07	0.08	-2.76	-0.07	0.09	-4.41
24.92	-0.06	0.02	0.00	-0.07	0.06	-1.45	-0.07	0.08	-3.52	-0.07	0.09	-5.12
24.50	-0.06	0.02	0.04	-0.07	0.06	-2.23	-0.07	0.08	-4.31	-0.07	0.09	-5.85
24.08	-0.06	0.02	0.15	-0.07	0.06	-2.89	-0.07	0.08	-4.97	-0.07	0.09	-6.43
23.67	-0.06	0.02	0.38	-0.07	0.06	-3.29	-0.07	0.08	-5.32	-0.07	0.08	-6.69
23.67	-0.06	0.02	0.38	-0.07	0.06	-3.29	-0.07	0.08	-5.32	-0.07	0.08	-6.69
23.25	-0.06	0.02	0.73	-0.07	0.06	-3.37	-0.07	0.08	-5.29	-0.07	0.08	-6.55
22.83	-0.06	0.02	0.93	-0.07	0.06	-2.84	-0.07	0.08	-4.42	-0.07	0.08	-5.42
22.42	-0.06	0.02	0.74	-0.07	0.06	-1.68	-0.07	0.08	-2.61	-0.07	0.08	-3.20
22.00	-0.06	0.02	0.00	-0.07	0.06	0.00	-0.07	0.08	0.00	-0.07	0.08	0.00

B.2.2 For depth of excavation of 9m

1.5m				10m			15m			20m		
Y [m]	Ux [m]	Uy [m]	M [kNm/m]	Ux [m]	Uy [m]	M [kNm/m]	Ux [m]	Uy [m]	M [kNm/m]	Ux [m]	Uy [m]	M [kNm/m]
40.00	0.06	0.04	0.00	0.06	0.08	0.00	0.03	0.10	0.00	0.01	0.11	0.00
39.50	0.05	0.04	5.62	0.05	0.08	0.11	0.03	0.10	0.52	0.00	0.11	0.96
39.00	0.05	0.04	17.74	0.04	0.08	0.38	0.02	0.10	1.31	-0.01	0.11	2.67
38.50	0.04	0.04	36.63	0.03	0.08	0.72	0.01	0.10	2.17	-0.02	0.11	4.79
38.00	0.03	0.04	62.85	0.02	0.08	1.10	0.00	0.10	2.98	-0.02	0.11	7.05
32.00	-0.05	0.04	-51.02	0.02	0.08	1.10	0.00	0.10	2.98	-0.02	0.11	7.05
31.75	-0.05	0.04	-64.44	0.01	0.08	-3.96	-0.01	0.10	-1.54	-0.03	0.11	2.20
31.50	-0.06	0.04	-69.37	0.01	0.08	-9.00	-0.01	0.10	-6.07	-0.03	0.11	-2.60
31.25	-0.06	0.04	-64.28	0.00	0.08	-14.02	-0.02	0.10	-10.60	-0.03	0.11	-7.36
31.00	-0.06	0.04	-47.31	0.00	0.08	-19.02	-0.02	0.10	-15.13	-0.04	0.11	-12.07
38.00	0.03	0.04	62.85	0.00	0.08	-19.02	-0.02	0.10	-15.13	-0.04	0.11	-12.07
37.75	0.03	0.04	43.58	-0.01	0.08	-28.98	-0.03	0.10	-24.20	-0.05	0.11	-21.41
37.50	0.02	0.04	26.49	-0.02	0.08	-38.84	-0.04	0.10	-33.30	-0.05	0.11	-30.64
37.25	0.02	0.04	11.64	-0.03	0.08	-48.65	-0.05	0.10	-42.41	-0.06	0.11	-39.77
37.00	0.02	0.04	-0.91	-0.04	0.08	-58.45	-0.05	0.10	-51.54	-0.07	0.11	-48.83
37.00	0.02	0.04	-0.91	-0.04	0.08	-58.45	-0.05	0.10	-51.54	-0.07	0.11	-48.83
36.50	0.01	0.04	-18.61	-0.05	0.08	-68.09	-0.06	0.10	-61.18	-0.07	0.11	-58.99
36.00	0.00	0.04	-25.64	-0.05	0.08	-77.77	-0.06	0.10	-70.82	-0.07	0.11	-68.62
35.50	-0.01	0.04	-21.14	-0.06	0.08	-87.37	-0.07	0.10	-80.26	-0.08	0.11	-77.56
35.00	-0.02	0.04	-4.15	-0.06	0.08	-96.71	-0.07	0.10	-89.25	-0.08	0.11	-85.62
23.50	-0.07	0.05	-7.02	-0.06	0.08	-96.71	-0.07	0.10	-89.25	-0.08	0.11	-85.62
23.06	-0.07	0.05	-6.75	-0.06	0.08	-105.43	-0.07	0.10	-97.48	-0.08	0.11	-92.61
22.63	-0.07	0.05	-6.28	-0.07	0.09	-113.12	-0.08	0.10	-104.66	-0.08	0.11	-98.32
22.19	-0.07	0.05	-5.60	-0.07	0.09	-119.47	-0.08	0.10	-110.45	-0.08	0.11	-102.41
21.75	-0.07	0.05	-4.68	-0.07	0.09	-124.17	-0.08	0.10	-114.47	-0.09	0.11	-104.56
25.25	-0.07	0.05	-6.96	-0.07	0.09	-124.17	-0.08	0.10	-114.47	-0.09	0.11	-104.56
24.81	-0.07	0.05	-7.01	-0.08	0.09	-129.10	-0.08	0.10	-117.82	-0.09	0.11	-105.50
24.38	-0.07	0.05	-7.09	-0.08	0.09	-133.06	-0.08	0.10	-119.94	-0.09	0.11	-105.01
23.94	-0.07	0.05	-7.12	-0.08	0.09	-134.93	-0.09	0.10	-119.91	-0.09	0.11	-102.32
23.50	-0.07	0.05	-7.02	-0.08	0.09	-133.61	-0.09	0.10	-116.74	-0.09	0.11	-96.60
27.00	-0.07	0.04	-13.85	-0.08	0.09	-133.61	-0.09	0.10	-116.74	-0.09	0.11	-96.60
26.56	-0.07	0.04	-9.86	-0.09	0.09	-127.64	-0.09	0.10	-109.30	-0.09	0.11	-86.95
26.13	-0.07	0.04	-7.93	-0.09	0.09	-115.86	-0.09	0.10	-96.44	-0.09	0.11	-72.41
25.69	-0.07	0.04	-7.20	-0.09	0.09	-96.37	-0.09	0.10	-76.78	-0.09	0.11	-51.83
25.25	-0.07	0.05	-6.96	-0.09	0.09	-67.22	-0.09	0.10	-48.80	-0.09	0.11	-23.99
29.00	-0.07	0.04	-51.49	-0.09	0.09	-67.22	-0.09	0.10	-48.80	-0.09	0.11	-23.99
28.50	-0.07	0.04	-41.38	-0.09	0.09	-39.67	-0.09	0.10	-26.47	-0.09	0.11	-5.43
28.00	-0.07	0.04	-31.67	-0.09	0.09	-32.97	-0.09	0.10	-22.35	-0.09	0.11	-4.92
27.50	-0.07	0.04	-22.47	-0.09	0.09	-34.98	-0.09	0.10	-25.52	-0.09	0.11	-11.20

27.00	-0.07	0.04	-13.85	-0.09	0.09	-34.36	-0.09	0.10	-26.45	-0.09	0.11	-14.76
33.00	-0.04	0.04	-83.60	-0.09	0.09	-34.36	-0.09	0.10	-26.45	-0.09	0.11	-14.76
32.75	-0.05	0.04	-81.63	-0.09	0.09	-24.42	-0.09	0.10	-19.67	-0.09	0.11	-12.30
32.50	-0.05	0.04	-76.46	-0.09	0.09	-16.09	-0.09	0.10	-13.84	-0.09	0.11	-9.86
32.25	-0.05	0.04	-66.75	-0.09	0.09	-9.06	-0.09	0.10	-8.73	-0.09	0.11	-7.34
32.00	-0.05	0.04	-51.02	-0.09	0.09	-2.98	-0.09	0.10	-4.11	-0.09	0.11	-4.64
35.00	-0.02	0.04	-4.15	-0.09	0.09	-2.98	-0.09	0.10	-4.11	-0.09	0.11	-4.64
34.75	-0.02	0.04	-25.32	-0.09	0.09	-0.87	-0.09	0.10	-2.51	-0.09	0.11	-3.80
34.50	-0.02	0.04	-43.22	-0.09	0.09	-0.52	-0.09	0.10	-2.30	-0.09	0.11	-3.89
34.25	-0.03	0.04	-57.84	-0.09	0.09	-1.15	-0.09	0.10	-2.87	-0.09	0.11	-4.49
34.00	-0.03	0.04	-69.18	-0.09	0.09	-2.12	-0.09	0.10	-3.72	-0.09	0.11	-5.26
31.00	-0.06	0.04	-47.31	-0.09	0.09	-2.12	-0.09	0.10	-3.72	-0.09	0.11	-5.26
30.50	-0.06	0.04	-36.37	-0.09	0.09	-3.25	-0.09	0.10	-4.71	-0.09	0.11	-6.13
30.00	-0.06	0.04	-39.69	-0.09	0.09	-4.34	-0.09	0.10	-5.70	-0.09	0.11	-7.01
29.50	-0.07	0.04	-47.63	-0.09	0.09	-5.33	-0.09	0.10	-6.63	-0.09	0.11	-7.86
29.00	-0.07	0.04	-51.49	-0.08	0.08	-6.17	-0.09	0.10	-7.45	-0.09	0.11	-8.64
34.00	-0.03	0.04	-69.18	-0.08	0.08	-6.17	-0.09	0.10	-7.45	-0.09	0.11	-8.64
33.75	-0.03	0.04	-77.45	-0.08	0.08	-6.82	-0.09	0.10	-8.13	-0.09	0.11	-9.33
33.50	-0.04	0.04	-82.54	-0.08	0.08	-7.23	-0.09	0.10	-8.59	-0.09	0.11	-9.84
33.25	-0.04	0.04	-84.57	-0.08	0.08	-7.34	-0.08	0.10	-8.74	-0.09	0.11	-10.05
33.00	-0.04	0.04	-83.60	-0.08	0.08	-7.07	-0.08	0.10	-8.48	-0.08	0.11	-9.84
21.75	-0.07	0.05	-4.68	-0.08	0.08	-7.07	-0.08	0.10	-8.48	-0.08	0.11	-9.84
21.31	-0.07	0.05	-3.55	-0.08	0.08	-6.43	-0.08	0.10	-7.82	-0.08	0.11	-9.20
20.88	-0.07	0.05	-2.28	-0.08	0.08	-4.88	-0.08	0.10	-6.01	-0.08	0.11	-7.23
20.44	-0.07	0.05	-1.04	-0.08	0.08	-2.62	-0.08	0.10	-3.25	-0.08	0.11	-4.05
20.00	-0.07	0.05	0.00	-0.08	0.08	0.00	-0.08	0.10	0.00	-0.08	0.11	0.00

B.2.3 For depth of excavation of 11m

	1.5m			10m			15m			20m		
Y	Ux	Uy	M	Ux	Uy	M	Ux	Uy	M	Ux	Uy	M
[m]	[m]	[m]	[kNm/m]	[m]	[m]	[kNm/m]	[m]	[m]	[kNm/m]	[m]	[m]	[kNm/m]
40.00	0.03	0.06	0.00	0.04	0.10	0.00	0.02	0.12	0.00	-0.01	0.13	0.00
39.50	0.03	0.06	6.90	0.03	0.10	0.71	0.01	0.12	1.22	-0.02	0.13	1.68
39.00	0.02	0.06	21.50	0.02	0.10	2.45	0.00	0.12	3.59	-0.03	0.13	5.13
38.50	0.01	0.06	43.72	0.01	0.10	5.11	-0.01	0.12	6.79	-0.04	0.13	9.94
38.00	0.00	0.06	73.82	-0.01	0.10	8.62	-0.02	0.12	10.61	-0.04	0.13	15.82
38.00	0.00	0.06	73.82	-0.01	0.10	8.62	-0.02	0.12	10.61	-0.04	0.13	15.82
37.75	0.00	0.06	54.62	-0.01	0.10	3.99	-0.03	0.12	6.42	-0.05	0.13	10.92
37.50	-0.01	0.06	37.68	-0.02	0.10	-0.45	-0.03	0.12	2.38	-0.05	0.13	6.29
37.25	-0.01	0.06	23.00	-0.02	0.10	-4.71	-0.04	0.12	-1.51	-0.06	0.13	1.90
37.00	-0.02	0.06	10.63	-0.03	0.10	-8.83	-0.04	0.12	-5.27	-0.06	0.13	-2.25
37.00	-0.02	0.06	10.63	-0.03	0.10	-8.83	-0.04	0.12	-5.27	-0.06	0.13	-2.25
36.50	-0.02	0.06	-6.92	-0.04	0.10	-16.75	-0.06	0.12	-12.46	-0.07	0.13	-9.95
36.00	-0.03	0.06	-14.22	-0.05	0.10	-24.33	-0.07	0.12	-19.29	-0.08	0.13	-16.94
35.50	-0.04	0.06	-10.73	-0.07	0.10	-31.75	-0.08	0.12	-25.94	-0.09	0.13	-23.42
35.00	-0.05	0.06	4.13	-0.08	0.10	-39.14	-0.09	0.12	-32.55	-0.10	0.13	-29.60
35.00	-0.05	0.06	4.13	-0.08	0.10	-39.14	-0.09	0.12	-32.55	-0.10	0.13	-29.60
34.75	-0.06	0.06	-21.50	-0.08	0.10	-52.50	-0.09	0.12	-45.67	-0.10	0.13	-43.10
34.50	-0.06	0.06	-44.22	-0.09	0.10	-65.92	-0.10	0.12	-58.81	-0.10	0.13	-56.15
34.25	-0.06	0.06	-64.00	-0.09	0.10	-79.34	-0.10	0.12	-71.89	-0.11	0.13	-68.66
34.00	-0.07	0.06	-80.84	-0.10	0.10	-92.70	-0.10	0.12	-84.80	-0.11	0.13	-80.49
34.00	-0.07	0.06	-80.84	-0.10	0.10	-92.70	-0.10	0.12	-84.80	-0.11	0.13	-80.49
33.75	-0.07	0.06	-95.02	-0.10	0.10	-105.99	-0.11	0.12	-97.27	-0.11	0.13	-91.51
33.50	-0.08	0.06	-106.45	-0.11	0.10	-118.79	-0.11	0.12	-109.11	-0.12	0.13	-101.60
33.25	-0.08	0.06	-115.25	-0.11	0.10	-130.82	-0.12	0.12	-120.01	-0.12	0.13	-110.48
33.00	-0.08	0.06	-121.53	-0.12	0.10	-141.73	-0.12	0.12	-129.63	-0.12	0.13	-117.85
33.00	-0.08	0.06	-121.53	-0.12	0.10	-141.73	-0.12	0.12	-129.63	-0.12	0.13	-117.85
32.75	-0.09	0.06	-127.66	-0.12	0.10	-153.97	-0.12	0.12	-139.54	-0.13	0.13	-124.92
32.50	-0.09	0.06	-131.72	-0.12	0.10	-166.72	-0.13	0.12	-149.54	-0.13	0.13	-131.79
32.25	-0.09	0.06	-132.49	-0.13	0.10	-179.09	-0.13	0.12	-158.95	-0.13	0.13	-137.93
32.00	-0.09	0.06	-128.79	-0.13	0.10	-190.28	-0.13	0.12	-167.08	-0.13	0.13	-142.82
32.00	-0.09	0.06	-128.79	-0.13	0.10	-190.28	-0.13	0.12	-167.08	-0.13	0.13	-142.82
31.75	-0.10	0.06	-159.73	-0.13	0.10	-211.88	-0.13	0.12	-185.11	-0.13	0.13	-157.34
31.50	-0.10	0.06	-183.97	-0.13	0.10	-230.24	-0.13	0.12	-200.19	-0.13	0.13	-169.27
31.25	-0.10	0.06	-199.49	-0.14	0.10	-243.53	-0.14	0.12	-210.90	-0.14	0.13	-177.53
31.00	-0.10	0.06	-204.20	-0.14	0.10	-249.92	-0.14	0.12	-215.82	-0.14	0.13	-181.03
31.00	-0.10	0.06	-204.20	-0.14	0.10	-249.92	-0.14	0.12	-215.82	-0.14	0.13	-181.03
30.75	-0.10	0.06	-191.13	-0.14	0.10	-244.65	-0.14	0.12	-211.78	-0.14	0.13	-177.57
30.50	-0.10	0.06	-167.60	-0.14	0.10	-231.61	-0.14	0.12	-200.84	-0.13	0.13	-167.99
30.25	-0.10	0.06	-133.86	-0.13	0.10	-210.76	-0.14	0.12	-182.85	-0.13	0.13	-152.07

30.00	-0.10	0.06	-90.32	-0.13	0.10	-182.20	-0.13	0.12	-157.72	-0.13	0.13	-129.60
30.00	-0.10	0.06	-90.32	-0.13	0.10	-182.20	-0.13	0.12	-157.72	-0.13	0.13	-129.60
29.75	-0.10	0.06	-72.76	-0.13	0.10	-144.84	-0.13	0.12	-124.55	-0.13	0.13	-99.85
29.50	-0.09	0.06	-44.56	-0.13	0.11	-98.67	-0.13	0.12	-83.15	-0.13	0.13	-62.56
29.25	-0.09	0.06	-4.56	-0.13	0.11	-42.46	-0.13	0.12	-32.52	-0.13	0.13	-16.89
29.00	-0.09	0.06	48.24	-0.12	0.11	24.89	-0.13	0.12	28.26	-0.12	0.13	37.93
29.00	-0.09	0.06	48.24	-0.12	0.11	24.89	-0.13	0.12	28.26	-0.12	0.13	37.93
28.50	-0.09	0.06	88.98	-0.12	0.11	87.09	-0.12	0.12	79.65	-0.12	0.13	80.19
28.00	-0.09	0.06	87.95	-0.12	0.11	99.00	-0.12	0.12	87.07	-0.12	0.13	83.01
27.50	-0.09	0.06	69.12	-0.11	0.11	86.71	-0.12	0.12	74.19	-0.12	0.13	68.16
27.00	-0.09	0.06	52.27	-0.11	0.11	71.88	-0.11	0.12	60.34	-0.11	0.13	53.46
27.00	-0.09	0.06	52.27	-0.11	0.11	71.88	-0.11	0.12	60.34	-0.11	0.13	53.46
26.55	-0.09	0.06	35.25	-0.11	0.11	54.79	-0.11	0.12	45.10	-0.11	0.13	38.71
26.10	-0.09	0.06	20.36	-0.11	0.11	38.82	-0.11	0.12	31.15	-0.11	0.13	25.67
25.65	-0.09	0.06	8.27	-0.11	0.11	25.05	-0.11	0.12	19.28	-0.11	0.13	14.85
25.20	-0.09	0.06	-0.62	-0.11	0.11	14.22	-0.11	0.12	10.03	-0.11	0.13	6.57
25.20	-0.09	0.06	-0.62	-0.11	0.11	14.22	-0.11	0.12	10.03	-0.11	0.13	6.57
24.75	-0.09	0.06	-6.88	-0.11	0.11	5.97	-0.11	0.12	3.03	-0.11	0.13	0.41
24.30	-0.09	0.06	-10.97	-0.11	0.10	-0.05	-0.11	0.12	-2.05	-0.11	0.13	-4.00
23.85	-0.09	0.06	-13.40	-0.11	0.10	-4.28	-0.11	0.12	-5.62	-0.11	0.13	-7.07
23.40	-0.09	0.06	-14.63	-0.10	0.10	-7.17	-0.11	0.12	-8.08	-0.11	0.13	-9.17
23.40	-0.09	0.06	-14.63	-0.10	0.10	-7.17	-0.11	0.12	-8.08	-0.11	0.13	-9.17
22.95	-0.09	0.06	-15.01	-0.10	0.10	-9.07	-0.11	0.12	-9.75	-0.11	0.13	-10.61
22.50	-0.09	0.06	-14.85	-0.10	0.10	-10.32	-0.11	0.12	-10.90	-0.11	0.13	-11.65
22.05	-0.09	0.06	-14.30	-0.10	0.10	-11.11	-0.11	0.12	-11.71	-0.11	0.13	-12.44
21.60	-0.09	0.06	-13.52	-0.10	0.10	-11.61	-0.11	0.12	-12.31	-0.11	0.13	-13.09
21.60	-0.09	0.06	-13.52	-0.10	0.10	-11.61	-0.11	0.12	-12.31	-0.11	0.13	-13.09
21.15	-0.09	0.06	-12.55	-0.10	0.10	-11.90	-0.10	0.12	-12.76	-0.11	0.13	-13.65
20.70	-0.09	0.06	-11.41	-0.10	0.10	-11.97	-0.10	0.12	-13.03	-0.10	0.13	-14.06
20.25	-0.09	0.06	-10.07	-0.10	0.10	-11.76	-0.10	0.12	-13.02	-0.10	0.13	-14.20
19.80	-0.09	0.06	-8.49	-0.10	0.10	-11.18	-0.10	0.12	-12.61	-0.10	0.13	-13.94
19.80	-0.09	0.06	-8.49	-0.10	0.10	-11.18	-0.10	0.12	-12.61	-0.10	0.13	-13.94
19.35	-0.09	0.06	-6.66	-0.10	0.10	-10.12	-0.10	0.12	-11.64	-0.10	0.13	-13.05
18.90	-0.09	0.06	-4.44	-0.10	0.10	-7.89	-0.10	0.12	-9.26	-0.10	0.13	-10.56
18.45	-0.09	0.06	-2.10	-0.09	0.10	-4.44	-0.10	0.12	-5.31	-0.10	0.13	-6.17
18.00	-0.09	0.06	0.00	-0.09	0.10	0.00	-0.10	0.12	0.00	-0.10	0.13	0.00

B.2.4 For depth of excavation of 13m

1.5m				10m			15m			20m		
Y	Ux	Uy	M	Ux	Uy	M	Ux	Uy	M	Ux	Uy	M
[m]	[m]	[m]	[kNm/m]	[m]	[m]	[kNm/m]	[m]	[m]	[kNm/m]	[m]	[m]	[kNm/m]
40.00	0.01	0.07	0.00	0.01	0.11	0.00	-0.01	0.13	0.00	-0.03	0.14	0.00
39.75	0.00	0.07	4.65	0.00	0.11	0.27	-0.02	0.13	0.45	-0.04	0.14	0.90
39.50	0.00	0.07	13.97	0.00	0.11	0.92	-0.02	0.13	1.39	-0.04	0.14	2.80
39.25	-0.01	0.07	27.34	-0.01	0.11	1.92	-0.03	0.13	2.67	-0.05	0.14	5.53
39.00	-0.01	0.07	44.19	-0.02	0.11	3.19	-0.03	0.13	4.21	-0.05	0.14	8.94
39.00	-0.01	0.07	44.19	-0.02	0.11	3.19	-0.03	0.13	4.21	-0.05	0.14	8.94
38.50	-0.02	0.07	17.77	-0.03	0.11	-0.46	-0.04	0.13	0.85	-0.06	0.14	3.40
38.00	-0.03	0.07	1.95	-0.04	0.11	-2.96	-0.06	0.13	-1.47	-0.07	0.14	-0.37
37.50	-0.04	0.07	-4.43	-0.06	0.11	-4.33	-0.07	0.13	-2.70	-0.08	0.14	-2.42
37.00	-0.06	0.07	-2.22	-0.07	0.11	-4.57	-0.08	0.13	-2.74	-0.09	0.14	-2.74
37.00	-0.06	0.07	-2.22	-0.07	0.11	-4.57	-0.08	0.13	-2.74	-0.09	0.14	-2.74
36.75	-0.06	0.07	2.23	-0.08	0.11	-4.29	-0.09	0.13	-2.29	-0.10	0.14	-2.22
36.50	-0.07	0.07	9.14	-0.08	0.11	-3.76	-0.09	0.13	-1.53	-0.10	0.14	-1.25
36.25	-0.07	0.07	18.83	-0.09	0.11	-2.98	-0.10	0.13	-0.46	-0.11	0.14	0.17
36.00	-0.08	0.07	31.66	-0.10	0.11	-1.95	-0.10	0.13	0.94	-0.11	0.14	2.07
36.00	-0.08	0.07	31.66	-0.10	0.11	-1.95	-0.10	0.13	0.94	-0.11	0.14	2.07
35.75	-0.08	0.07	9.38	-0.10	0.11	-9.57	-0.11	0.13	-6.46	-0.12	0.14	-6.01
35.50	-0.09	0.07	-9.61	-0.11	0.11	-16.94	-0.12	0.13	-13.61	-0.12	0.14	-13.67
35.25	-0.09	0.07	-25.49	-0.12	0.11	-24.09	-0.12	0.13	-20.52	-0.13	0.14	-20.96
35.00	-0.10	0.07	-38.45	-0.12	0.11	-31.03	-0.13	0.13	-27.23	-0.13	0.14	-27.93
35.00	-0.10	0.07	-38.45	-0.12	0.11	-31.03	-0.13	0.13	-27.23	-0.13	0.14	-27.93
34.75	-0.10	0.07	-48.20	-0.13	0.11	-37.76	-0.13	0.13	-33.75	-0.14	0.14	-34.61
34.50	-0.11	0.07	-55.20	-0.14	0.12	-44.44	-0.14	0.13	-40.15	-0.14	0.14	-40.86
34.25	-0.11	0.07	-59.35	-0.14	0.12	-51.02	-0.14	0.13	-46.41	-0.15	0.14	-46.53
34.00	-0.12	0.07	-60.60	-0.15	0.12	-57.43	-0.15	0.13	-52.48	-0.15	0.14	-51.46
34.00	-0.12	0.07	-60.60	-0.15	0.12	-57.43	-0.15	0.13	-52.48	-0.15	0.14	-51.46
33.75	-0.12	0.07	-59.02	-0.16	0.12	-63.73	-0.16	0.13	-58.13	-0.16	0.14	-55.50
33.50	-0.13	0.07	-54.35	-0.16	0.12	-69.58	-0.16	0.13	-63.09	-0.16	0.14	-58.47
33.25	-0.13	0.07	-46.55	-0.17	0.12	-74.70	-0.17	0.13	-67.08	-0.16	0.14	-60.16
33.00	-0.14	0.07	-35.60	-0.17	0.12	-78.83	-0.17	0.13	-69.82	-0.17	0.14	-60.30
33.00	-0.14	0.07	-35.60	-0.17	0.12	-78.83	-0.17	0.13	-69.82	-0.17	0.14	-60.30
32.50	-0.15	0.07	-106.66	-0.18	0.12	-133.63	-0.18	0.13	-117.48	-0.18	0.14	-100.06
32.00	-0.16	0.07	-167.13	-0.19	0.12	-190.12	-0.19	0.13	-165.46	-0.18	0.14	-139.22
31.50	-0.16	0.07	-210.38	-0.20	0.12	-242.55	-0.20	0.13	-209.57	-0.19	0.14	-175.07
31.00	-0.17	0.07	-228.60	-0.21	0.12	-284.71	-0.20	0.13	-245.18	-0.19	0.14	-204.54
31.00	-0.17	0.07	-228.60	-0.21	0.12	-284.71	-0.20	0.13	-245.18	-0.19	0.14	-204.54
30.50	-0.17	0.07	-293.53	-0.21	0.12	-329.80	-0.20	0.13	-288.33	-0.20	0.14	-245.63
30.00	-0.17	0.07	-323.85	-0.21	0.12	-351.56	-0.20	0.13	-311.32	-0.20	0.14	-268.27
29.50	-0.17	0.07	-317.97	-0.21	0.12	-347.08	-0.20	0.13	-310.38	-0.19	0.14	-269.40

29.00	-0.16	0.07	-272.24	-0.20	0.12	-311.91	-0.20	0.13	-280.09	-0.19	0.14	-245.18
29.00	-0.16	0.07	-272.24	-0.20	0.12	-311.91	-0.20	0.13	-280.09	-0.19	0.14	-245.18
28.75	-0.16	0.07	-226.52	-0.20	0.12	-276.11	-0.19	0.13	-249.58	-0.19	0.14	-219.62
28.50	-0.15	0.07	-170.90	-0.19	0.12	-232.33	-0.19	0.13	-211.55	-0.18	0.14	-187.15
28.25	-0.15	0.07	-105.63	-0.19	0.12	-180.72	-0.18	0.13	-166.18	-0.18	0.14	-147.77
28.00	-0.14	0.07	-30.97	-0.18	0.12	-121.51	-0.18	0.13	-113.54	-0.17	0.14	-101.52
28.00	-0.14	0.07	-30.97	-0.18	0.12	-121.51	-0.18	0.13	-113.54	-0.17	0.14	-101.52
27.75	-0.14	0.07	16.84	-0.17	0.12	-54.78	-0.17	0.13	-53.76	-0.17	0.14	-48.31
27.50	-0.13	0.08	74.03	-0.17	0.12	19.69	-0.17	0.13	13.52	-0.16	0.14	12.06
27.25	-0.12	0.08	140.61	-0.16	0.12	101.97	-0.16	0.13	88.36	-0.16	0.14	79.75
27.00	-0.12	0.08	216.52	-0.15	0.12	192.09	-0.16	0.13	170.83	-0.15	0.14	154.86
27.00	-0.12	0.08	216.52	-0.15	0.12	192.09	-0.16	0.13	170.83	-0.15	0.14	154.86
26.54	-0.11	0.08	258.23	-0.14	0.12	260.77	-0.15	0.13	229.16	-0.15	0.14	203.37
26.08	-0.11	0.08	236.90	-0.14	0.12	255.50	-0.14	0.13	222.56	-0.14	0.14	194.97
25.63	-0.10	0.08	187.04	-0.13	0.12	213.26	-0.14	0.13	184.48	-0.14	0.14	159.93
25.17	-0.10	0.08	137.63	-0.13	0.12	166.08	-0.13	0.13	143.17	-0.13	0.14	123.25
25.17	-0.10	0.08	137.63	-0.13	0.12	166.08	-0.13	0.13	143.17	-0.13	0.14	123.25
24.71	-0.10	0.08	92.68	-0.12	0.12	120.37	-0.13	0.13	103.20	-0.13	0.14	87.97
24.25	-0.10	0.08	56.83	-0.12	0.12	82.18	-0.13	0.13	69.91	-0.13	0.14	58.76
23.79	-0.10	0.08	29.61	-0.12	0.12	51.82	-0.13	0.13	43.50	-0.13	0.14	35.71
23.33	-0.10	0.08	10.30	-0.12	0.12	29.21	-0.13	0.13	23.87	-0.13	0.14	18.64
23.33	-0.10	0.08	10.30	-0.12	0.12	29.21	-0.13	0.13	23.87	-0.13	0.14	18.64
22.88	-0.10	0.08	-2.77	-0.12	0.12	12.96	-0.12	0.13	9.78	-0.13	0.14	6.43
22.42	-0.10	0.08	-11.11	-0.12	0.12	1.75	-0.12	0.13	0.03	-0.13	0.14	-2.00
21.96	-0.10	0.08	-15.95	-0.12	0.12	-5.62	-0.12	0.13	-6.41	-0.13	0.14	-7.59
21.50	-0.10	0.08	-18.43	-0.12	0.12	-10.28	-0.12	0.13	-10.55	-0.12	0.14	-11.24
21.50	-0.10	0.08	-18.43	-0.12	0.12	-10.28	-0.12	0.13	-10.55	-0.12	0.14	-11.24
21.04	-0.10	0.08	-19.30	-0.12	0.12	-13.02	-0.12	0.13	-13.08	-0.12	0.14	-13.57
20.58	-0.10	0.08	-19.21	-0.12	0.12	-14.56	-0.12	0.13	-14.63	-0.12	0.14	-15.12
20.13	-0.10	0.08	-18.51	-0.12	0.12	-15.29	-0.12	0.13	-15.54	-0.12	0.14	-16.24
19.67	-0.10	0.08	-17.49	-0.12	0.12	-15.58	-0.12	0.13	-16.15	-0.12	0.14	-17.18
19.67	-0.10	0.08	-17.49	-0.12	0.12	-15.58	-0.12	0.13	-16.15	-0.12	0.14	-17.18
19.21	-0.10	0.08	-16.26	-0.11	0.12	-15.56	-0.12	0.13	-16.56	-0.12	0.14	-18.07
18.75	-0.10	0.08	-14.86	-0.11	0.12	-15.29	-0.12	0.13	-16.77	-0.12	0.14	-18.85
18.29	-0.10	0.08	-13.26	-0.11	0.12	-14.69	-0.11	0.13	-16.68	-0.12	0.14	-19.39
17.83	-0.10	0.08	-11.40	-0.11	0.12	-13.71	-0.11	0.13	-16.20	-0.11	0.14	-19.56
17.83	-0.10	0.08	-11.40	-0.11	0.12	-13.71	-0.11	0.13	-16.20	-0.11	0.14	-19.56
17.38	-0.10	0.08	-9.23	-0.11	0.12	-12.18	-0.11	0.13	-15.02	-0.11	0.14	-18.86
16.92	-0.10	0.08	-6.38	-0.11	0.12	-9.07	-0.11	0.13	-11.83	-0.11	0.14	-15.75
16.46	-0.10	0.08	-3.15	-0.11	0.12	-4.75	-0.11	0.13	-6.69	-0.11	0.14	-9.59
16.00	-0.10	0.08	0.00	-0.10	0.12	0.00	-0.11	0.13	0.00	-0.11	0.14	0.00

B.3 Effect of Change in Pile diameter on pile

B.3.1 For depth of excavation of 7m

	40cm			60cm			80cm		
Y	Ux	Uy	M	Ux	Uy	M	Ux	Uy	M
[m]	[m]	[m]	[kNm/m]	[m]	[m]	[kNm/m]	[m]	[m]	[kNm/m]
40.00	0.09	0.02	0.00	0.06	0.01	0.00	0.06	-0.02	0.00
39.75	0.08	0.02	3.67	0.06	0.01	3.74	0.06	-0.02	3.31
39.50	0.08	0.02	11.14	0.06	0.01	11.27	0.05	-0.02	9.94
39.25	0.08	0.02	22.02	0.06	0.01	22.06	0.05	-0.02	19.39
39.00	0.07	0.02	35.97	0.05	0.01	35.63	0.05	-0.02	31.22
39.00	0.07	0.02	35.97	0.05	0.01	35.63	0.05	-0.02	31.22
38.50	0.06	0.02	6.63	0.05	0.01	4.90	0.04	-0.02	-5.62
38.00	0.06	0.02	-13.02	0.04	0.01	-17.33	0.04	-0.02	-35.17
37.50	0.05	0.02	-23.64	0.03	0.01	-31.61	0.04	-0.02	-57.70
37.00	0.04	0.02	-25.46	0.03	0.01	-38.12	0.03	-0.02	-73.09
37.00	0.04	0.02	-25.46	0.03	0.01	-38.12	0.03	-0.02	-73.09
36.75	0.04	0.02	-22.58	0.03	0.01	-37.99	0.03	-0.02	-77.56
36.50	0.03	0.02	-16.88	0.02	0.01	-35.40	0.03	-0.02	-79.61
36.25	0.03	0.02	-7.95	0.02	0.01	-30.09	0.02	-0.02	-78.95
36.00	0.02	0.02	4.58	0.02	0.01	-21.83	0.02	-0.02	-75.35
36.00	0.02	0.02	4.58	0.02	0.01	-21.83	0.02	-0.02	-75.35
35.75	0.02	0.02	-8.17	0.01	0.01	-40.53	0.02	-0.02	-99.14
35.50	0.02	0.02	-16.95	0.01	0.01	-56.18	0.02	-0.02	-119.85
35.25	0.01	0.02	-21.64	0.01	0.01	-68.58	0.01	-0.02	-137.22
35.00	0.01	0.02	-22.18	0.01	0.01	-77.56	0.01	-0.02	-151.04
35.00	0.01	0.02	-22.18	0.01	0.01	-77.56	0.01	-0.02	-151.04
34.75	0.00	0.02	-17.81	0.00	0.01	-82.04	0.01	-0.02	-160.05
34.50	0.00	0.02	-9.33	0.00	0.01	-82.73	0.01	-0.02	-165.06
34.25	0.00	0.02	3.28	0.00	0.01	-79.61	0.00	-0.02	-166.01
34.00	-0.01	0.02	20.02	-0.01	0.01	-72.67	0.00	-0.02	-162.82
34.00	-0.01	0.02	20.02	-0.01	0.01	-72.67	0.00	-0.02	-162.82
33.75	-0.01	0.02	4.52	-0.01	0.01	-98.28	0.00	-0.02	-191.65
33.50	-0.01	0.02	-7.03	-0.01	0.01	-120.06	0.00	-0.02	-215.98
33.25	-0.02	0.02	-14.74	-0.01	0.01	-138.03	0.00	-0.02	-235.89
33.00	-0.02	0.02	-18.75	-0.02	0.01	-152.23	-0.01	-0.02	-251.50
33.00	-0.02	0.02	-18.75	-0.02	0.01	-152.23	-0.01	-0.02	-251.50
32.96	-0.02	0.02	-19.51	-0.02	0.01	-154.49	-0.01	-0.02	-253.94
32.93	-0.02	0.02	-20.64	-0.02	0.01	-157.26	-0.01	-0.02	-256.92
32.89	-0.02	0.02	-22.05	-0.02	0.01	-160.44	-0.01	-0.02	-260.40
32.86	-0.02	0.02	-23.62	-0.02	0.01	-163.91	-0.01	-0.02	-264.30
32.86	-0.02	0.02	-23.62	-0.02	0.01	-163.91	-0.01	-0.02	-264.30
32.75	-0.02	0.02	-29.27	-0.02	0.01	-176.26	-0.01	-0.02	-278.76

32.64	-0.03	0.02	-35.42	-0.02	0.01	-189.85	-0.01	-0.02	-295.41
32.52	-0.03	0.02	-41.77	-0.02	0.01	-204.17	-0.01	-0.02	-313.52
32.41	-0.03	0.02	-48.09	-0.02	0.01	-218.82	-0.01	-0.02	-332.45
32.41	-0.03	0.02	-48.09	-0.02	0.01	-218.82	-0.01	-0.02	-332.45
32.06	-0.03	0.02	-66.94	-0.03	0.01	-265.10	-0.01	-0.02	-394.38
31.71	-0.04	0.02	-83.46	-0.03	0.01	-308.01	-0.02	-0.02	-454.16
31.35	-0.04	0.02	-96.33	-0.03	0.01	-343.89	-0.02	-0.02	-506.85
31.00	-0.05	0.02	-103.80	-0.04	0.01	-368.93	-0.02	-0.02	-547.51
31.00	-0.05	0.02	-103.80	-0.04	0.01	-368.93	-0.02	-0.02	-547.51
30.50	-0.05	0.02	-94.58	-0.04	0.01	-374.82	-0.03	-0.02	-573.18
30.00	-0.05	0.02	-85.65	-0.04	0.01	-370.34	-0.03	-0.02	-583.95
29.50	-0.06	0.02	-77.07	-0.05	0.01	-356.36	-0.03	-0.02	-580.09
29.00	-0.06	0.02	-66.69	-0.05	0.01	-331.78	-0.04	-0.02	-560.14
29.00	-0.06	0.02	-66.69	-0.05	0.01	-331.78	-0.04	-0.02	-560.14
28.50	-0.06	0.02	-48.32	-0.05	0.01	-292.70	-0.04	-0.02	-520.85
28.00	-0.06	0.02	-32.61	-0.05	0.01	-251.81	-0.04	-0.02	-474.60
27.50	-0.06	0.02	-19.52	-0.05	0.01	-211.02	-0.04	-0.02	-423.75
27.00	-0.06	0.02	-8.70	-0.05	0.01	-171.91	-0.04	-0.02	-370.37
27.00	-0.06	0.02	-8.70	-0.05	0.01	-171.91	-0.04	-0.02	-370.37
26.58	-0.06	0.02	-4.04	-0.06	0.01	-144.13	-0.05	-0.02	-327.90
26.17	-0.06	0.02	-1.59	-0.06	0.01	-119.79	-0.05	-0.02	-286.97
25.75	-0.06	0.02	-0.52	-0.06	0.01	-98.35	-0.05	-0.02	-247.55
25.33	-0.06	0.02	-0.09	-0.06	0.01	-79.37	-0.05	-0.02	-209.68
25.33	-0.06	0.02	-0.09	-0.06	0.01	-79.37	-0.05	-0.02	-209.68
24.92	-0.06	0.02	0.00	-0.06	0.01	-62.57	-0.05	-0.02	-173.56
24.50	-0.06	0.02	0.04	-0.06	0.01	-47.69	-0.05	-0.02	-139.38
24.08	-0.06	0.02	0.15	-0.06	0.01	-34.62	-0.05	-0.02	-107.60
23.67	-0.06	0.02	0.38	-0.06	0.01	-23.30	-0.06	-0.02	-78.68
23.67	-0.06	0.02	0.38	-0.06	0.01	-23.30	-0.06	-0.02	-78.68
23.25	-0.06	0.02	0.73	-0.06	0.01	-13.75	-0.06	-0.02	-53.35
22.83	-0.06	0.02	0.93	-0.06	0.01	-6.45	-0.06	-0.02	-31.98
22.42	-0.06	0.02	0.74	-0.06	0.01	-1.77	-0.06	-0.02	-14.27
22.00	-0.06	0.02	0.00	-0.06	0.01	0.00	-0.06	-0.02	0.00

B.3.2 For depth of excavation of 9m

40cm				60cm			80cm		
Y	Ux	Uy	M	Ux	Uy	M	Ux	Uy	M
[m]	[m]	[m]	[kNm/m]	[m]	[m]	[kNm/m]	[m]	[m]	[kNm/m]
40.00	0.06	0.04	0.00	0.03	0.03	0.00	0.03	0.00	0.00
39.50	0.05	0.04	5.62	0.03	0.03	7.20	0.02	0.00	5.80
39.00	0.05	0.04	17.74	0.02	0.03	21.84	0.02	0.00	17.21
38.50	0.04	0.04	36.63	0.02	0.03	42.56	0.02	0.00	33.03
38.00	0.03	0.04	62.85	0.01	0.03	68.25	0.01	0.00	52.34
32.00	-0.05	0.04	-51.02	-0.04	0.03	-230.02	-0.03	0.00	-345.30
31.75	-0.05	0.04	-64.44	-0.05	0.03	-246.15	-0.03	0.00	-358.50
31.50	-0.06	0.04	-69.37	-0.05	0.03	-252.86	-0.03	0.00	-361.26
31.25	-0.06	0.04	-64.28	-0.05	0.03	-248.42	-0.04	0.00	-352.28
31.00	-0.06	0.04	-47.31	-0.05	0.03	-231.05	-0.04	0.00	-329.95
38.00	0.03	0.04	62.85	0.01	0.03	68.25	0.01	0.00	52.34
37.75	0.03	0.04	43.58	0.01	0.03	45.84	0.01	0.00	24.90
37.50	0.02	0.04	26.49	0.01	0.03	24.65	0.01	0.00	-1.69
37.25	0.02	0.04	11.64	0.01	0.03	4.76	0.01	0.00	-27.26
37.00	0.02	0.04	-0.91	0.00	0.03	-13.72	0.00	0.00	-51.66
37.00	0.02	0.04	-0.91	0.00	0.03	-13.72	0.00	0.00	-51.66
36.50	0.01	0.04	-18.61	0.00	0.03	-45.65	0.00	0.00	-95.84
36.00	0.00	0.04	-25.64	-0.01	0.03	-69.21	0.00	0.00	-131.91
35.50	-0.01	0.04	-21.14	-0.01	0.03	-83.18	-0.01	0.00	-158.27
35.00	-0.02	0.04	-4.15	-0.02	0.03	-86.41	-0.01	0.00	-173.37
23.50	-0.07	0.05	-7.02	-0.07	0.03	-56.86	-0.06	0.00	-142.49
23.06	-0.07	0.05	-6.75	-0.07	0.03	-48.51	-0.06	0.00	-122.48
22.63	-0.07	0.05	-6.28	-0.07	0.03	-40.38	-0.06	0.00	-102.54
22.19	-0.07	0.05	-5.60	-0.07	0.03	-32.49	-0.07	0.00	-83.01
21.75	-0.07	0.05	-4.68	-0.07	0.03	-24.89	-0.07	0.00	-64.23
25.25	-0.07	0.05	-6.96	-0.07	0.03	-93.79	-0.06	0.00	-219.11
24.81	-0.07	0.05	-7.01	-0.07	0.03	-83.79	-0.06	0.00	-200.73
24.38	-0.07	0.05	-7.09	-0.07	0.03	-74.39	-0.06	0.00	-181.76
23.94	-0.07	0.05	-7.12	-0.07	0.03	-65.45	-0.06	0.00	-162.31
23.50	-0.07	0.05	-7.02	-0.07	0.03	-56.86	-0.06	0.00	-142.49
27.00	-0.07	0.04	-13.85	-0.07	0.03	-146.15	-0.05	0.00	-288.75
26.56	-0.07	0.04	-9.86	-0.07	0.03	-130.25	-0.06	0.00	-271.36
26.13	-0.07	0.04	-7.93	-0.07	0.03	-116.64	-0.06	0.00	-254.25
25.69	-0.07	0.04	-7.20	-0.07	0.03	-104.67	-0.06	0.00	-236.94
25.25	-0.07	0.05	-6.96	-0.07	0.03	-93.79	-0.06	0.00	-219.11
29.00	-0.07	0.04	-51.49	-0.06	0.03	-227.04	-0.05	0.00	-349.63
28.50	-0.07	0.04	-41.38	-0.06	0.03	-209.39	-0.05	0.00	-340.60
28.00	-0.07	0.04	-31.67	-0.06	0.03	-189.39	-0.05	0.00	-327.10
27.50	-0.07	0.04	-22.47	-0.06	0.03	-168.02	-0.05	0.00	-309.64

27.00	-0.07	0.04	-13.85	-0.07	0.03	-146.15	-0.05	0.00	-288.75
33.00	-0.04	0.04	-83.60	-0.04	0.03	-240.71	-0.02	0.00	-358.35
32.75	-0.05	0.04	-81.63	-0.04	0.03	-245.99	-0.03	0.00	-364.57
32.50	-0.05	0.04	-76.46	-0.04	0.03	-246.80	-0.03	0.00	-365.28
32.25	-0.05	0.04	-66.75	-0.04	0.03	-241.89	-0.03	0.00	-359.27
32.00	-0.05	0.04	-51.02	-0.04	0.03	-230.02	-0.03	0.00	-345.30
35.00	-0.02	0.04	-4.15	-0.02	0.03	-86.41	-0.01	0.00	-173.37
34.75	-0.02	0.04	-25.32	-0.02	0.03	-117.37	-0.01	0.00	-209.62
34.50	-0.02	0.04	-43.22	-0.02	0.03	-145.20	-0.01	0.00	-242.39
34.25	-0.03	0.04	-57.84	-0.02	0.03	-169.73	-0.02	0.00	-271.50
34.00	-0.03	0.04	-69.18	-0.03	0.03	-190.80	-0.02	0.00	-296.82
31.00	-0.06	0.04	-47.31	-0.05	0.03	-231.05	-0.04	0.00	-329.95
30.50	-0.06	0.04	-36.37	-0.05	0.03	-218.54	-0.04	0.00	-317.45
30.00	-0.06	0.04	-39.69	-0.06	0.03	-221.90	-0.04	0.00	-326.30
29.50	-0.07	0.04	-47.63	-0.06	0.03	-228.63	-0.04	0.00	-341.47
29.00	-0.07	0.04	-51.49	-0.06	0.03	-227.04	-0.05	0.00	-349.63
34.00	-0.03	0.04	-69.18	-0.03	0.03	-190.80	-0.02	0.00	-296.82
33.75	-0.03	0.04	-77.45	-0.03	0.03	-208.55	-0.02	0.00	-318.44
33.50	-0.04	0.04	-82.54	-0.03	0.03	-222.76	-0.02	0.00	-335.96
33.25	-0.04	0.04	-84.57	-0.03	0.03	-233.48	-0.02	0.00	-349.27
33.00	-0.04	0.04	-83.60	-0.04	0.03	-240.71	-0.02	0.00	-358.35
21.75	-0.07	0.05	-4.68	-0.07	0.03	-24.89	-0.07	0.00	-64.23
21.31	-0.07	0.05	-3.55	-0.07	0.03	-17.49	-0.07	0.00	-46.59
20.88	-0.07	0.05	-2.28	-0.07	0.03	-11.39	-0.07	0.00	-31.24
20.44	-0.07	0.05	-1.04	-0.07	0.03	-6.01	-0.07	0.00	-16.48
20.00	-0.07	0.05	0.00	-0.07	0.03	0.00	-0.07	0.00	0.00

B.3.3 For depth of excavation of 11m

	40cm			60cm			80cm		
Y	Ux	Uy	M	Ux	Uy	M	Ux	Uy	M
[m]	[m]	[m]	[kNm/m]	[m]	[m]	[kNm/m]	[m]	[m]	[kNm/m]
40.00	0.03	0.06	0.00	0.01	0.05	0.00	0.00	0.02	0.00
39.50	0.03	0.06	6.90	0.00	0.05	7.68	0.00	0.02	5.08
39.00	0.02	0.06	21.50	0.00	0.05	22.84	-0.01	0.02	14.59
38.50	0.01	0.06	43.72	-0.01	0.05	43.68	-0.01	0.02	27.26
38.00	0.00	0.06	73.82	-0.01	0.05	68.78	-0.01	0.02	42.09
38.00	0.00	0.06	73.82	-0.01	0.05	68.78	-0.01	0.02	42.09
37.75	0.00	0.06	54.62	-0.01	0.05	42.80	-0.02	0.02	8.16
37.50	-0.01	0.06	37.68	-0.02	0.05	17.83	-0.02	0.02	-25.21
37.25	-0.01	0.06	23.00	-0.02	0.05	-6.09	-0.02	0.02	-57.89
37.00	-0.02	0.06	10.63	-0.02	0.05	-28.85	-0.02	0.02	-89.73
37.00	-0.02	0.06	10.63	-0.02	0.05	-28.85	-0.02	0.02	-89.73
36.50	-0.02	0.06	-6.92	-0.03	0.05	-70.26	-0.03	0.02	-149.85
36.00	-0.03	0.06	-14.22	-0.03	0.05	-104.67	-0.03	0.02	-203.20
35.50	-0.04	0.06	-10.73	-0.04	0.05	-130.99	-0.03	0.02	-248.19
35.00	-0.05	0.06	4.13	-0.05	0.05	-148.17	-0.04	0.02	-283.28
35.00	-0.05	0.06	4.13	-0.05	0.05	-148.17	-0.04	0.02	-283.28
34.75	-0.06	0.06	-21.50	-0.05	0.05	-188.59	-0.04	0.02	-331.12
34.50	-0.06	0.06	-44.22	-0.05	0.05	-226.18	-0.04	0.02	-375.78
34.25	-0.06	0.06	-64.00	-0.05	0.05	-260.76	-0.04	0.02	-417.01
34.00	-0.07	0.06	-80.84	-0.06	0.05	-292.13	-0.04	0.02	-454.59
34.00	-0.07	0.06	-80.84	-0.06	0.05	-292.13	-0.04	0.02	-454.59
33.75	-0.07	0.06	-95.02	-0.06	0.05	-320.42	-0.05	0.02	-488.72
33.50	-0.08	0.06	-106.45	-0.06	0.05	-345.40	-0.05	0.02	-518.95
33.25	-0.08	0.06	-115.25	-0.06	0.05	-367.11	-0.05	0.02	-545.15
33.00	-0.08	0.06	-121.53	-0.07	0.05	-385.54	-0.05	0.02	-567.20
33.00	-0.08	0.06	-121.53	-0.07	0.05	-385.54	-0.05	0.02	-567.20
32.75	-0.09	0.06	-127.66	-0.07	0.05	-402.30	-0.05	0.02	-586.33
32.50	-0.09	0.06	-131.72	-0.07	0.05	-414.92	-0.05	0.02	-599.96
32.25	-0.09	0.06	-132.49	-0.07	0.05	-422.08	-0.05	0.02	-606.81
32.00	-0.09	0.06	-128.79	-0.07	0.05	-422.51	-0.06	0.02	-605.61
32.00	-0.09	0.06	-128.79	-0.07	0.05	-422.51	-0.06	0.02	-605.61
31.75	-0.10	0.06	-159.73	-0.07	0.05	-449.73	-0.06	0.02	-628.05
31.50	-0.10	0.06	-183.97	-0.07	0.05	-467.74	-0.06	0.02	-640.08
31.25	-0.10	0.06	-199.49	-0.08	0.05	-474.49	-0.06	0.02	-639.86
31.00	-0.10	0.06	-204.20	-0.08	0.05	-467.98	-0.06	0.02	-625.59
31.00	-0.10	0.06	-204.20	-0.08	0.05	-467.98	-0.06	0.02	-625.59
30.75	-0.10	0.06	-191.13	-0.08	0.05	-442.15	-0.06	0.02	-591.74
30.50	-0.10	0.06	-167.60	-0.08	0.05	-405.02	-0.06	0.02	-546.24
30.25	-0.10	0.06	-133.86	-0.08	0.05	-357.00	-0.06	0.02	-489.56

30.00	-0.10	0.06	-90.32	-0.08	0.05	-298.74	-0.06	0.02	-422.37
30.00	-0.10	0.06	-90.32	-0.08	0.05	-298.74	-0.06	0.02	-422.37
29.75	-0.10	0.06	-72.76	-0.08	0.05	-266.31	-0.06	0.02	-380.85
29.50	-0.09	0.06	-44.56	-0.08	0.05	-223.21	-0.06	0.02	-328.52
29.25	-0.09	0.06	-4.56	-0.08	0.05	-168.58	-0.06	0.02	-264.63
29.00	-0.09	0.06	48.24	-0.08	0.05	-101.74	-0.07	0.02	-188.58
29.00	-0.09	0.06	48.24	-0.08	0.05	-101.74	-0.07	0.02	-188.58
28.50	-0.09	0.06	88.98	-0.08	0.05	-27.39	-0.07	0.02	-101.45
28.00	-0.09	0.06	87.95	-0.08	0.05	4.78	-0.07	0.02	-61.37
27.50	-0.09	0.06	69.12	-0.08	0.05	14.20	-0.07	0.02	-47.33
27.00	-0.09	0.06	52.27	-0.08	0.05	16.98	-0.07	0.02	-41.84
27.00	-0.09	0.06	52.27	-0.08	0.05	16.98	-0.07	0.02	-41.84
26.55	-0.09	0.06	35.25	-0.08	0.05	11.14	-0.07	0.02	-46.27
26.10	-0.09	0.06	20.36	-0.08	0.05	2.01	-0.07	0.02	-54.62
25.65	-0.09	0.06	8.27	-0.08	0.05	-8.47	-0.07	0.02	-64.65
25.20	-0.09	0.06	-0.62	-0.08	0.05	-18.65	-0.07	0.02	-74.43
25.20	-0.09	0.06	-0.62	-0.08	0.05	-18.65	-0.07	0.02	-74.43
24.75	-0.09	0.06	-6.88	-0.08	0.05	-27.94	-0.07	0.02	-83.12
24.30	-0.09	0.06	-10.97	-0.08	0.05	-35.78	-0.08	0.02	-89.96
23.85	-0.09	0.06	-13.40	-0.09	0.05	-41.98	-0.08	0.02	-94.63
23.40	-0.09	0.06	-14.63	-0.09	0.05	-46.41	-0.08	0.02	-96.84
23.40	-0.09	0.06	-14.63	-0.09	0.05	-46.41	-0.08	0.02	-96.84
22.95	-0.09	0.06	-15.01	-0.09	0.05	-49.05	-0.08	0.02	-96.56
22.50	-0.09	0.06	-14.85	-0.09	0.05	-49.96	-0.08	0.02	-93.79
22.05	-0.09	0.06	-14.30	-0.09	0.05	-49.23	-0.08	0.02	-88.69
21.60	-0.09	0.06	-13.52	-0.09	0.05	-46.94	-0.08	0.02	-81.42
21.60	-0.09	0.06	-13.52	-0.09	0.05	-46.94	-0.08	0.02	-81.42
21.15	-0.09	0.06	-12.55	-0.09	0.05	-43.23	-0.08	0.02	-72.25
20.70	-0.09	0.06	-11.41	-0.09	0.05	-38.25	-0.08	0.02	-61.53
20.25	-0.09	0.06	-10.07	-0.09	0.05	-32.21	-0.08	0.02	-49.72
19.80	-0.09	0.06	-8.49	-0.09	0.05	-25.32	-0.08	0.02	-37.30
19.80	-0.09	0.06	-8.49	-0.09	0.05	-25.32	-0.08	0.02	-37.30
19.35	-0.09	0.06	-6.66	-0.09	0.05	-17.97	-0.08	0.02	-24.97
18.90	-0.09	0.06	-4.44	-0.09	0.05	-10.60	-0.08	0.02	-13.91
18.45	-0.09	0.06	-2.10	-0.09	0.05	-4.22	-0.08	0.02	-5.25
18.00	-0.09	0.06	0.00	-0.09	0.05	0.00	-0.08	0.02	0.00

B.3.4 For depth of excavation of 13m

40cm				60cm			80cm		
Y	Ux	Uy	M	Ux	Uy	M	Ux	Uy	M
[m]	[m]	[m]	[kNm/m]	[m]	[m]	[kNm/m]	[m]	[m]	[kNm/m]
40.00	0.01	0.07	0.00	-0.01	0.06	0.00	-0.02	0.03	0.00
39.75	0.00	0.07	4.65	-0.01	0.06	4.33	-0.02	0.03	2.94
39.50	0.00	0.07	13.97	-0.02	0.06	12.84	-0.03	0.03	8.58
39.25	-0.01	0.07	27.34	-0.02	0.06	24.76	-0.03	0.03	16.35
39.00	-0.01	0.07	44.19	-0.02	0.06	39.37	-0.03	0.03	25.71
39.00	-0.01	0.07	44.19	-0.02	0.06	39.37	-0.03	0.03	25.71
38.50	-0.02	0.07	17.77	-0.03	0.06	-0.40	-0.04	0.03	-36.90
38.00	-0.03	0.07	1.95	-0.04	0.06	-33.26	-0.04	0.03	-95.67
37.50	-0.04	0.07	-4.43	-0.05	0.06	-60.40	-0.05	0.03	-151.02
37.00	-0.06	0.07	-2.22	-0.05	0.06	-82.71	-0.05	0.03	-203.08
37.00	-0.06	0.07	-2.22	-0.05	0.06	-82.71	-0.05	0.03	-203.08
36.75	-0.06	0.07	2.23	-0.06	0.06	-91.89	-0.05	0.03	-227.50
36.50	-0.07	0.07	9.14	-0.06	0.06	-99.68	-0.06	0.03	-250.65
36.25	-0.07	0.07	18.83	-0.07	0.06	-105.89	-0.06	0.03	-272.25
36.00	-0.08	0.07	31.66	-0.07	0.06	-110.33	-0.06	0.03	-292.01
36.00	-0.08	0.07	31.66	-0.07	0.06	-110.33	-0.06	0.03	-292.01
35.75	-0.08	0.07	9.38	-0.07	0.06	-152.48	-0.06	0.03	-349.17
35.50	-0.09	0.07	-9.61	-0.08	0.06	-192.60	-0.07	0.03	-404.27
35.25	-0.09	0.07	-25.49	-0.08	0.06	-230.59	-0.07	0.03	-457.11
35.00	-0.10	0.07	-38.45	-0.08	0.06	-266.38	-0.07	0.03	-507.52
35.00	-0.10	0.07	-38.45	-0.08	0.06	-266.38	-0.07	0.03	-507.52
34.75	-0.10	0.07	-48.20	-0.09	0.06	-299.18	-0.07	0.03	-554.42
34.50	-0.11	0.07	-55.20	-0.09	0.06	-329.42	-0.07	0.03	-598.36
34.25	-0.11	0.07	-59.35	-0.09	0.06	-356.90	-0.08	0.03	-639.08
34.00	-0.12	0.07	-60.60	-0.10	0.06	-381.41	-0.08	0.03	-676.35
34.00	-0.12	0.07	-60.60	-0.10	0.06	-381.41	-0.08	0.03	-676.35
33.75	-0.12	0.07	-59.02	-0.10	0.06	-403.10	-0.08	0.03	-710.33
33.50	-0.13	0.07	-54.35	-0.10	0.06	-421.72	-0.08	0.03	-740.67
33.25	-0.13	0.07	-46.55	-0.10	0.06	-437.25	-0.08	0.03	-767.24
33.00	-0.14	0.07	-35.60	-0.11	0.06	-449.69	-0.08	0.03	-789.96
33.00	-0.14	0.07	-35.60	-0.11	0.06	-449.69	-0.08	0.03	-789.96
32.50	-0.15	0.07	-106.66	-0.11	0.06	-551.70	-0.09	0.03	-898.38
32.00	-0.16	0.07	-167.13	-0.12	0.06	-635.22	-0.09	0.03	-981.14
31.50	-0.16	0.07	-210.38	-0.12	0.06	-689.28	-0.09	0.03	-1027.60
31.00	-0.17	0.07	-228.60	-0.12	0.06	-702.51	-0.09	0.03	-1026.91
31.00	-0.17	0.07	-228.60	-0.12	0.06	-702.51	-0.09	0.03	-1026.91
30.50	-0.17	0.07	-293.53	-0.12	0.06	-733.67	-0.10	0.03	-1035.65
30.00	-0.17	0.07	-323.85	-0.12	0.06	-722.08	-0.10	0.03	-999.26

29.50	-0.17	0.07	-317.97	-0.12	0.06	-667.45	-0.10	0.03	-918.01
29.00	-0.16	0.07	-272.24	-0.12	0.06	-567.84	-0.10	0.03	-790.65
29.00	-0.16	0.07	-272.24	-0.12	0.06	-567.84	-0.10	0.03	-790.65
28.75	-0.16	0.07	-226.52	-0.12	0.06	-495.01	-0.10	0.03	-704.19
28.50	-0.15	0.07	-170.90	-0.12	0.06	-412.17	-0.10	0.03	-607.65
28.25	-0.15	0.07	-105.63	-0.12	0.06	-319.62	-0.10	0.03	-501.33
28.00	-0.14	0.07	-30.97	-0.12	0.06	-217.73	-0.10	0.03	-385.58
28.00	-0.14	0.07	-30.97	-0.12	0.06	-217.73	-0.10	0.03	-385.58
27.75	-0.14	0.07	16.84	-0.12	0.06	-143.34	-0.10	0.03	-297.25
27.50	-0.13	0.08	74.03	-0.12	0.06	-59.76	-0.10	0.03	-199.64
27.25	-0.12	0.08	140.61	-0.11	0.06	32.83	-0.10	0.03	-92.94
27.00	-0.12	0.08	216.52	-0.11	0.06	134.20	-0.10	0.03	22.57
27.00	-0.12	0.08	216.52	-0.11	0.06	134.20	-0.10	0.03	22.57
26.54	-0.11	0.08	258.23	-0.11	0.06	230.47	-0.10	0.03	144.76
26.08	-0.11	0.08	236.90	-0.11	0.06	262.93	-0.09	0.03	200.60
25.63	-0.10	0.08	187.04	-0.11	0.06	257.72	-0.09	0.03	215.56
25.17	-0.10	0.08	137.63	-0.11	0.06	236.96	-0.09	0.03	211.27
25.17	-0.10	0.08	137.63	-0.11	0.06	236.96	-0.09	0.03	211.27
24.71	-0.10	0.08	92.68	-0.10	0.06	206.16	-0.09	0.03	193.36
24.25	-0.10	0.08	56.83	-0.10	0.06	172.16	-0.09	0.03	168.87
23.79	-0.10	0.08	29.61	-0.10	0.06	137.67	-0.09	0.03	140.91
23.33	-0.10	0.08	10.30	-0.10	0.06	105.05	-0.09	0.03	112.29
23.33	-0.10	0.08	10.30	-0.10	0.06	105.05	-0.09	0.03	112.29
22.88	-0.10	0.08	-2.77	-0.10	0.06	75.24	-0.09	0.03	84.44
22.42	-0.10	0.08	-11.11	-0.10	0.06	48.94	-0.09	0.03	58.54
21.96	-0.10	0.08	-15.95	-0.10	0.06	26.36	-0.09	0.03	35.24
21.50	-0.10	0.08	-18.43	-0.10	0.06	7.64	-0.09	0.03	15.09
21.50	-0.10	0.08	-18.43	-0.10	0.06	7.64	-0.09	0.03	15.09
21.04	-0.10	0.08	-19.30	-0.10	0.06	-7.34	-0.09	0.03	-1.68
20.58	-0.10	0.08	-19.21	-0.10	0.06	-18.76	-0.09	0.03	-14.97
20.13	-0.10	0.08	-18.51	-0.10	0.06	-26.84	-0.09	0.03	-24.80
19.67	-0.10	0.08	-17.49	-0.10	0.06	-31.82	-0.09	0.03	-31.26
19.67	-0.10	0.08	-17.49	-0.10	0.06	-31.82	-0.09	0.03	-31.26
19.21	-0.10	0.08	-16.26	-0.10	0.06	-33.96	-0.09	0.03	-34.56
18.75	-0.10	0.08	-14.86	-0.10	0.06	-33.53	-0.09	0.03	-34.99
18.29	-0.10	0.08	-13.26	-0.10	0.06	-30.84	-0.09	0.03	-32.90
17.83	-0.10	0.08	-11.40	-0.10	0.06	-26.20	-0.09	0.03	-28.68
17.83	-0.10	0.08	-11.40	-0.10	0.06	-26.20	-0.09	0.03	-28.68
17.38	-0.10	0.08	-9.23	-0.10	0.06	-20.12	-0.09	0.03	-22.60
16.92	-0.10	0.08	-6.38	-0.10	0.06	-12.97	-0.09	0.03	-17.03
16.46	-0.10	0.08	-3.15	-0.10	0.06	-5.84	-0.09	0.03	-10.59
16.00	-0.10	0.08	0.00	-0.10	0.06	0.00	-0.09	0.03	0.00

B.4 Effect of Change in embedment length on pile

B.4.1 For depth of excavation of 7m

	3m			3.5m			4m		
Y	Ux	Uy	M	Ux	Uy	M	Ux	Uy	M
[m]	[m]	[m]	[kNm/m]	[m]	[m]	[kNm/m]	[m]	[m]	[kNm/m]
40.00	0.09	0.02	0.00	0.09	0.02	0.00	0.09	0.02	0.00
39.75	0.08	0.02	3.67	0.08	0.02	3.68	0.08	0.02	3.68
39.50	0.08	0.02	11.14	0.08	0.02	11.16	0.08	0.02	11.17
39.25	0.08	0.02	22.02	0.07	0.02	22.04	0.07	0.02	22.08
39.00	0.07	0.02	35.97	0.07	0.02	35.98	0.07	0.02	36.06
39.00	0.07	0.02	35.97	0.07	0.02	35.98	0.07	0.02	36.06
38.50	0.06	0.02	6.63	0.06	0.02	6.69	0.06	0.02	6.92
38.00	0.06	0.02	-13.02	0.05	0.02	-12.92	0.05	0.02	-12.48
37.50	0.05	0.02	-23.64	0.05	0.02	-23.49	0.05	0.02	-22.78
37.00	0.04	0.02	-25.46	0.04	0.02	-25.22	0.04	0.02	-24.23
37.00	0.04	0.02	-25.46	0.04	0.02	-25.22	0.04	0.02	-24.23
36.75	0.04	0.02	-22.58	0.03	0.02	-22.29	0.03	0.02	-21.16
36.50	0.03	0.02	-16.88	0.03	0.02	-16.53	0.03	0.02	-15.30
36.25	0.03	0.02	-7.95	0.03	0.02	-7.58	0.03	0.02	-6.27
36.00	0.02	0.02	4.58	0.02	0.02	4.96	0.02	0.02	6.30
36.00	0.02	0.02	4.58	0.02	0.02	4.96	0.02	0.02	6.30
35.75	0.02	0.02	-8.17	0.02	0.02	-7.81	0.02	0.02	-6.44
35.50	0.02	0.02	-16.95	0.02	0.02	-16.62	0.01	0.02	-15.25
35.25	0.01	0.02	-21.64	0.01	0.02	-21.38	0.01	0.02	-20.02
35.00	0.01	0.02	-22.18	0.01	0.02	-22.02	0.01	0.02	-20.70
35.00	0.01	0.02	-22.18	0.01	0.02	-22.02	0.01	0.02	-20.70
34.75	0.00	0.02	-17.81	0.00	0.02	-17.80	0.00	0.02	-16.52
34.50	0.00	0.02	-9.33	0.00	0.02	-9.50	0.00	0.02	-8.27
34.25	0.00	0.02	3.28	0.00	0.02	2.90	0.00	0.02	4.07
34.00	-0.01	0.02	20.02	-0.01	0.02	19.40	-0.01	0.02	20.50
34.00	-0.01	0.02	20.02	-0.01	0.02	19.40	-0.01	0.02	20.50
33.75	-0.01	0.02	4.52	-0.01	0.02	3.63	-0.01	0.02	4.66
33.50	-0.01	0.02	-7.03	-0.01	0.02	-8.21	-0.01	0.02	-7.25
33.25	-0.02	0.02	-14.74	-0.02	0.02	-16.24	-0.02	0.02	-15.37
33.00	-0.02	0.02	-18.75	-0.02	0.02	-20.58	-0.02	0.02	-19.80
33.00	-0.02	0.02	-18.75	-0.02	0.02	-20.58	-0.02	0.02	-19.80
32.96	-0.02	0.02	-19.51	-0.02	0.02	-21.39	-0.02	0.02	-20.62
32.93	-0.02	0.02	-20.64	-0.02	0.02	-22.58	-0.02	0.02	-21.82
32.89	-0.02	0.02	-22.05	-0.02	0.02	-24.04	-0.02	0.02	-23.29
32.86	-0.02	0.02	-23.62	-0.02	0.02	-25.67	-0.02	0.02	-24.94
32.86	-0.02	0.02	-23.62	-0.02	0.02	-25.67	-0.02	0.02	-24.94

32.75	-0.02	0.02	-29.27	-0.02	0.02	-31.51	-0.02	0.02	-30.82
32.64	-0.03	0.02	-35.42	-0.03	0.02	-37.86	-0.03	0.02	-37.21
32.52	-0.03	0.02	-41.77	-0.03	0.02	-44.42	-0.03	0.02	-43.82
32.41	-0.03	0.02	-48.09	-0.03	0.02	-50.95	-0.03	0.02	-50.39
32.41	-0.03	0.02	-48.09	-0.03	0.02	-50.95	-0.03	0.02	-50.39
32.06	-0.03	0.02	-66.94	-0.03	0.02	-70.47	-0.03	0.02	-70.05
31.71	-0.04	0.02	-83.46	-0.04	0.02	-87.63	-0.04	0.02	-87.32
31.35	-0.04	0.02	-96.33	-0.04	0.02	-101.02	-0.04	0.02	-100.81
31.00	-0.05	0.02	-103.80	-0.05	0.02	-108.82	-0.05	0.02	-108.69
31.00	-0.05	0.02	-103.80	-0.05	0.02	-108.82	-0.05	0.02	-108.69
30.50	-0.05	0.02	-94.58	-0.05	0.02	-99.72	-0.05	0.02	-99.63
30.00	-0.05	0.02	-85.65	-0.05	0.02	-90.63	-0.05	0.02	-90.57
29.50	-0.06	0.02	-77.07	-0.06	0.02	-81.68	-0.06	0.02	-81.63
29.00	-0.06	0.02	-66.69	-0.06	0.02	-70.75	-0.06	0.02	-70.71
29.00	-0.06	0.02	-66.69	-0.06	0.02	-70.75	-0.06	0.02	-70.71
28.50	-0.06	0.02	-48.32	-0.06	0.02	-51.69	-0.06	0.02	-51.65
28.00	-0.06	0.02	-32.61	-0.06	0.02	-35.32	-0.06	0.02	-35.27
27.50	-0.06	0.02	-19.52	-0.06	0.02	-21.62	-0.06	0.02	-21.57
27.00	-0.06	0.02	-8.70	-0.06	0.02	-10.30	-0.06	0.02	-10.29
27.00	-0.06	0.02	-8.70	-0.06	0.02	-10.30	-0.06	0.02	-10.29
26.58	-0.06	0.02	-4.04	-0.06	0.02	-4.69	-0.06	0.02	-5.23
26.17	-0.06	0.02	-1.59	-0.06	0.02	-2.12	-0.06	0.02	-2.69
25.75	-0.06	0.02	-0.52	-0.06	0.02	-1.32	-0.06	0.02	-1.75
25.33	-0.06	0.02	-0.09	-0.06	0.02	-1.23	-0.06	0.02	-1.59
25.33	-0.06	0.02	-0.09	-0.06	0.02	-1.23	-0.06	0.02	-1.59
24.92	-0.06	0.02	0.00	-0.06	0.02	-1.42	-0.06	0.02	-1.89
24.50	-0.06	0.02	0.04	-0.06	0.02	-1.56	-0.06	0.02	-2.32
24.08	-0.06	0.02	0.15	-0.06	0.02	-1.51	-0.06	0.02	-2.75
23.67	-0.06	0.02	0.38	-0.06	0.02	-1.19	-0.06	0.02	-3.07
23.67	-0.06	0.02	0.38	-0.06	0.02	-1.19	-0.06	0.02	-3.07
23.25	-0.06	0.02	0.73	-0.06	0.02	-0.62	-0.06	0.02	-3.24
22.83	-0.06	0.02	0.93	-0.06	0.02	0.04	-0.06	0.02	-3.24
22.42	-0.06	0.02	0.74	-0.06	0.02	0.39	-0.06	0.02	-3.10
22.00	-0.06	0.02	0.00	-0.06	0.02	0.00	-0.06	0.02	-2.80

B.4.2 For depth of excavation of 9m

	5m			5.5m			6m		
Y	Ux	Uy	M	Ux	Uy	M	Ux	Uy	M
[m]	[m]	[m]	[kNm/m]	[m]	[m]	[kNm/m]	[m]	[m]	[kNm/m]
40.00	0.06	0.04	0.00	0.06	0.04	0.00	0.06	0.04	0.00
39.50	0.05	0.04	5.62	0.05	0.04	5.61	0.05	0.04	5.61
39.00	0.05	0.04	17.74	0.05	0.04	17.70	0.05	0.04	17.70
38.50	0.04	0.04	36.63	0.04	0.04	36.57	0.04	0.04	36.56
38.00	0.03	0.04	62.85	0.03	0.04	62.76	0.03	0.04	62.76
32.00	-0.05	0.04	-51.02	0.03	0.04	62.76	0.03	0.04	62.76
31.75	-0.05	0.04	-64.44	0.03	0.04	43.54	0.03	0.04	43.59
31.50	-0.06	0.04	-69.37	0.02	0.04	26.51	0.02	0.04	26.60
31.25	-0.06	0.04	-64.28	0.02	0.04	11.71	0.02	0.04	11.86
31.00	-0.06	0.04	-47.31	0.02	0.04	-0.77	0.02	0.04	-0.58
38.00	0.03	0.04	62.85	0.02	0.04	-0.77	0.02	0.04	-0.58
37.75	0.03	0.04	43.58	0.01	0.04	-18.35	0.01	0.04	-18.07
37.50	0.02	0.04	26.49	0.00	0.04	-25.26	0.00	0.04	-24.87
37.25	0.02	0.04	11.64	-0.01	0.04	-20.65	-0.01	0.04	-20.17
37.00	0.02	0.04	-0.91	-0.02	0.04	-3.58	-0.02	0.04	-3.03
37.00	0.02	0.04	-0.91	-0.02	0.04	-3.58	-0.02	0.04	-3.03
36.50	0.01	0.04	-18.61	-0.02	0.04	-24.69	-0.02	0.04	-24.10
36.00	0.00	0.04	-25.64	-0.02	0.04	-42.54	-0.02	0.04	-41.93
35.50	-0.01	0.04	-21.14	-0.03	0.04	-57.12	-0.03	0.04	-56.49
35.00	-0.02	0.04	-4.15	-0.03	0.04	-68.43	-0.03	0.04	-67.79
23.50	-0.07	0.05	-7.02	-0.03	0.04	-68.43	-0.03	0.04	-67.79
23.06	-0.07	0.05	-6.75	-0.03	0.04	-76.68	-0.03	0.04	-76.02
22.63	-0.07	0.05	-6.28	-0.04	0.04	-81.76	-0.04	0.04	-81.09
22.19	-0.07	0.05	-5.60	-0.04	0.04	-83.77	-0.04	0.04	-83.10
21.75	-0.07	0.05	-4.68	-0.04	0.04	-82.80	-0.04	0.04	-82.13
25.25	-0.07	0.05	-6.96	-0.04	0.04	-82.80	-0.04	0.04	-82.13
24.81	-0.07	0.05	-7.01	-0.05	0.04	-80.86	-0.05	0.04	-80.21
24.38	-0.07	0.05	-7.09	-0.05	0.04	-75.69	-0.05	0.04	-75.06
23.94	-0.07	0.05	-7.12	-0.05	0.04	-65.96	-0.05	0.04	-65.36
23.50	-0.07	0.05	-7.02	-0.05	0.04	-50.34	-0.05	0.04	-49.76
27.00	-0.07	0.04	-13.85	-0.05	0.04	-50.34	-0.05	0.04	-49.76
26.56	-0.07	0.04	-9.86	-0.05	0.04	-63.77	-0.05	0.04	-63.21
26.13	-0.07	0.04	-7.93	-0.06	0.04	-68.89	-0.06	0.04	-68.34
25.69	-0.07	0.04	-7.20	-0.06	0.04	-63.93	-0.06	0.04	-63.38
25.25	-0.07	0.05	-6.96	-0.06	0.04	-46.98	-0.06	0.04	-46.42
29.00	-0.07	0.04	-51.49	-0.06	0.04	-46.98	-0.06	0.04	-46.42
28.50	-0.07	0.04	-41.38	-0.06	0.04	-35.37	-0.06	0.04	-34.87
28.00	-0.07	0.04	-31.67	-0.06	0.04	-39.38	-0.06	0.04	-38.95

27.50	-0.07	0.04	-22.47	-0.07	0.04	-48.10	-0.07	0.04	-47.73
27.00	-0.07	0.04	-13.85	-0.07	0.04	-51.12	-0.07	0.04	-50.91
33.00	-0.04	0.04	-83.60	-0.07	0.04	-51.12	-0.07	0.04	-50.91
32.75	-0.05	0.04	-81.63	-0.07	0.04	-41.14	-0.07	0.04	-40.98
32.50	-0.05	0.04	-76.46	-0.07	0.04	-31.46	-0.07	0.04	-31.35
32.25	-0.05	0.04	-66.75	-0.07	0.04	-22.32	-0.07	0.04	-22.25
32.00	-0.05	0.04	-51.02	-0.07	0.04	-13.78	-0.07	0.04	-13.74
35.00	-0.02	0.04	-4.15	-0.07	0.04	-13.78	-0.07	0.04	-13.74
34.75	-0.02	0.04	-25.32	-0.07	0.04	-9.50	-0.07	0.04	-9.74
34.50	-0.02	0.04	-43.22	-0.07	0.04	-7.65	-0.07	0.04	-7.86
34.25	-0.03	0.04	-57.84	-0.07	0.04	-7.14	-0.07	0.04	-7.21
34.00	-0.03	0.04	-69.18	-0.07	0.04	-7.10	-0.07	0.04	-7.06
31.00	-0.06	0.04	-47.31	-0.07	0.04	-7.10	-0.07	0.04	-7.06
30.50	-0.06	0.04	-36.37	-0.07	0.04	-7.29	-0.07	0.04	-7.21
30.00	-0.06	0.04	-39.69	-0.07	0.05	-7.48	-0.07	0.04	-7.43
29.50	-0.07	0.04	-47.63	-0.07	0.05	-7.58	-0.07	0.04	-7.63
29.00	-0.07	0.04	-51.49	-0.07	0.05	-7.52	-0.07	0.04	-7.76
34.00	-0.03	0.04	-69.18	-0.07	0.05	-7.52	-0.07	0.04	-7.76
33.75	-0.03	0.04	-77.45	-0.07	0.05	-7.30	-0.07	0.04	-7.81
33.50	-0.04	0.04	-82.54	-0.07	0.05	-6.88	-0.07	0.04	-7.77
33.25	-0.04	0.04	-84.57	-0.07	0.05	-6.23	-0.07	0.04	-7.64
33.00	-0.04	0.04	-83.60	-0.07	0.05	-5.32	-0.07	0.05	-7.41
21.75	-0.07	0.05	-4.68	-0.07	0.05	-5.32	-0.07	0.05	-7.41
21.31	-0.07	0.05	-3.55	-0.07	0.05	-4.15	-0.07	0.05	-7.06
20.88	-0.07	0.05	-2.28	-0.07	0.05	-2.70	-0.07	0.05	-6.57
20.44	-0.07	0.05	-1.04	-0.07	0.05	-1.22	-0.07	0.05	-5.90
20.00	-0.07	0.05	0.00	-0.07	0.05	0.00	-0.07	0.05	-5.03

B.4.3 For depth of excavation of 11m

7m				7.5m			8m		
Y	Ux	Uy	M	Ux	Uy	M	Ux	Uy	M
[m]	[m]	[m]	[kNm/m]	[m]	[m]	[kNm/m]	[m]	[m]	[kNm/m]
40.00	0.03	0.06	0.00	0.03	0.06	0.00	0.03	0.06	0.00
39.50	0.03	0.06	6.90	0.02	0.06	6.85	0.02	0.06	6.89
39.00	0.02	0.06	21.50	0.02	0.06	21.35	0.02	0.06	21.45
38.50	0.01	0.06	43.72	0.01	0.06	43.47	0.01	0.06	43.61
38.00	0.00	0.06	73.82	0.00	0.06	73.50	0.00	0.06	73.63
38.00	0.00	0.06	73.82	0.00	0.06	73.50	0.00	0.06	73.63
37.75	0.00	0.06	54.62	0.00	0.06	54.33	0.00	0.06	54.51
37.50	-0.01	0.06	37.68	-0.01	0.06	37.42	-0.01	0.06	37.63
37.25	-0.01	0.06	23.00	-0.01	0.06	22.80	-0.01	0.06	23.03
37.00	-0.02	0.06	10.63	-0.02	0.06	10.50	-0.02	0.06	10.74
37.00	-0.02	0.06	10.63	-0.02	0.06	10.50	-0.02	0.06	10.74
36.50	-0.02	0.06	-6.92	-0.03	0.06	-6.86	-0.03	0.06	-6.62
36.00	-0.03	0.06	-14.22	-0.03	0.06	-13.91	-0.03	0.06	-13.57
35.50	-0.04	0.06	-10.73	-0.04	0.06	-10.14	-0.04	0.06	-9.72
35.00	-0.05	0.06	4.13	-0.05	0.06	5.01	-0.05	0.06	5.34
35.00	-0.05	0.06	4.13	-0.05	0.06	5.01	-0.05	0.06	5.34
34.75	-0.06	0.06	-21.50	-0.06	0.06	-20.47	-0.06	0.06	-20.24
34.50	-0.06	0.06	-44.22	-0.06	0.06	-43.03	-0.06	0.06	-42.95
34.25	-0.06	0.06	-64.00	-0.06	0.06	-62.66	-0.06	0.06	-62.75
34.00	-0.07	0.06	-80.84	-0.07	0.06	-79.36	-0.07	0.06	-79.66
34.00	-0.07	0.06	-80.84	-0.07	0.06	-79.36	-0.07	0.06	-79.66
33.75	-0.07	0.06	-95.02	-0.07	0.06	-93.40	-0.07	0.06	-93.93
33.50	-0.08	0.06	-106.45	-0.08	0.06	-104.70	-0.08	0.06	-105.47
33.25	-0.08	0.06	-115.25	-0.08	0.06	-113.37	-0.08	0.06	-114.40
33.00	-0.08	0.06	-121.53	-0.08	0.06	-119.53	-0.08	0.06	-120.80
33.00	-0.08	0.06	-121.53	-0.08	0.06	-119.53	-0.08	0.06	-120.80
32.75	-0.09	0.06	-127.66	-0.09	0.06	-125.59	-0.09	0.06	-127.02
32.50	-0.09	0.06	-131.72	-0.09	0.06	-129.58	-0.09	0.06	-131.14
32.25	-0.09	0.06	-132.49	-0.09	0.06	-130.32	-0.09	0.06	-131.98
32.00	-0.09	0.06	-128.79	-0.09	0.06	-126.60	-0.09	0.06	-128.32
32.00	-0.09	0.06	-128.79	-0.09	0.06	-126.60	-0.09	0.06	-128.32
31.75	-0.10	0.06	-159.73	-0.10	0.06	-157.54	-0.10	0.06	-159.27
31.50	-0.10	0.06	-183.97	-0.10	0.06	-181.81	-0.10	0.06	-183.50
31.25	-0.10	0.06	-199.49	-0.10	0.06	-197.37	-0.10	0.06	-199.00
31.00	-0.10	0.06	-204.20	-0.10	0.06	-202.15	-0.10	0.06	-203.66
31.00	-0.10	0.06	-204.20	-0.10	0.06	-202.15	-0.10	0.06	-203.66
30.75	-0.10	0.06	-191.13	-0.10	0.06	-189.14	-0.10	0.06	-190.51
30.50	-0.10	0.06	-167.60	-0.10	0.06	-165.67	-0.10	0.06	-166.89

30.25	-0.10	0.06	-133.86	-0.10	0.06	-132.00	-0.10	0.06	-133.03
30.00	-0.10	0.06	-90.32	-0.10	0.06	-88.52	-0.10	0.06	-89.36
30.00	-0.10	0.06	-90.32	-0.10	0.06	-88.52	-0.10	0.06	-89.36
29.75	-0.10	0.06	-72.76	-0.10	0.06	-71.02	-0.09	0.06	-71.65
29.50	-0.09	0.06	-44.56	-0.09	0.06	-42.86	-0.09	0.06	-43.29
29.25	-0.09	0.06	-4.56	-0.09	0.06	-2.87	-0.09	0.06	-3.11
29.00	-0.09	0.06	48.24	-0.09	0.06	49.93	-0.09	0.06	49.89
29.00	-0.09	0.06	48.24	-0.09	0.06	49.93	-0.09	0.06	49.89
28.50	-0.09	0.06	88.98	-0.09	0.06	89.96	-0.09	0.06	90.72
28.00	-0.09	0.06	87.95	-0.09	0.06	88.34	-0.09	0.06	89.49
27.50	-0.09	0.06	69.12	-0.09	0.06	69.20	-0.08	0.06	70.32
27.00	-0.09	0.06	52.27	-0.08	0.06	52.06	-0.08	0.06	53.08
27.00	-0.09	0.06	52.27	-0.08	0.06	52.06	-0.08	0.06	53.08
26.55	-0.09	0.06	35.25	-0.09	0.06	33.09	-0.08	0.06	35.47
26.10	-0.09	0.06	20.36	-0.09	0.06	17.11	-0.09	0.06	20.18
25.65	-0.09	0.06	8.27	-0.09	0.06	4.71	-0.09	0.06	7.86
25.20	-0.09	0.06	-0.62	-0.09	0.06	-3.84	-0.09	0.06	-1.09
25.20	-0.09	0.06	-0.62	-0.09	0.06	-3.84	-0.09	0.06	-1.09
24.75	-0.09	0.06	-6.88	-0.09	0.06	-9.41	-0.09	0.06	-7.30
24.30	-0.09	0.06	-10.97	-0.09	0.06	-12.69	-0.09	0.06	-11.30
23.85	-0.09	0.06	-13.40	-0.09	0.06	-14.31	-0.09	0.06	-13.62
23.40	-0.09	0.06	-14.63	-0.09	0.06	-14.87	-0.09	0.06	-14.75
23.40	-0.09	0.06	-14.63	-0.09	0.06	-14.87	-0.09	0.06	-14.75
22.95	-0.09	0.06	-15.01	-0.09	0.06	-14.75	-0.09	0.06	-15.07
22.50	-0.09	0.06	-14.85	-0.09	0.06	-14.26	-0.09	0.06	-14.90
22.05	-0.09	0.06	-14.30	-0.09	0.06	-13.56	-0.09	0.06	-14.43
21.60	-0.09	0.06	-13.52	-0.09	0.06	-12.78	-0.09	0.06	-13.85
21.60	-0.09	0.06	-13.52	-0.09	0.06	-12.78	-0.09	0.06	-13.85
21.15	-0.09	0.06	-12.55	-0.09	0.06	-11.94	-0.09	0.06	-13.21
20.70	-0.09	0.06	-11.41	-0.09	0.06	-11.03	-0.09	0.06	-12.59
20.25	-0.09	0.06	-10.07	-0.09	0.06	-9.98	-0.09	0.06	-11.98
19.80	-0.09	0.06	-8.49	-0.09	0.06	-8.72	-0.09	0.06	-11.39
19.80	-0.09	0.06	-8.49	-0.09	0.06	-8.72	-0.09	0.06	-11.39
19.35	-0.09	0.06	-6.66	-0.09	0.06	-7.15	-0.09	0.06	-10.78
18.90	-0.09	0.06	-4.44	-0.09	0.06	-4.95	-0.09	0.06	-10.07
18.45	-0.09	0.06	-2.10	-0.08	0.06	-2.41	-0.09	0.06	-9.19
18.00	-0.09	0.06	0.00	-0.08	0.06	0.00	-0.08	0.06	-8.05

B.4.4 For depth of excavation of 13m

	9m			9.5m			10m		
Y	Ux	Uy	M	Ux	Uy	M	Ux	Uy	M
[m]	[m]	[m]	[kNm/m]	[m]	[m]	[kNm/m]	[m]	[m]	[kNm/m]
40.00	0.01	0.07	0.00	0.01	0.07	0.00	0.01	0.07	0.00
39.75	0.00	0.07	4.65	0.00	0.07	4.63	0.00	0.07	4.63
39.50	0.00	0.07	13.97	0.00	0.07	13.94	0.00	0.07	13.94
39.25	-0.01	0.07	27.34	-0.01	0.07	27.31	-0.01	0.07	27.30
39.00	-0.01	0.07	44.19	-0.01	0.07	44.16	-0.01	0.07	44.15
39.00	-0.01	0.07	44.19	-0.01	0.07	44.16	-0.01	0.07	44.15
38.50	-0.02	0.07	17.77	-0.02	0.07	18.17	-0.02	0.07	18.18
38.00	-0.03	0.07	1.95	-0.03	0.07	2.62	-0.03	0.07	2.69
37.50	-0.04	0.07	-4.43	-0.04	0.07	-3.67	-0.05	0.07	-3.46
37.00	-0.06	0.07	-2.22	-0.06	0.07	-1.49	-0.06	0.07	-1.06
37.00	-0.06	0.07	-2.22	-0.06	0.07	-1.49	-0.06	0.07	-1.06
36.75	-0.06	0.07	2.23	-0.06	0.07	2.95	-0.06	0.07	3.53
36.50	-0.07	0.07	9.14	-0.07	0.07	9.85	-0.07	0.07	10.57
36.25	-0.07	0.07	18.83	-0.07	0.07	19.57	-0.07	0.07	20.40
36.00	-0.08	0.07	31.66	-0.08	0.07	32.41	-0.08	0.07	33.30
36.00	-0.08	0.07	31.66	-0.08	0.07	32.41	-0.08	0.07	33.30
35.75	-0.08	0.07	9.38	-0.08	0.07	10.08	-0.08	0.07	11.01
35.50	-0.09	0.07	-9.61	-0.09	0.07	-8.96	-0.09	0.07	-8.01
35.25	-0.09	0.07	-25.49	-0.09	0.07	-24.88	-0.09	0.07	-23.93
35.00	-0.10	0.07	-38.45	-0.10	0.07	-37.87	-0.10	0.07	-36.94
35.00	-0.10	0.07	-38.45	-0.10	0.07	-37.87	-0.10	0.07	-36.94
34.75	-0.10	0.07	-48.20	-0.10	0.07	-47.64	-0.10	0.07	-46.75
34.50	-0.11	0.07	-55.20	-0.11	0.07	-54.65	-0.11	0.07	-53.82
34.25	-0.11	0.07	-59.35	-0.11	0.07	-58.80	-0.11	0.07	-58.06
34.00	-0.12	0.07	-60.60	-0.12	0.07	-60.05	-0.12	0.07	-59.39
34.00	-0.12	0.07	-60.60	-0.12	0.07	-60.05	-0.12	0.07	-59.39
33.75	-0.12	0.07	-59.02	-0.12	0.07	-58.50	-0.12	0.07	-57.92
33.50	-0.13	0.07	-54.35	-0.13	0.07	-53.86	-0.13	0.07	-53.36
33.25	-0.13	0.07	-46.55	-0.13	0.07	-46.11	-0.13	0.07	-45.67
33.00	-0.14	0.07	-35.60	-0.14	0.07	-35.20	-0.14	0.07	-34.84
33.00	-0.14	0.07	-35.60	-0.14	0.07	-35.20	-0.14	0.07	-34.84
32.50	-0.15	0.07	-106.66	-0.15	0.07	-106.33	-0.15	0.07	-106.11
32.00	-0.16	0.07	-167.13	-0.16	0.07	-166.87	-0.16	0.07	-166.74
31.50	-0.16	0.07	-210.38	-0.16	0.07	-210.16	-0.16	0.07	-210.08
31.00	-0.17	0.07	-228.60	-0.17	0.07	-228.39	-0.17	0.07	-228.30
31.00	-0.17	0.07	-228.60	-0.17	0.07	-228.39	-0.17	0.07	-228.30
30.50	-0.17	0.07	-293.53	-0.17	0.07	-293.20	-0.17	0.07	-293.17
30.00	-0.17	0.07	-323.85	-0.17	0.07	-323.36	-0.17	0.07	-323.35

29.50	-0.17	0.07	-317.97	-0.17	0.07	-317.30	-0.16	0.07	-317.28
29.00	-0.16	0.07	-272.24	-0.16	0.07	-271.33	-0.16	0.07	-271.28
29.00	-0.16	0.07	-272.24	-0.16	0.07	-271.33	-0.16	0.07	-271.28
28.75	-0.16	0.07	-226.52	-0.15	0.07	-225.48	-0.15	0.07	-225.40
28.50	-0.15	0.07	-170.90	-0.15	0.07	-169.72	-0.15	0.07	-169.61
28.25	-0.15	0.07	-105.63	-0.15	0.07	-104.30	-0.14	0.07	-104.15
28.00	-0.14	0.07	-30.97	-0.14	0.07	-29.50	-0.14	0.07	-29.30
28.00	-0.14	0.07	-30.97	-0.14	0.07	-29.50	-0.14	0.07	-29.30
27.75	-0.14	0.07	16.84	-0.13	0.07	18.48	-0.13	0.07	18.73
27.50	-0.13	0.08	74.03	-0.13	0.07	75.84	-0.13	0.07	76.15
27.25	-0.12	0.08	140.61	-0.12	0.07	142.59	-0.12	0.07	142.98
27.00	-0.12	0.08	216.52	-0.12	0.07	218.70	-0.12	0.07	219.16
27.00	-0.12	0.08	216.52	-0.12	0.07	218.70	-0.12	0.07	219.16
26.54	-0.11	0.08	258.23	-0.11	0.07	258.55	-0.11	0.07	260.77
26.08	-0.11	0.08	236.90	-0.11	0.08	229.86	-0.11	0.07	238.29
25.63	-0.10	0.08	187.04	-0.10	0.08	172.96	-0.10	0.07	187.06
25.17	-0.10	0.08	137.63	-0.10	0.08	120.52	-0.10	0.07	136.30
25.17	-0.10	0.08	137.63	-0.10	0.08	120.52	-0.10	0.07	136.30
24.71	-0.10	0.08	92.68	-0.10	0.08	75.15	-0.10	0.07	90.76
24.25	-0.10	0.08	56.83	-0.10	0.08	40.89	-0.10	0.07	54.74
23.79	-0.10	0.08	29.61	-0.10	0.08	16.40	-0.10	0.07	27.66
23.33	-0.10	0.08	10.30	-0.10	0.08	0.16	-0.10	0.08	8.65
23.33	-0.10	0.08	10.30	-0.10	0.08	0.16	-0.10	0.08	8.65
22.88	-0.10	0.08	-2.77	-0.10	0.08	-9.94	-0.10	0.08	-4.05
22.42	-0.10	0.08	-11.11	-0.10	0.08	-15.68	-0.10	0.08	-12.00
21.96	-0.10	0.08	-15.95	-0.10	0.08	-18.42	-0.10	0.08	-16.48
21.50	-0.10	0.08	-18.43	-0.10	0.08	-19.35	-0.10	0.08	-18.67
21.50	-0.10	0.08	-18.43	-0.10	0.08	-19.35	-0.10	0.08	-18.67
21.04	-0.10	0.08	-19.30	-0.10	0.08	-19.16	-0.10	0.08	-19.34
20.58	-0.10	0.08	-19.21	-0.10	0.08	-18.44	-0.10	0.08	-19.13
20.13	-0.10	0.08	-18.51	-0.10	0.08	-17.45	-0.10	0.08	-18.42
19.67	-0.10	0.08	-17.49	-0.10	0.08	-16.42	-0.10	0.08	-17.53
19.67	-0.10	0.08	-17.49	-0.10	0.08	-16.42	-0.10	0.08	-17.53
19.21	-0.10	0.08	-16.26	-0.10	0.08	-15.38	-0.10	0.08	-16.61
18.75	-0.10	0.08	-14.86	-0.10	0.08	-14.33	-0.10	0.08	-15.78
18.29	-0.10	0.08	-13.26	-0.10	0.08	-13.16	-0.10	0.08	-15.03
17.83	-0.10	0.08	-11.40	-0.10	0.08	-11.73	-0.10	0.08	-14.38
17.83	-0.10	0.08	-11.40	-0.10	0.08	-11.73	-0.10	0.08	-14.38
17.38	-0.10	0.08	-9.23	-0.10	0.08	-9.89	-0.10	0.08	-13.77
16.92	-0.10	0.08	-6.38	-0.10	0.08	-7.31	-0.10	0.08	-13.11
16.46	-0.10	0.08	-3.15	-0.09	0.08	-3.97	-0.10	0.08	-12.27
16.00	-0.10	0.08	0.00	-0.09	0.08	0.00	-0.10	0.08	-11.11

Reference

1. Aiza Malik (2015) "Geotechnical Statistical Evaluation of Lahore Site Data and Deep Excavation Design".
2. A.T.C. Goh, K.S.Wong, C.I.Teh & D.Wen (2003) " Pile Response Adjacent to Braced Excavation" Journal of Geotechnical and Geo environmental Engineering, Vol. 129, No. 4.
3. Brinkgreve et al. 2004 PLAXIS is a finite element package intended for analysis of deformation, stability and groundwater flow problems in geotechnical engineering.
4. Bolton M.D. et al (1994) studied the non linear stress-strain behavior of over consolidated clays.
5. Bowles, J.E. (1996). "Foundation Analysis and Design", Fifth Edition, McGraw-Hill, New York. Fourth Edition, 1988.
6. Broms and Wong (1989) proposed a simplified method to estimate the lateral deformation of braced sheet pile walls in clay with average to good workman ship.
7. Cecconi M. et al.(2002) developed a constitutive model for granular materials within the framework of strain–hardening elasto plasticity.
8. Clough, G., & O'Rourke, T. (1990). Construction induced movements of in-situ walls. Proceeding of ASCE Special Conference on Design and Performance of Earth Retaining Structures, (pp. 439-470). Cornell University, New York.
9. E. Erbì and F.M. Soccodato (2011) discussed the results of a 3D numerical study of deep excavations in soft clayey soils.
10. Finno and Sabatini (2002) presented the damage caused by an adjacent in soft clay. in which the excavation support system was secant pile wall braced by both cross-lot struts and tiebacks on a three-story school supported by shallow foundations.
11. Gebru's (2016) analysis of Contiguous Pile wall as deep excavation support system in silty soil in case of Adam Town.
12. Fourier and Potts (1984) studies at the behavior of a propped retaining wall by finite element method.
13. Garvin, R. and Boward, J. (1992) described the cut-and-cover construction of a five level underground parking structure in Pittsburgh.
14. Hancock et al (1977) described the performance of multi-propped deep excavation in sand and gravel.

15. Hatiya (2016) An analysis of secant pile wall as deep excavation support system on silty sand soil in case of Hawassa town.
16. Hsieh, P., & Ou, C. (1997). Use of the modified hyperbolic model in excavation analysis under un drained conditions.
17. Johansson et.al (2014) presented and compared the forces and deformations measured at a multi-anchored sheet pile wall.
18. Kenney et.al (1972) used the finite element method to evaluate the relative importance of different parameters on the important of a braced excavation at Oslo subway in Norway.
19. Liao et al.(1998) The bending moment (M) of the shoring pile can be calculated through the measurements from the reinforcement bar strain gauges.
20. Lings, M. L. et al (1991) presented and compared the performance of a deep excavation constructed by top-down methods in Gault Clay to design predictions.
21. Maria A. et al (2011) studied the performance of the deep excavation support system for 20m diaphragm wall with a single row of prestressed anchors in Berlin using finite element program.
22. M. Mitew (2005) conducted numerical analysis and parameter study taking into account two calculation methods, based on different constitutive soil models.
23. Ou, C., Hsieh, P., & Chion, D. (1993). Characteristics of ground surface settlement during excavation. Canadian Geotechnical Journal
24. Popa et al (2007). Presented "Numerical modeling and experimental measurements for a retaining wall of a deep excavation in Bucharest, Romania."
25. Poul V. L.(1990). A constitutive model with a single yield surface has been developed for the behavior of frictional materials, such as clay, sand, concrete, and rock.
26. Schanz et al. (1999) A comprehensive description of the Hardening Soil model.
27. Schweiger (2005) studied the analysis of a deep excavation project in clayey silt in Salzburg.
28. Teferra, A. (1992). "Foundation Engineering" Addis Ababa: Addis Ababa University Press.
29. Tianteng zhou (2015) "3D FEM analysis for sequential excavation"
30. Tung G. and Kung C. (2015) the Modified Pseudo-Plasticity model by conduction a series of small strain triaxial tests.
31. Whittle 1987 complexity of the constitutive model should be closely tied to the major aspects of the problem.

32. Winter, E. et al (1992) described the performance of a 10-m deep excavation supported by a shoring with tiebacks.
33. Yang C. et al. (2008) developed a constitutive model, Plastic Bounding Surface Model for unsaturated cemented and loessic soils under cyclic loading.
34. Yu Ou C.Y et al. (2012) studied the characteristics of ground surface settlement during excavation.